BUILDING A MECHANISTIC UNDERSTANDING OF STREAM PRIMARY PRODUCTIVITY TO INFORM WATER MANAGEMENT

by

CAITLIN C. CONN

(Under the Direction of Seth Wenger and Amy Rosemond)

ABSTRACT

Streamflow strongly influences river ecosystem structure, function, and the services they provide. River biota are adapted to regional flow regimes in unmanaged systems, and changes in land use, climate, and water management alter hydrology in ways that impact ecosystem function. While prior research has established a strong understanding of river ecosystem structure and large-scale processes, we know considerably less about the mechanisms through which river biota affect ecosystem function or how such understanding can inform river management. This dissertation addresses that knowledge gap using a mid-sized temperate river in Athens, Georgia, the Middle Oconee River, to evaluate producer-mediated effects of antecedent flow conditions on stream primary productivity and assessing how modeling decisions influence ecological inference.

I first examined how antecedent flow affected the biomass and distribution of primary producer groups, including the foundation species *Podostemum ceratophyllum*, which is of conservation concern, in the Middle Oconee River over a three-year period. High and low flows drove producer biomass and distribution, and sustained drought and floods produced distinct, producer-specific effects. I then conducted laboratory incubations using producers collected from

the same reach to quantify gross primary productivity and combined these rates with biomass data to assess each producer's potential contribution to overall stream productivity. Producers differed in their mass-specific productivity rates, reflecting variation in their responses to light availability, and their potential contributions to total productivity varied with biomass dynamics driven by antecedent flow conditions.

Lastly, I evaluated how key decisions in hydraulic model design and hydrologic representation influenced ecological inference about habitat provisioning. Higher resolution models consistently outperformed simpler models, and a complementary approach using time-weighted and targeted discharge statistics provided the most accurate and comprehensive depiction of how streamflow variability affects habitat provisioning. The value of increased modeling investment depended on the risks of uncertainty for a given ecological outcome, demonstrating the importance of evaluating modeling trade-offs in light of project objectives and risk tolerance. Collectively, this dissertation establishes producer-mediated effects of antecedent flow as a mechanism driving variation in stream function and underscores the importance of incorporating ecological mechanisms into modeling efforts to better inform river management.

INDEX WORDS: Antecedent flow conditions, Flow ecology, Primary producer biomass, *Podostemum ceratophyllum*, Gross primary productivity, Habitat provisioning, Hydraulic models, Hydrology, Streamflow, Ecological inference, River management

BUILDING A MECHANISTIC UNDERSTANDING OF STREAM PRIMARY PRODUCTIVITY TO INFORM WATER MANAGEMENT

by

CAITLIN C. CONN

B.A., Hendrix College, 2010

A Dissertation Submitted to the Graduate Faculty of The University of Georgia in Partial Fulfillment of the Requirements for the Degree

DOCTOR OF PHILOSPHY

ATHENS, GEORGIA

2025

BUILDING A MECHANISTIC UNDERSTANDING OF STREAM PRIMARY PRODUCTIVITY TO INFORM WATER MANAGEMENT

by

CAITLIN C. CONN

Major Professor:	Seth Wenger
	Amy Rosemond
Committee:	Mary Freeman
	Kyle McKay

Electronic Version Approved:

Ron Walcott
Vice Provost for Graduate Education and Dean of the Graduate School
The University of Georgia
December 2025

DEDICATION

This dissertation is dedicated to Little Bear. I can’t wait to meet you.

ACKNOWLEDGEMENTS

I have made it here because of countless colleagues, committee members, undergraduate assistants, faculty, teammates, medical professionals, friends, partners, and family members who have offered up their assistance, expertise, and on many occasions, their sanity.

To the lab mates, undergraduate assistants, and first and foremost, Phillip Bumpers, who made my lab and field work possible, thank you. Phillip, you are a rock, in the best and most steadfast of ways.

To my committee members Kyle McKay and Mary Freeman, your expertise and mentorship has shaped who I am as a scientist. Kyle, every conversation with you feels like a pragmatic takeover of the world, complete with schematics and an outline. Mary, every conversation with you feels like an invitation to explore. I don't know if I've ever met someone so intelligent and insightful who is simultaneously so humble and collaborative. I am a better scientist for knowing both of you. Thank you.

To my advisors Seth Wenger and Amy Rosemond, you have provided me with years of support with a patience and compassion I can only hope to achieve in my own mentorship. Seth, thank you for always letting me barge into your office, for re-explaining the same statistics five times over, and for continuing to support me despite your own ever-growing commitments. Amy, you are a fountain of intelligence, creativity, and love. I feel honored to be your final graduate. UGA and the scientific community at-large have been lucky to have you both.

To the family who so fully accept and believe in me, thank you.

And lastly, to my partner Audrey Moss, I don't have adequate words to describe how important your love and support have been to me, but I'll give it a try. You cared for me when my body and brain failed me, and you believed in me when my own confidence faltered. Every single day, I feel lucky to know you. Thank you, a thousand times over. I love you.

TABLE OF CONTENTS

Page

LIST OF TABLES

Page

LIST OF FIGURES

Page

CHAPTER 1

INTRODUCTION

Streamflow shapes the structure and function of riverine ecosystems (Poff et al. 1997, Hart and Finelli 1999, Biggs et al. 2005), and in turn, the goods and services that rivers and streams provide for human use and enjoyment (Baron et al. 2002). As a modern society, we are inextricably connected to these aquatic systems, yet through various actions – extraction, diversion, damming, and numerous other alterations – we have fundamentally reshaped natural flow regimes (Millenium Ecosystem Assessment 2005). A central challenge of the Anthropocene – the era of human dominance in which we now find ourselves – is to understand the consequences of these impacts and, where possible, mitigate them (Richter et al. 1996, Poff et al. 2010, Sun et al. 2017). However, our capacity to effectively manage for healthy rivers and streams is limited by (1) a knowledge gap – the incomplete understanding of the mechanisms by which streamflow affects ecosystem processes (Poff and Zimmerman 2010, Bernhardt et al. 2018) and (2) a methodological gap - the uncertainties and shortcomings of current methods of forecasting ecological responses to streamflow scenarios (Dietze et al. 2018, Brauman et al. 2021).

Analogous to human medicine, evaluating stream functional components alongside structural ones is necessary for a full understanding of ecosystem health (Palmer and Febria 2012). In fact, researchers have proposed that ecosystem functions be considered as management objectives alongside ecosystem structural attributes due to their importance in maintaining ecosystem services (Wenger et al. 2009, Tank et al. 2010). Because energy is a fundamental

limitation of all ecosystems, metabolic rates – gross primary productivity, ecosystem respiration, and net ecosystem productivity – could be valuable functional targets for water managers and restoration practitioners (Bernhardt et al. 2018).

Gross primary productivity (GPP) is a measure of the conversion of solar energy into fixed organic energy by autotrophs (i.e., primary producers), whereas ecosystem respiration (ER) is a measure of both autotrophic and heterotrophic activity as this energy moves through the system. The difference between the two, net ecosystem productivity (NEP) or metabolism, describes the balance between energy production and energy consumption within the ecosystem (Odum 1956). Due to technological advancements over the last two decades, recent research has been able to elucidate patterns in these functional rates for small and large streams (Appling et al. 2018, Savoy et al. 2019).

Even in largely heterotrophic streams, where energy consumption is greater than energy production (ER > GPP), there can be critical semi-annual or annual periods of high primary production (Carter et al. 2024), and due to the labile natural of autotrophic carbon in comparison to that of terrestrial carbon, primary producers can disproportionately contribute to consumer biomass (Thorp and Delong 2002). Primary producers can also provide habitat complexity for numerous stream biota (Cardinale et al. 2011, Wood and Freeman 2017, Vadeboncoeur and Power 2017, Kendrick et al. 2019), and their productivity is inextricably linked to other important stream processes, such as nutrient uptake (Johnson and Tank 2009, Hanrahan et al. 2018, Myrstener et al. 2021, Reisinger et al. 2021, Schlenker et al. 2024). Despite the structural and functional importance of stream primary production and the availability of whole-stream metabolic data, current research does not yet provide the mechanistic understanding of whole stream metabolism necessary for it to be an interpretable and effective management objective.

Like all stream biota, primary producers are adapted to the natural flow regime – the characteristic magnitude, timing, frequency, and rate of change of flows that shapes the stream environment – and they are subject to the same global stressors as higher-order consumers (Poff et al. 1997, Lytle and Poff 2004). Yet prior flow ecology research (i.e., research identifying predictive relationships between streamflow and ecological responses) has largely focused on consumers, such as macroinvertebrates and fishes, or riparian vegetation (Lytle and Poff 2004, Poff and Zimmerman 2010). Further, while differences in morphology and physiology have been documented as drivers of variability in producer responses to local conditions, this research has heavily focused on stream algae, and even then, we know considerably less about how producer traits and water velocity dynamics play out at the temporal and spatial scales relevant to conservation and management efforts (but see Power 1992, Power et al. 2008).

In addition to identifying flow ecology relationships for a more diverse set of primary producers and at scales relevant to management, structural and functional components of primary production need to be quantified and connected to determine whole-stream consequences of changing streamflow variability. Palmer and Ruhi (2019) describe these linkages as the 'flow-biota-ecosystem-process-nexus,' noting both the dual roles of ecosystem structure and function and their dynamic, multi-directional relationships with flow. Past research has quantified instantaneous metabolic rates in laboratory incubations and small-scale *in-situ* mesocosm experiments (e.g., Steinman and McIntire 1986, Rosemond 1993, Bott et al. 1997) and the more recent studies have documented whole-stream metabolic patterns (Dodds et al. 2013, Appling et al. 2018, Savoy et al. 2019, Bernhardt et al. 2022), but fewer studies have linked the different ecological scales. Connecting the scales, however, is crucial for a mechanistic understanding of how flow effects extend from individual organisms to whole streams, which is needed for stream

metabolic functions to be effective targets of subsequent conservation and restoration efforts (e.g., as an indicator of ecosystem health) (Palmer and Ruhi 2019).

In order to integrate both the ecological and physical aspects of stream systems, restoration practitioners and water managers increasingly rely upon integrated modeling, which provides a framework for combining multiple models across scales and disciplines (Borsuk et al. 2004, Uusitalo et al. 2015). However, developing such models requires navigating a challenging trade-off between a better representation of the stream dynamics and a more feasible, often more interpretable, model (Schultz et al. 2010, Harris et al. 2023). Understanding how modeling decisions shape our inferences about the ecosystem is key to finding the appropriate level of model complexity (Larsen et al. 2016). Thus, in addition to a more mechanistic understanding of flow-ecology relationships, we also need to evaluate how different model choices influence our understanding of those relationships.

In this dissertation, I investigated the mechanisms underlying stream primary productivity in a mid-sized, temperate river and evaluated how modeling decisions shape ecological inferences within the same system. The overarching goal of this research is to build a mechanistic understanding of how stream flow affects primary productivity in order to better predict the ecological outcomes of future management and climate scenarios. Chapters 2 and 3 were initiated with a grant from the United States Army Corps of Engineers to evaluate the effects of flow-variability on ecosystem function. Chapter 4 was conducted in partnership with the Engineer Research and Development Center of the United States Army Corps of Engineers.

In Chapter 2, I examined the mechanisms through which streamflow affects stream function by evaluating how antecedent flow conditions influenced the distribution and biomass of primary producers in a mid-sized temperate river. I used an observational approach,

comprehensively surveying an approximately 500 m-long river reach to quantify primary producer biomass over a period of three years. I then tested producer-specific flow ecology hypotheses to determine the effects of high- and low-flow disturbances on three morphologically distinct producer groups: *Podostemum ceratophyllum*, benthic algae containing biofilms, and filamentous algae predominantly comprised of *Rhizoclonium* sp. These hypotheses were grounded in evidence and theory of how differences in producer traits convey advantages and/or disadvantages to different aspects of the flow regime. Prior flow ecology studies have largely focused on consumers or riparian vegetation (Poff and Zimmerman 2010), with research on how producer traits shape responses to environmental stimuli having typically been limited to smaller spatial scales and shorter time periods (e.g., Biggs et al. 1998, Riis and Biggs 2001, Hart et al. 2013, Rott and Wehr 2016). This study provides empirical evidence of producer-specific flow ecology relationships at management and policy-relevant scales, showing that differences in producer traits can determine resistance and resilience to hydrologic disturbance.

In Chapter 3, I continued building a mechanistic understanding by linking structure to function. I used an experimental approach to evaluate gross primary productivity (GPP) of the same primary producer groups in laboratory incubations under different experimental light conditions and then incorporated observational biomass data from Chapter 2 to assess their potential contributions to stream primary productivity. By further separating producers into types — biofilms containing algae on soft and hard substrates and from different light environments, *Podostemum ceratophyllum* from different light environments, the filamentous green alga *Rhizoclonium* sp., and the filamentous cyanobacterium *Lyngbya* sp. — I was able to quantify functional responses relative to both experimental and antecedent light availability. This study provides empirical data (i.e., GPP rates) for a diverse set of primary producers, exhibiting

differences in morphological and functional traits, while quantifying the effects of light availability. Further, by incorporating field and biomass data from Chapter 2, I illustrate how antecedent flow conditions could create variability in stream metabolism through distinct primary producer morphological and functional traits.

In Chapter 4, I shifted research focus from the ecological knowledge gap to the methodological knowledge gap. I evaluated how modeling decisions can shape our understanding of stream ecosystem responses to flow by employing a simulation-based approach in the same mid-sized temperate river examined in Chapters 2 and 3, using hydraulic models and streamflow statistics widely applied in water-resource management. To assess how differences in model complexity and hydrologic representation influence our understanding of fish habitat provisioning, I varied three aspects of the hydraulic model (i.e., data input resolution, sampling design, and dimensionality) along with the selection of discharge metrics, including traditional central-tendency and percentile statistics, time-weighted variants of these statistics, and regulatory low-flow statistics.

While researchers have developed frameworks for assessing risk (Schultz et al. 2010) and guiding model complexity decisions (Larsen et al. 2016), determining the appropriate level of representational detail remains a central challenge in modeling flow-ecology dynamics. This study demonstrates that the project objectives and risk tolerance determine whether increased investment in model complexity and hydrologic representation is worth the trade-off. The continued reliance on ecological proxies, a common substitute in hydraulic-habitat models, also highlights the need for more informative ecological inputs, potentially including the mechanistic insights of stream function developed in Chapters 2 and 3.

Understanding how different management and climate change scenarios affect a stream ecosystem requires a more mechanistic understanding of both the processes that shape the ecological system and those that shape its modeling. This dissertation addresses both ecological and methodological dimensions of this knowledge gap. By quantifying individual steps in the producer-mediated pathway that ultimately determine reach-scale primary productivity, this dissertation advances the mechanistic understanding of how flow variation affects stream primary productivity. It also provides insights into modeling stream ecological responses by evaluating how key decisions in hydraulic model design and hydrologic representation affect fish habitat provisioning across variable streamflow conditions.

REFERENCES

Appling, A. P., J. S. Read, L. A. Winslow, M. Arroita, E. S. Bernhardt, N. A. Griffiths, R. O. Hall, J. W. Harvey, J. B. Heffernan, E. H. Stanley, E. G. Stets, and C. B. Yackulic. 2018. The metabolic regimes of 356 rivers in the United States. Scientific Data 2018 5:1 63:S99–S118.

Baron, J. S., N. L. Poff, P. L. Angermeier, C. N. Dahm, P. H. Gleick, N. G. Hairston, R. B. Jackson, C. A. Johnston, B. D. Richter, and A. D. Steinman. 2002. Meeting Ecological and Society Needs for Freshwater. Ecological Applications 12:1247–1260.

Bernhardt, E. S., J. B. Heffernan, N. B. Grimm, E. H. Stanley, J. W. Harvey, M. Arroita, A. P. Appling, M. J. Cohen, W. H. McDowell, R. O. Hall, J. S. Read, B. J. Roberts, E. G. Stets, and C. B. Yackulic. 2018. The metabolic regimes of flowing waters. Limnology and Oceanography 63:S99–S118.

Bernhardt, E. S., P. Savoy, M. J. Vlah, A. P. Appling, L. E. Koenig, R. O. Hall, M. Arroita, J. R. Blaszczak, A. M. Carter, M. Cohen, J. W. Harvey, J. B. Heffernan, A. M. Helton, J. D. Hosen, L. Kirk, W. H. McDowell, E. H. Stanley, C. B. Yackulic, and N. B. Grimm. 2022. Light and flow regimes regulate the metabolism of rivers. Proceedings of the National Academy of Sciences of the United States of America 119:e2121976119.

Biggs, B. J. F., D. G. Goring, and V. I. Nikora. 1998. Subsidy and stress responses of stream periphyton to gradients in water velocity as a function of community growth form. Journal of Phycology 34:598–607.

Biggs, B. J. F., V. I. Nikora, and T. H. Snelder. 2005. Linking scales of flow variability to lotic ecosystem structure and function. River Research and Applications 21:283–298.

Borsuk, M. E., C. A. Stow, and K. H. Reckhow. 2004. A Bayesian network of eutrophication models for synthesis, prediction, and uncertainty analysis. Ecological Modelling 173:219–239.

Bott, T. L., J. T. Brock, A. Baattrup-Pedersen, P. A. Chambers, W. K. Dodds, K. T. Himbeault, J. R. Lawrence, D. Planas, E. Snyder, and G. M. Wolfaardt. 1997. An evaluation of techniques for measuring periphyton metabolisms in chambers. Canadian Journal of Fisheries and Aquatic Sciences 54:715–725.

Brauman, K. A., L. L. Bremer, P. Hamel, B. F. Ochoa-Tocachi, F. Roman-Dañobeytia, V. Bonnesoeur, E. Arapa, and G. Gammie. 2021. Producing valuable information from hydrologic models of nature-based solutions for water. Integrated Environmental Assessment and Management 18:135–147.

Cardinale, B. J., K. L. Matulich, D. U. Hooper, J. E. Byrnes, E. Duffy, L. Gamfeldt, P. Balvanera, M. I. O'Connor, and A. Gonzalez. 2011. The functional role of producer diversity in ecosystems. American Journal of Botany 98:572–592.

Dietze, M. C., A. Fox, L. M. Beck-Johnson, J. L. Betancourt, M. B. Hooten, C. S. Jarnevich, T. H. Keitt, M. A. Kenney, C. M. Laney, L. G. Larsen, H. W. Loescher, C. K. Lunch, B. C. Pijanowski, J. T. Randerson, E. K. Read, A. T. Tredennick, R. Vargas, K. C. Weathers, and E. P. White. 2018. Iterative near-term ecological forecasting: Needs, opportunities, and challenges. Proceedings of the National Academy of Sciences 115:1424–1432.

Hanrahan, B. R., J. L. Tank, A. F. Aubeneau, and D. Bolster. 2018. Substrate-specific biofilms control nutrient uptake in experimental streams. Freshwater Science 37:456–471.

Harris, A., N. Richards, and S. K. Mckay. 2023. Defining levels of effort for ecological models. Vicksburg.

Hart, D. D., B. J. Biggs, V. I. Nikora, and C. A. Flinders. 2013. Flow effects on periphyton patches and their ecological consequences in a New Zealand river. Freshwater Biology:1588–1602.

Hart, D. D., and C. M. Finelli. 1999. Physical-biological coupling in streams: The pervasive effects of flow on benthic organisms. Annual Review of Ecology and Systematics 30:363–395.

Johnson, L. T., and J. L. Tank. 2009. Diurnal variations in dissolved organic matter and ammonium uptake in six open-canopy streams. Journal of the North American Benthological Society 28:694–708.

Kendrick, M. R., A. E. Hershey, and A. D. Huryn. 2019. Disturbance, nutrients, and antecedent flow conditions affect macroinvertebrate community structure and productivity in an Arctic river. Limnology and Oceanography 64:S93–S104.

Larsen, L. G., M. B. Eppinga, P. Passalacqua, W. M. Getz, K. A. Rose, and M. Liang. 2016. Appropriate complexity landscape modeling. Earth-Science Reviews 160:111–130.

Lytle, D. A., and N. L. Poff. 2004. Adaptation to natural flow regimes. Trends in Ecology & Evolution 19:94–100.

Millenium Ecosystem Assessment. 2005. Ecosystems and Human Well-being: Synthesis. Washington D.C.

Myrstener, M., L. Gómez-Gener, G. Rocher-Ros, R. Giesler, and R. A. Sponseller. 2021. Nutrients influence seasonal metabolic patterns and total productivity of Arctic streams. Limnology and Oceanography 66:S182–S196.

Odum, H. T. 1956. Primary production in flowing waters. Limnology and Oceanography 1:102–117.

Palmer, M. A., and C. M. Febria. 2012. The Heartbeat of Ecosystems. Science 336:1393–1394.

Palmer, M., and A. Ruhi. 2019. Linkages between flow regime, biota, and ecosystem processes: Implications for river restoration. Science 365:147–170.

Poff, N. L., J. D. Allan, M. B. Bain, J. R. Karr, K. L. Prestegaard, B. D. Richter, R. E. Sparks, and J. C. Stromberg. 1997. The Natural Flow Regime. BioScience 47:769–784.

Poff, N. L., B. D. Richter, A. H. Arthington, S. E. Bunn, R. J. Naiman, E. Kendy, M. Acreman, C. Apse, B. P. Bledsoe, M. C. Freeman, J. Hendriksen, R. B. Jacobson, J. G. Kennen, D. M. Merritt, J. H. O'keeffe, J. D. Olden, K. Rogers, R. E. Tharme, and A. Warner. 2010. The ecological limits of hydrologic alteration (ELOHA): A new framework for developing regional environmental flow standards. Freshwater Biology 55:147–170.

Poff, N. L., and J. K. H. Zimmerman. 2010. Ecological responses to altered flow regimes: a literature review to inform the science and management of environmental flows. Freshwater Biology 55:194–205.

Power, M. E. 1992. Hydrologic and trophic controls of seasonal algal blooms in northern California rivers. Hydrobiologia 125:385–410.

Power, M. E., M. S. Parker, and W. E. Dietrich. 2008. Seasonal reassembly of a river food web: Floods, droughts, and impacts of fish. Ecological Monographs 78:263–282.

Reisinger, A. J., J. L. Tank, R. O. Hall, E. J. Rosi, M. A. Baker, and L. Genzoli. 2021. Water column contributions to the metabolism and nutrient dynamics of mid-sized rivers. Biogeochemistry 153:67–84.

Richter, B. D., J. V Baumgartner, J. Powell, and D. P. Braun. 1996. A Method for Assessing Hydrologic Alteration within Ecosystems. Conservation Biology 10:1163–1174.

Riis, T., and B. J. F. Biggs. 2001. Distribution of macrophytes in New Zealand streams and lakes in relation to disturbance frequency and resource supply - A synthesis and conceptual model. New Zealand Journal of Marine and Freshwater Research 35:255–267.

Rosemond, A. D. 1993. Interactions among irradiance, nutrients, and herbivores constrain a stream algal community. Oecologia 94:585–594.

Rott, E., and J. D. Wehr. 2016. The spatio-temporal development of macroalgae in rivers. Pages 159–195 River Algae. Springer International Publishing, Cham.

Savoy, P., A. P. Appling, J. B. Heffernan, E. G. Stets, J. S. Read, J. W. Harvey, and E. S. Bernhardt. 2019. Metabolic rhythms in flowing waters: An approach for classifying river productivity regimes. Limnology and Oceanography 64:1835–1851.

Schlenker, A., M. Brauns, P. Fink, and M. Weitere. 2024. Beyond biomass: Resource effects on primary production and consumer nutrient assimilation in streams. Freshwater Biology 69:1353–1363.

Schultz, M. T., K. N. Mitchell, B. K. Harper, and T. S. Bridges. 2010. ERDC TR-10-12 "Decision Making Under Uncertainty."

Steinman, A. D., and C. D. McIntire. 1986. Effects of current velocity and light energy on the structure of periphyton assemblage in laboratory streams. Journal of Phycology 22:352–361.

Sun, G., D. Hallema, and H. Asbjornsen. 2017. Ecohydrological processes and ecosystem services in the Anthropocene: a review. Ecological Processes 6:1–9.

Tank, J. L., E. J. Rosi-Marshall, N. A. Griffiths, S. A. Entrekin, and M. L. Stephen. 2010. A review of allochthonous organic matter dynamics and metabolism in streams. Journal of the North American Benthological Society 29:118–146.

Thorp, J. H., and M. D. Delong. 2002. Dominance of autochthonous autotrophic carbon in food webs of heterotrophic rivers. Oikos 96:543–550.

Uusitalo, L., A. Lehikoinen, I. Helle, and K. Myrberg. 2015. An overview of methods to evaluate uncertainty of deterministic models in decision support. Environmental Modelling & Software 63:24–31.

Vadeboncoeur, Y., and M. E. Power. 2017. Attached algae: The cryptic base of inverted trophic pyramids in freshwaters. Annual Review of Ecology, Evolution, and Systematics 48:255–279.

Wenger, S. J., A. H. Roy, C. R. Jackson, E. S. Bernhardt, T. L. Carter, S. Filoso, C. A. Gibson, W. C. Hession, S. S. Kaushal, E. Martí, J. L. Meyer, M. A. Palmer, M. J. Paul, A. H. Purcell, A. Ramírez, A. D. Rosemond, K. A. Schofield, E. B. Sudduth, and C. J. Walsh. 2009. Twenty-six key research questions in urban stream ecology: an assessment of the state of the science. Journal of the North American Benthological Society 28:1080–1098.

Wood, J., and M. Freeman. 2017. Ecology of the macrophyte Podostemum ceratophyllum Michx. (Hornleaf riverweed), a widespread foundation species of eastern North American rivers. Aquatic Botany 139:65–74.

CHAPTER 2

ANTECEDENT FLOW CONDITIONS DRIVE PATTERNS OF PRIMARY PRODUCER BIOMASS IN A MID-SIZED TEMPERATE RIVER[1]

[1] Conn, C. C., A. D. Rosemond, P. M. Bumpers, M. C. Freeman, S. K. McKay, S. J. Wenger. To be submitted to a peer-reviewed journal.

ABSTRACT

Effective management of riverine ecosystems requires an understanding of how abiotic conditions affect essential ecosystem processes such as primary production. It is reasonable to expect that different primary producer types (e.g., macrophytes vs algae) will respond differently to different physical conditions, but this has received only limited attention to date. We examined how antecedent flow conditions affected the biomass and distribution of distinct producer groups in a mid-sized, temperate river over a 3-year period. We compared monthly biomass of three major producer groups —a submerged vascular plant (*Podostemum ceratophyllum*), benthic biofilms containing algae, and filamentous algae — with metrics of antecedent discharge over the study period. We found that antecedent flow conditions, notably both high and low flows, were a strong driver of the biomass and distribution of producer groups. Temporal patterns in peak biomass indicated that sustained drought and floods had strong producer-specific effects. We also found support for most producer-specific hypotheses, which were grounded in evidence and theory of how producer traits, largely growth form, determine responses to local water velocity conditions and disturbance. Our findings provide empirical evidence that organismal traits can determine producer resistance and resilience to hydrologic disturbance at management and policy-relevant spatial and temporal scales. Determining the functional contributions of similarly distinct producer groups is an important next step in quantifying the potential impacts of hydrologic regime shifts on producer-mediated ecosystem processes.

INTRODUCTION

Stream flow has a major influence on ecosystem structure, function, and the corresponding goods and services provided by rivers, such as water supply and recreation (Palmer and Ruhi 2019). Because most river biota are adapted to specific flow conditions (Lytle

and Poff 2004; Kennedy et al. 2016), changes in land use, climate, and river management can affect the flow regime in ways that degrade — or perhaps enhance — ecological structure and function (e.g., Mulholland et al. 1997, Dosdogru et al. 2020). Thus, it is essential to identify predictive relationships between streamflow and ecological responses (i.e. flow ecology relationships) to understand how ecosystems will be affected by hydrologic change under future management and climate scenarios (Poff et al. 2010). Past research on ecological responses to altered flow regimes (Poff and Zimmerman 2010), adaptation of biota to natural flow regimes (Lytle and Poff 2004), and recommendations for management guidelines (Richter et al. 2006) have largely focused on consumers (e.g., Davis et al. 2020), such as fishes and macroinvertebrates, or riparian vegetation. However, primary producers are integral to ecosystem function, serving as the base of the food web (Vadeboncoeur and Power 2017, Kendrick et al. 2019), and are subject to the same global change stressors as higher-order consumers (Kominoski and Rosemond 2012).

Despite the gaps in flow ecology relationships for primary producers (hereafter "producers"), there has been considerable research on the physiology and morphology of some groups, particularly algae (Wehr et al. 2015), and the responses of certain producers to environmental stimuli such as water velocity, nutrients, light, and herbivory (Asaeda and Son 2000, Arnon et al. 2007, Hill et al. 2011). Prior research has shown substantial variability in producer biology — such as differences in growth form, growth rate, and reproduction (Allan et al. 2021) — both within (e.g. stalked versus prostrate algal growth) and among (e.g., benthic algae versus macrophytes) groups (Steinman et al. 1992a). These differences in morphology and physiology have been documented as drivers of variability in producer responses to local conditions (Biggs et al. 1998, Riis and Biggs 2001, Hart et al. 2013, Rott and Wehr 2016). For

example, algal growth and instantaneous water velocity are often correlated: adnate and prostrate algal forms may be found in high water velocity areas, while stalked and filamentous algae are usually limited to moderate and low velocity areas (Biggs 1996b). However, researchers know considerably less about how these producer traits and water velocity dynamics play out over longer time periods and at larger spatial scales (but see Power 1992, Power et al. 2008).

Variability in the resistance and resilience of different producers to flow conditions, along with any accompanying producer interactions, is particularly important to consider in mid-sized open-canopy rivers where primary production can account for a substantial portion of the base of food webs and multiple producer groups often co-exist (Vannote et al. 1980). Even systems that are predominantly heterotrophic at an annual scale may experience seasonal periods of high primary production (Carter et al. 2024). Mid-sized river systems also provide valuable ecosystem services, not least of which is municipal drinking water. Human use of these aquatic systems can affect local and downstream hydrologic conditions (Poff and Zimmerman 2010b). These human activities complicate, and often exacerbate, the effects of climate change, particularly by increasing the frequency, duration, and severity of low-flow events (Core Writing Team 2023). Thus, to adequately predict how mid-sized systems will respond to hydrologic change, researchers need to establish flow ecology relationships of how diverse producer groups will respond to natural and managed flow conditions.

While prior literature provides some understanding of flow ecology relationships of higher order consumers, there is still an ongoing need to identify the mechanisms underlying organism-specific relationships and to evaluate and quantify how these mechanisms affect ecosystem functions such as primary productivity and stream metabolism (Bernhardt et al. 2022, Blaszczak et al. 2023). We propose that the effects of hydrology on primary-producer driven

functions are mediated by differential responses of distinct producer groups. We hypothesize that producers differ in their resistance and resilience to events like floods and droughts, and these differences explain patterns in whole ecosystem processes such as stream metabolism. The first step in testing this hypothesis is to identify how antecedent flow conditions affect the biomass and distribution of diverse producer groups.

Here we ask how antecedent flow conditions, focusing on low-flow and high-flow disturbances, affect the biomass and distribution of multiple producer groups in a mid-sized, open-canopy, temperate river. We address this question by surveying producers comprehensively within one river reach, measuring the biomass of a submerged vascular plant (*Podostemum ceratophyllum*), benthic biofilms containing algae (hereafter "biofilm"), and filamentous algae. We test producer-specific flow ecology hypotheses by modeling the biomass of each group as a function of antecedent flow conditions at different time scales. Of the three groups, *Podostemum ceratophyllum* (hereafter "*Podostemum*") provides a particularly interesting opportunity to examine a flow ecology relationship that likely has significant implications for ecosystem function. *Podostemum* plays a foundational role (sensu Ellison 2019) in supporting production of stream consumers in mid-sized rivers (Rosi-Marshall and Wallace 2002, Hutchens et al. 2004) and is currently the subject of conservation concerns about declines in its abundance (Wood and Freeman 2017). Understanding flow ecology relationships, especially those involving foundation species, is essential to guide management decisions that support healthy ecosystem functioning and in turn, the ecosystem goods and services that support society.

METHODS

Site Description

We conducted our research in Athens, GA, USA, on a segment of the Middle Oconee River, a 6th-order tributary of the Altamaha River basin that flows through the Piedmont physiographic province (Figure 2.1). This river has been the focus of numerous studies of benthic communities and hydrologic patterns for over half a century (Nelson and Scott 1962, Grubaugh and Wallace 1995, Pahl 2009b, McKay 2014, Katz et al. 2015, Rack 2025) and provides a context of common management issues, including land use change, water extraction, and flow regulation that have resulted in periodic extreme low flows. Our study section of the Middle Oconee is largely an open-canopy system with a sequence of sandy runs and cobble and bedrock shoals.

Field Methods

From June of 2016 to August of 2018, we quantified primary producer standing stock biomass. Although bryophytes and a red alga (*Lemanea* sp.) were occasionally observed in our samples, we focused on the three consistently dominant producer groups: *Podostemum*, biofilm, and filamentous algae. Quantifying aquatic vascular plant biomass requires mass measurements rather than chlorophyll *a* (Chl-*a*) extractions (Bowden et al. 2017), so we used ash-free dry mass (AFDM) to compare biomass of the three dominant producer groups. However, we also quantified biofilm biomass as Chl-*a* to assess only the algal components. To determine whether there was significant mass or algal content of seston, we took grab samples from the water column. We refer to the mass of biofilm and seston as biofilm AFDM and seston AFDM, respectively. Likewise, we refer to the algal content of biofilm and seston as biofilm Chl-*a* and seston Chl-*a*. We sampled monthly whenever the river was wadable (≤ 11.33 m^3 s^{-1}). This

resulted in 19 sampling events, spanning one winter and one spring season, three summer seasons, and two fall seasons. We established 7 permanent transects to capture the diversity of velocity, light, and bed substrate found within the stream (Figure 2.1). Transects 1–3 were established below a municipal water intake and a first-order tributary, in what we call the 'lower shoal', characterized by a mix of bedrock and coarse substrates (primarily cobble and gravel). Transects 4–6 were established above the tributary within a sandy run, though transects 5 and 6 included rock outcroppings. Transect 7 was the uppermost transect, established on the river left portion of an island in what we call the 'upper shoal', which consisted solely of bedrock.

We conducted random stratified sampling (Figure 2.1). For each sampling event, we established five equal blocks along the wetted width of each transect to ensure representative sampling of habitats across the stream (particularly shaded edge vs. open canopy). While the transect line was permanently established, the specific location of each block varied from month to month as river flows changed the wetted width. Each block extended 5-m upstream and 5-m downstream from the transect line. We took one destructive sample per block per permanent transect per sampling event (n = 35 per sampling event), with the exception of June 2018 when only the lower shoal transects were sampled (n = 15). To prevent resampling a location, we randomly generated non-repeating coordinates for every sampling location for the entire season.

Prior to sampling producer biomass, we measured water depth and instantaneous water velocity and recorded the benthic substrate category as bedrock or other fixed rock (boulders or large cobbles that were not readily removable), large removable rock (cobble), small removable rock (gravel), or sand and soft substrate. We determined the appropriate field sampling method based on the primary bed substrate. For bedrock and other fixed rock, we used a razor blade and a modified Surber sampler known as a t-sampler (Wood et al. 2019) to remove all producer

material within a 102-cm^2 opening. Because removed material was caught within a 250-µm mesh sleeve, the t-sample method only reliably captured larger producer material. All other sampling methods, however, were able to capture both fine and coarse particles. To sample large removable rocks, we used a razor blade to scrape any organic material within a 29-cm^2 template and then brushed and rinsed the template area to remove any remaining fine particulate material in a slurry. For small rocks, we used the t-sampler to collect surface gravel from a 102-cm^2 area of the streambed. For soft sediment and sand, we used a PVC pipe corer with an opening of 45-cm^2 to collect a sample volume of approximately 227-cm^3. Producer material was not removed from t-samples of small rocks (TSR) or core samples of sand and soft sediment until laboratory processing. For water column samples, we collected a 1-L grab sample aggregated from three points across the wetted channel, at two locations of the stream reach (below and above the tributary/municipal intake). All biomass samples were refrigerated and processed in the laboratory within 48 hours of the sampling event.

We collected data on the physical and chemical properties of the water column at each sampling event and then at additional site visits to increase sample size. Both above and below the tributary/municipal water intake, we collected an unfiltered 60-ml water sample, aggregated in the same fashion as the biomass grab samples, to measure total nitrogen (TN) and total phosphorus (TP). We also collected a filtered (0.7 µm glass fiber filters (GFF)) 60-ml water sample to measure dissolved nitrogen (NH_4-N + NO_3-N) and dissolved phosphorus as soluble reactive phosphorus (SRP). We measured turbidity, water temperature, dissolved oxygen, and conductivity at the same locations. All water samples were frozen within 24 hours for later analysis.

Laboratory Processing

We processed samples according to the method of collection to determine the biomass of *Podostemum* and filamentous algae as large particulate matter (> 500 µm) and benthic biofilm as fine particulate organic matter (FPOM; which we define here as < 500 µm and > 0.7 µm). . We rinsed t-samples over nested 500-µm and 120-µm sieves. Larger producer material was caught in the 500-µm sieve and FPOM in the 120-µm sieve. We rinsed template samples over a 500-µm sieve to collect larger material and then collected the resulting slurry to filter FPOM. For TSRs, we placed the sample in a tray and used a razor blade to collect larger material from any of the rocks. We then brushed and rinsed any rocks larger than 23-mm^2 and collected the resulting slurry to filter FPOM. We dumped core samples into a bucket, elutriated the contents, and first collected any larger material. If any small rocks were present, we followed the protocols for TSR but dumped the resulting slurry back into the bucket. Finally, we elutriated the remaining contents of the bucket and took a subsample to filter FPOM. We dry-weighed the entirety of any larger material found in each sample, unless it was too large to fit into the weigh tins, in which case we subsampled. We then combusted the samples or subsamples at 500° C and reweighed them to determine AFDM (g m^{-2}). FPOM from water samples, slurries, or 120-µm sieve contents suspended in tap water was filtered, or subsampled and filtered, through pre-ashed and pre-weighed 0.7-µm GFFs to determine AFDM. Separately, water column samples and slurries were filtered, or subsampled and filtered, through 0.7-µm GFFs to freeze for Chl-*a* quantification. Since t-samples excluded material finer than 120-µm, they were not analyzed for Chl-*a*.

For benthic samples, we used the area of collection to calculate Chl-*a* per mg-m^2 or AFDM as g per m^2. For water column samples, we calculated Chl-*a* per ml and AFDM as g per ml. We began quantifying Chl-*a* using the hot-ethanol extraction and spectrophotometer methods

described by Sartory and Grobbelaar (1984) and modified by Parker et al. (2016) to use a 45-minute post-acidification time in place of 90-seconds. Due to high sample sizes, we were unable to continue using a 45-minute post-acidification time, so starting in August of 2016, we used a post-acidification time of 90 seconds and applied the correction factor described in Parker et al. (2016) to account for under-acidification. Acid with double the concentration was accidentally used for December 2017 samples. We developed a correction factor for these samples by running subsamples under both concentrations and regressing the correct concentration (100 µL) against the doubled concentration (200 µL) to yield a relationship of $y = -0.85267 \times -0.06989$ ($R^2 = 0.86$).

Nutrient analysis of water samples was conducted by the University of Georgia Center for Applied Isotope Studies. Concentrations of DIN (NH_4-N + NO_3-N) and SRP (PO_4-P) were measured via continuous flow colorimetry of the filtered water samples with an Alpkem Rapid Flow Analyzer 300. Following acid digestion of the unfiltered water samples, total N and P concentrations were measured using the same device.

Evaluating Patterns in the Timing, Location, and Substrates Associated with Producer Biomass

We used R for all data preparation, analysis, and modeling (R Core Team 2025). We aggregated biomass by month and examined patterns in mean monthly biomass across the entire reach and for transects grouped by the following river segments: lower shoal, run, and upper shoal (Figure 2.1). For benthic biomass measured as AFDM — *Podostemum*, filamentous algae, and biofilm — we also examined the proportion each producer comprised of each month's mean biomass across the entire reach and river segment, as well as the proportion each producer comprised of the mean monthly biomass per substrate type across the entire reach.

Predicting Biomass and Testing Producer-Specific Flow Ecology Hypotheses

The core of our analysis was to test hypotheses of how high and low flows affect the biomass of each producer (Table 1). We quantified varying degrees of 'high' and 'low' flow based on exceedance probabilities of the historic flow record, up to the time of our study, and included any relevant metrics currently used in policy (Table 2.2). These hypotheses were based on 1) mechanisms with existing empirical support, 2) mechanisms that have been documented for a similar producer, and 3) mechanisms previously hypothesized in existing literature, but not yet demonstrated (e.g., Suren and Riis 2010).

The hypothesized mechanisms, in part, were based on producer growth form, especially susceptibility to high-flow conditions. We hypothesized that high flows via scour and shear stress would negatively affect producers that are more loosely adherent to substrates and/or have higher accumulation, such as macrophytic filamentous algae or larger quantities of biofilm. We expected a producer like *Podostemum*, which is more tightly adherent to substrates, to respond positively to high flows due to increased nutrient supply and protection from herbivory. In contrast, low flows can result in greater susceptibility to herbivory for some producer groups, as has been found for *Podostemum* (Wood et al 2019), as well as decreased nutrient supply or competition from other producers that thrive in lower flow conditions. Thus, we hypothesized that low flows would negatively affect producers.

We conducted ordinary least squares linear regression modeling of the date-specific mean and maximum biomass for the following producer categories: *Podostemum*, filamentous algae, biofilm Chl-*a*, biofilm AFDM, and seston AFDM. Because samples showed weak autocorrelation (Pearsons' r = -0.19 to 0.18), we treated sampling dates as independent. Although we observed bryophytes and the red alga *Lemanea*, we did not collect sufficient samples to

model their dynamics. Similarly, we were unable to model seston Chl-*a* as values were near zero.

We used instantaneous discharge data from a USGS gage (02217500) located immediately downstream from 01 January 2016 to 29 August 2018 to calculate metrics for antecedent flow. Due to the sample size (n = 18 or 19 when June of 2018 is included), we limited models to one or two explanatory variables. Because of the potential for correlation for variables within the 'high' and 'low' flow categories, we considered the variables within each category exclusive to one another; a model could only have one low-flow and one high-flow variable as opposed to two high-flow variables or two low-flow variables. Pearson correlation coefficients for variables in reported models were less than 0.5. Subject to this restriction, we ran all possible combinations of one or two predictor variables for each of the biomass response variables, including but not limited to the variables related to our hypotheses.

We ranked models using the Akaike information criterion (AIC) (Burnham and Anderson 2002) and included all models with Δ AIC ≤ 2 as "top models" for evaluating support for our hypotheses (Table 2.2). We considered models to have a "dominant variable" when explanatory power (i.e., R^2) of the model with that variable as a single predictor was: 1) at least 70% as good at explaining biomass variability as the best model and 2) at least twice as strong as the model with the other variable as the only predictor.

We considered a hypothesis to be supported if both the direction of the relationship and timeframe for any of the variables representing the hypothesis was found in one of the top models. We considered a hypothesis to be partially supported if the direction of the relationship for any of the variables representing the hypothesis was found in the top models, but the timeframe was different. A hypothesis was not supported if we did not find any variables

representing the hypothesis with the predicted direction of the relationship in one of the top models. As such, "not supported" can mean we failed to find the predicted relationship in one of the top models or that we found the opposite relationship in one of the top models.

RESULTS

Ambient Conditions During the Study Period

Chemical and physical properties of the reach during the study period were typical of mid-sized rivers with moderate nutrient inputs (Table 3). Compared to unimpacted rivers, total and dissolved N concentrations were elevated, while P concentrations were low (Scott et al. 2002, Manning et al. 2020). Stream temperatures captured seasonal highs (maximum temperature for the year), and pH was between 6.64 and 9 (Table 3). While we were able to opportunistically sample some high-flow events, our turbidity measurements are likely biased low since most of our collections occurred during relatively low flows. The most extreme hydrologic events occurred in 2016, with the highest flow event during the winter preceding sampling. The lowest flow occurred during a state-declared drought the following fall (Figure 2.2).

Patterns in the Timing, Location, and Substrates Associated with Producer Biomass

Biomass of the different producer communities varied throughout the study period, displaying producer-specific temporal and spatial patterns (Figure 2.3). During the summer (Jul. and Aug.) of 2016, we found high biomass of all four main benthic components — *Podostemum*, filamentous algae, biofilm Chl-*a*, and biofilm AFDM — in at least one river segment (Figure 2.3). The July 2016 summer spike was *Podostemum*'s highest biomass for the entire study period and was driven by samples in the lower shoal. Peak filamentous algal biomass also occurred

during this time as a green alga (genus *Rhizoclonium; Conn and Rosemond, personal observation)* bloomed across the entire reach. High biofilm Chl-*a* in the summer of 2016 rapidly decreased and then peaked again in late 2016 (Nov. and Dec.) with a diatom bloom (genus *Aulacoseria; Conn and Rosemond, personal observation*). With the exception of some *Podostemum* variability in the upper shoal, biomass of *Podostemum*, filamentous algae, and biofilm Chl-*a* in 2016 was high in comparison to biomass in 2017 and 2018.

In contrast to the other groups, biofilm AFDM was more variable over time due to frequent large fluctuations in standing stocks in the run. Biofilm AFDM was also positively related to biofilm Chl-*a* ($R^2 = 0.31$, p-value < 0.001), which included all samples except t-samples (data not shown). Biofilm AFDM and Chl-*a* spiked during the summer of 2016, but the highest overall biomass occurred in the run during the summer of 2017. While seston AFDM also spiked during the summers of 2016 and 2017, seston AFDM and biofilm AFDM were not correlated ($R^2 = 0.005$, p-value = 0.79), nor did we find any lagged increase of biofilm AFDM after an increase of seston AFDM (Figure A1). We found little evidence of algae in the water column as indicated by negligible levels of seston Chl-*a* (<0.00001 mg m^{-2}).

Of the producer biomass that was measured as AFDM*, Podostemum* dominated in 56% of months sampled, while biofilm AFDM dominated in 33% of months sampled (Figure 2.4). In the remaining 11% of sampling months, biomass was similar across producer groups. These overall patterns can largely be explained by peaks in either *Podostemum* or biofilm AFDM within the habitat each respectively dominated (Figure 2.4). *Podostemum* dominated the shoals while biofilm AFDM dominated the runs. Filamentous algae made up the least amount of biomass across river segments, with the exception of the *Rhizoclonium* bloom in June and July of 2016 when filamentous algal biomass exceeded *Podostemum* in the run (Figure 2.4).

Patterns in substrate association mirrored the patterns found by location, which is consistent with established expectations of substrates associated with different river segments. *Podostemum* biomass dominated rocky substrates, which were found in the shoals, while biofilm AFDM dominated sand and soft sediment, which were found in the run (Figure 2.5). Biofilm AFDM on bedrock and fixed rock could have been underestimated due to our inability to brush and/or filter all fine particulate material with the t-sample method. However, *Podostemum* still overwhelmingly dominated all hard substrate types even with a greater contribution from biofilm AFDM on the removable rock substrates where FPOM was comprehensively captured. Filamentous algae never dominated a habitat and was more evenly distributed amongst substrate types than other producer groups (Figure 2.5). While we did not capture biofilm Chl-*a* on bedrock or fixed rock, the mean biomass of biofilm Chl-*a* on soft substrate nearly tripled the combined biomass on small and large removable rocks for the majority of months we sampled (Figure A2).

Predicting Monthly Standing Stocks at the Reach Scale and Hypothesis Testing

We were able to predict both mean and maximum producer biomass with antecedent flow conditions, with varying degrees of strength (Table 2.4). Antecedent flow conditions were strongly correlated with mean and maximum biomass of *Podostemum* (R^2 = 0.87, 0.76; Figure 2.6 A,B respectively), filamentous algae (R^2 = 0.73, 0.73; Figure 2.6 C,D), and biofilm Chl-*a* (R^2 = 0.88, 0.86; Figure 2.6 E,F). However, when substrate was considered (Table A3), flow was a poor predictor of mean and maximum biofilm Chl-*a* on hard substrate (R^2 = 0.29, 0.36) while remaining a strong predictor on soft substrate (R^2 = 0.88, 0.86). The relationships between flow and biofilm AFDM (R^2 = 0.44, 0.45; Figure 6.2 G,H) and flow and seston AFDM (R^2 = 0.48,

0.59; Figure 2.6 I,J) were weaker. For benthic producers, antecedent flow conditions were more strongly correlated to mean biomass than maximum biomass while the opposite held for seston biomass.

A portion of the models included a dominant flow variable, and apart from the model predicting maximum biofilm AFDM, this dominant flow variable was consistently a low-flow variable. Less severe long-term minimum flows drove increases in maximum *Podostemum* biomass (single variable $R^2 = 0.54$) and mean and maximum filamentous algae biomass (single variable $R^2 = 0.55, 0.53$). Mid-term extreme low flows drove increases in both mean and maximum biofilm Chl-*a* (single variable $R^2 = 0.75, 0.81$). Mid-term high flows drove decreases in mean biofilm AFDM (single variable $R^2 = 0.36$), though the relationship was moderate at best with the best model explaining 44% of maximum biomass (Table 2.4).

Notably, we excluded both biofilm and seston AFDM from hypothesis-testing as biofilm AFDM was not strongly correlated to biofilm Chl-*a* (i.e., the algal components) and we found no detectible algal content of seston (i.e., negligible seston Chl-*a*). However, for the three producer groups for which we tested hypotheses — *Podostemum*, filamentous algae, and biofilm (Chl-*a*) — we found full support for the majority of hypotheses, including at least one effect of high flows and low flows for each producer (Table 2.5). For producer means, mid-term flow conditions were important for biofilm Chl-*a* and long-term flow conditions for *Podostemum*, while both short- and long-term flow conditions were important for filamentous algae. More specifically, biofilm Chl-*a* appeared to be positively affected by mid-term extreme low flows and negatively affected by mid-term events of extreme high flows. Filamentous algae were negatively affected by long-term low flows, but high flows had both positive and negative effects depending upon the timeframe. Short-term high flows appeared to have a negative effect while

long-term high and extreme high flows a positive effect. *Podostemum* was positively affected by long-term high flows and negatively affected by long-term extreme low flows. Overall, our hypotheses were similarly supported by the model results of producer maximums (Table 2.5). The exceptions were how biofilm Chl-*a* and *Podostemum* responded to short-term high flows. Maximum biofilm Chl-*a* was negatively affected by short-term events of extreme high flows (as opposed to mid-term events with mean), which fully supported our hypothesis, but maximum *Podostemum* biomass was negatively affected by short-term high flows, which was not an effect we hypothesized.

DISCUSSION

Overview

We found that antecedent flow conditions, both low and high flows, were a strong driver of the biomass and distribution of primary producers in the Middle Oconee River. We also found support for most of the producer-specific hypotheses, which were grounded in both evidence and theory of how producer traits may shape responses to water velocity and disturbance. We predicted, and found, both overlap and variability in producer responses at the larger scale of discharge (as opposed to water velocity). Our models indicated that *Podostemum* and filamentous algae were negatively affected by longer periods of drought and low flows, while benefiting from longer periods of high flows. However, filamentous algae and biofilm were negatively affected by shorter term extreme high flows, and biofilm was the only group positively associated with low flows. Data from the 2016 season also suggested that both drought and extreme high-flow events could cause producer-specific peaks in biomass. Current theory — that organismal traits can determine resistance and resilience to flow conditions — is based largely on research conducted at smaller spatial scales and across shorter timeframes, with few

studies including macrophytes and many studies occurring under controlled experimental conditions. Our findings provide empirical evidence that organismal traits can determine resistance and resilience to flow conditions for many producer groups at spatial scales and timeframes applicable to management and policy decisions. Understanding these relationships at these scales strengthens our ability to predict how producer communities will respond to changing flows, and thus different climate and management scenarios. Further, it is a key step in determining the mechanisms by which different scenarios affect ecosystem function.

Temporal Patterns: Disturbance vs. Stability

The multi-year nature of this study allowed us to capture and compare producer biomass during two major forms of natural disturbance – floods and droughts – to periods of relative stability. Peaks in monthly biomass in 2016 suggest that sustained drought and extreme high flows have strong producer-specific effects, as increased biomass of different producers occurred either simultaneously or in lagged proximity to both extreme flow events. In contrast, the 2017 and 2018 conditions of relative hydrologic stability corresponded to lower and less variable biomass across producers.

Antecedent flow conditions during the winter of 2015-2016 included the most extreme high-flow event recorded during the study period, which fell within the 90th percentile of all flows recorded since 1911 – a common threshold for floods (Rahimi et al. 2021). Maximum biomass of both *Podostemum* and filamentous algae occurred in the early part of the summer following the winter high flows. Long-term research in the Eel River system in California suggests that the winter high flows could be indirectly responsible for the peaks we observed in producer biomass via a top-down release of consumer pressure (Power et al. 2008). Power et al. (2008) found that winter flooding decreased consumer densities, which released herbivory

pressure and resulted in blooms of the filamentous algae *CIadophera* sp.in late spring and early summer. Given the susceptibility of *Podostemum* (Wood et al. 2019) and *Rhizoclonium* sp. to herbivory, reduced herbivory is a plausible mechanism by which the higher winter flows could have had an indirect effect on producer biomass in the warmer growing season. Further, depending upon the identity of the producer, and stream consumers, these blooms can negatively or positively affect the stream environment. Edible algae can be a large portion of the trophic base for stream consumers and can be a source of carbon and oxygen for other organisms and processes (Rüegg et al. 2020), but large blooms left unconsumed can lead to inhospitable conditions as they decompose and result in low or even depleted oxygen concentrations. Given *Podostemum*'s foundational role in stream environments, increased growth is likely a benefit, but it is unknown whether, like some algae, there are conditions under which growth is detrimental. In more general terms, these results suggest that floods have the potential to facilitate accumulations of primary producers that could have far-reaching positive or negative impacts depending upon producer identity, and potentially consumer dynamics.

While extreme high flows corresponded to a lagged increase in *Rhizoclonium* and *Podostemum* biomass, the fall drought of 2016 corresponded to an increase in biofilm biomass (measured as Chl-*a*) dominated by *Aulacoseria*. Importantly, only wetted areas of the benthos were included in this study, so our biomass means excluded zeros from dried areas within the stream. While there is a notable gap in research on the effects of both human-induced and naturally occurring low flows and drought in non-arid environments, especially for non-headwater perennial streams (Lake 2003), existing research suggests that the increase in biofilm biomass during the fall drought could also be a producer-specific effect of hydrology. In a 2018 meta-analysis, human-induced water stress resulted in an average of 3.3-fold increase in biofilm

biomass, measured as Chl-*a* (Sabater et al. 2018). Reduced flow velocity can lead to indirect and direct effects on algal biomass by increasing water clarity (indirect) and decreasing certain hydraulic stressors such as scouring (direct), which have been shown to limit algal growth (Biggs et al. 1999, Bernhardt et al. 2018). With an increase in water clarity and a decrease in water depth due to reduced water volume, more solar radiation can make it to the benthos, resulting in greater photosynthetic potential. And while severe or extreme droughts can eventually lead to decreased nutrients and increased herbivory (Dahm et al. 2003), less severe drought could lead to more favorable local conditions for algal accumulation, such as increased temperature and solar radiation (Paerl and Huisman 2008, Salmaso and Braioni 2008). Even in the face of herbivory, many diatom species remain highly productive (Vadeboncoeur and Power 2017). Decreased whole stream turbidity and mean water depth at the sampling locations does suggest that local conditions in 2016 were more favorable for producer growth. Thus, while floods, depending upon the season, may counterintuitively facilitate increases in certain producer groups via a release of herbivory pressure, drought may lead to increases in others. Increased hydrologic variability due to climate change likely means more years like 2016 with little chance that the consequences to different stream types (e.g., biome, order) will be uniform. In fact, Hosen et al. (2019) found that the effect of drought on primary production (GPP) in a temperate watershed was greater in larger river systems than in headwater systems, and attributed part of the increased primary production to an increase in producer biomass.

Spatial Patterns: Location as a Determinant of Identity and Biomass

The spatial patterns of producer biomass we observed over the study period are consistent with prior research that indicates stream location is an important determinant of producer biomass and identity. We found that *Podostemum*, which has been found to thrive in high

velocity areas due in part to the exclusion of herbivory (Wood et al. 2019), dominated shoal ecosystems while biofilm (measured as AFDM) dominated the lower velocity runs. Some algae, lacking the rooting structure *Podostemum* exhibits, is loosely adhered and more susceptible to scouring from high velocities and thus is better suited to lower velocity areas.

The distinction of shoal versus run corresponds to differences in local conditions, namely substrate, depth, and water velocity. These local conditions determine which producers can or cannot exist and/or thrive in each location (Biggs 1996d, Burkholder 1996, Hart and Finelli 1999), even at a sub-stratum scale (Murdock and Dodds 2007), and they shape how producers are affected by more extreme hydrologic disturbances. The subsidy-stress dynamics of a given location also have implications for how each producer contributes to whole stream processes (O'Donnell and Hotchkiss 2022). In a 2022 study on the resistance and resilience of stream metabolism to high-flow disturbances, O'Donnell and Hotchkiss (O'Donnell and Hotchkiss 2022) attributed the differences in ecosystem respiration and primary production responses to variable flows to differences in the energy sources and locations of autotrophs and heterotrophs.

Producer-specific Responses

The regression models predicting *Podostemum*, biofilm, and filamentous algae were consistent with our analysis of temporal patterns. Each analysis indicated both low flows and high flows were important determinants of producer biomass, and producer-specific traits appeared to determine which model variables best predicted each producer.

Podostemum

The top model for *Podostemum* mean biomass included longer-timeframe variables of high and low flows. Macrophytes, with significantly more robust plant structure than algae, require more growing time, which means there is a larger window of time — and corresponding

flow conditions — influencing plant growth. Our finding that the percentage of time spent above the long-term mean flow positively correlated with *Podostemum* biomass is consistent with our hypothesis that *Podostemum* would be positively affected by mid or long-term flows. However, we found that minimum flows over a longer time-period were the most important variable for predicting biomass. Our models support our hypothesis that antecedent drought severity negatively affects *Podostemum* growth. The specifics of *Podostemum* physiology – the relatively long regeneration time of an aquatic plant - could mean that even one low-flow event allowing increased herbivory or desiccation could have persistent negative effects on biomass.

Filamentous Algae

The top model for mean filamentous algae included a long-term high-flow variable that was positively correlated with biomass, while another model (which was nearly equivalent, in terms of support) included short-term high flow that was negatively correlated with biomass. Both findings demonstrate the relationships we hypothesized between high flows and filamentous algae biomass. Winter elimination of herbivores could have allowed for greater filamentous algae growth during the summer and fall of 2016, while the negative effect of short-term high flows might be due to shear stress in drag and/or sediment scour, effects demonstrated thoroughly in past studies (Biggs et al. 2005). Either or both of those mechanisms could have been occurring throughout the study period, but during the bloom of 2016, large quantities of filamentous algae, with extensive surface area, would have made the producer highly susceptible to drag.

While filamentous algae and diatom blooms are not uncommon for systems experiencing elevated nutrients from agricultural inputs, the filamentous algae bloom in the summer of 2016 occurred during nutrient conditions similar to those of the following years in which no algal

blooms occurred. Thus, current nutrient conditions do not explain the increase in filamentous algae, though prior exposure to elevated nutrients could have played a role. Unfortunately, we were not sampling nutrients before the bloom, so we could not test this hypothesis.

Biofilm

Unlike *Podostemum* and filamentous algae, biofilm Chl-*a* was best predicted by mid-term high and low flows; the top models included 90-day variables. The top biofilm Chl-*a* models also included a variable that measured a single event– the largest change in flow– as opposed to a percentage of time the stream experienced flow conditions, perhaps indicating that a single event can have lasting effects. The largest change in daily flow within 90-days (also 30-days in the case of maximum) of the sampling event (to predict mean vs. maximum biomass respectively) was negatively correlated with biofilm Chl-*a*. This was consistent with our hypothesis that high-flow events would negatively impact the algal components of biofilm. Unlike *Podostemum* with its hearty root structure, some biofilm components can be loosely adherent to substrate. These loosely adherent algae have been found to dominate low flow habitats (Cardinale 2011) and experience reductions in biomass from shear stress and sediment scour in higher water velocities (Francoeur and Biggs 2006). Thus, even if tightly adherent components of biofilm were somewhat resistant to high flows, reductions in loosely adherent components may explain the negative relationship we found between extreme high flows and biofilm Chl-*a*. Consistent with this and the established ability of biofilms to persist, even thrive, in lower flows through niche differentiation and shifts in community composition (Battin et al. 2016), we hypothesized that mid-term low flows would allow for the accumulation of biofilm biomass. This was supported by our finding that extreme low flows over a 90-day period was positively correlated with biofilm Chl-*a*. This correlation was likely driven by the proliferation of the diatom *Aulacoseria*

in biofilm that accrued during the fall 2016 drought. Interestingly, the low-flow variable was the percentage of days with extreme low flows. This indicates that nutrient supply was not an issue because while nutrient delivery generally decreases as flow decreases, we would expect to see a negative relationship with extreme low flows if nutrient supply were a limiting factor.

Notably, the strong relationships between flow and biofilm Chl-*a* only held for soft substrate, which on average had almost triple the combined biomass of biofilm on small and large removable rock. Our sampling methods did not reliably capture biofilm on bedrock or fixed rock (neither AFDM nor Chl-*a*). Thus, we do not know if the weak predictive relationship between flow and Chl-*a* on small and large removable rock is true across all hard substrate types (i.e. removable and fixed) or only true for combined removable rocks. In addition, the predictive relationship between flow and Chl-*a* on soft substrate was more heavily influenced by individual events than other producers.

The complex relationship between flow and biofilm AFDM reflect its mixed algal and detrital composition. Biofilm AFDM decreased with mid-term high flows, consistent with the Chl-*a* response, but increased with short-term higher-than-average flows, which could be the result of a greater detrital deposition from pulses of exogenous materials that masked the negative impact of high flows on algae. Maximum biofilm AFDM appeared to be driven by the short-term higher flows and low/extreme low flows within a longer time frame, a combination which facilitates both accumulation of algal biomass and retention of deposited detrital material.

In contrast, biofilm AFDM exhibited a divergent response to short-term low flows, depending upon the flow variable: a higher minimum flow within 7-14 days increased AFDM, whereas a high frequency of low-flow days within 7-30 days decreased AFDM. These results appear to be in conflict but could indicate different types of low flow events (e.g., a single, more

extreme low flow event vs. continued low flows) and/or interactions with high flows during the same time period. For instance, the top model has both a positive relationship with the proportion of flows above the 50th percentile of flows and the proportion of flows below the 25th percentile of flows. This could indicate a beneficial sequence where slightly higher flows provide detrital material and subsequent lows flows allow the material to settle. Thus, while mid-term and long-term low and extreme low flows appear to positively affect biofilm AFDM, more research is needed to clarify the impact(s) of short-term low flows.

Seston

We did not observe detectable algal content in our water column samples. While this result is consistent with Nelson and Scott's (1962) findings in the same system over half a century ago – that phytoplankton played an insignificant role – it contrasts with more recent studies of other mid-sized systems. Using 5 years of phytoplankton data from National Ecological Observatory Network sites across the US, Peipoch et al. (2025) found consistent patterns in the relationships between suspended Chl-*a* and discharge across a range of stream sizes. Not only did Peipoch et al. (2025) confirm the presence of phytoplankton, they were able to quantify the different contributions from benthic and planktonic origins. Additionally, using water column mesocosm data from 3 midwestern US watersheds, Reisenger et al. (2015) demonstrated that phytoplankton in mid-sized streams can be a significant contributor to stream metabolism and nutrient uptake (e.g., Reisinger et al. 2021). The negligible Chl-*a* levels in our study could be due to many factors, including but not limited to biological constraints or limitations of our sampling methods. Perhaps the volume of water we sampled wxas insufficient or the timing of sampling missed critical periods of activity. There is also the potential that ecological factors – P limitation as a demonstrated example from other systems (Klausmeier et

al. 2004) – constrained planktonic (e.g., Roeder 1977) and benthic algal contributions (e.g., Burrows et al. 2020). However, we consider P limitation, specifically, to be an unlikely explanation for our results given that the P concentrations of our samples, while low compared to impacted systems, were not necessarily low enough to inhibit algal growth.

Model Applicability

Capturing the responses of naturally occurring and morphologically distinct producers to a range of hydrologic events, including a notable flood and state-declared drought, increases our confidence about the relationships we modeled and their ability to inform future predictions of comparable systems. However, some of the flow relationships, as was the case with biofilm on soft substrate, were more heavily influenced by individual events than others, which highlights the importance of even longer-term datasets in confidently predicting the impacts of flow extremes.

CONCLUSION

The variety of producers we studied — vascular plants, filamentous algae, and biofilms containing a variety of organisms — is a good representation of producers in a mid-sized, open-canopy system. A growing body of literature also indicates the important role of macrophytes in stream processes and services (Alnoee et al. 2021, Thomaz 2021). While differing in traits from most other macrophytes, *Podostemum* is ubiquitous in many eastern areas of the United States (US) and plays an important role as a foundation species (Hill and Webster 1984, Hutchens et al. 2004, Wood and Freeman 2017). Importantly, *Podostemum* population declines have been recorded across its eastern US range, and various environmental stressors, such as sedimentation, low flows, and pollutants, have been implicated as potential causes (Wood and Freeman 2017). Our results demonstrate that increasing severity of low flows can negatively impact *Podostemum*

biomass. In contrast, the filamentous algae and biofilm blooms we observed during 2016 can be a common, sometimes problematic, occurrence for systems that experience low-flow conditions and elevated nutrients (Matthaei et al. 2010). Determining how biomass declines (as with *Podostemum*) or increases (as with *Rhizoclonium* and *Aulacoseria*) affect ecosystem function is an important next step in understanding the implications of these modeled relationships.

TABLES

Table 2.1: Hypothesized mechanisms by which hydrology may affect producer groups in the Middle Oconee River, Athens, GA. For timeframe, short-term refers to 7 – 30 days, mid-term refers to 90 days, and long-term refers to 180 days.

Producer group	Direction of relationship	Timeframe	Hydrologic Scenario	Mechanism	Example References
Podostemum	-	Mid- or long-term	Extreme low flows/drought	Desiccation	Pahl 2009
	-	Mid- or long-term	Low flows	Consumption by terrestrial and aquatic consumers	Parker et al. 2007
	+	Mid- or long-term	High flows	Protection from current herbivory	Wood et al. 2019
Filamentous algae	-	Mid-term	Low flows	Epiphyte competition	Stevenson and Stoermer 1982**
	-	Short-term	Extreme high flow event(s)	Shear stress/drag	Biggs and Thomsen 1995
	-	Short-term	Extreme high flow event(s)	Sediment scour	Francoeur and Biggs 2006
	+	Mid-term	High flows	Removal of herbivores or epiphytes	Power and Stewart 1987
	+	Long-term	Extreme high flow event(s)	Removal of next season herbivores	Power et al. 2008**
Biofilm	-	Mid-term	Extreme low flows/drought	Desiccation or insufficient nutrient delivery	Mosisch 2001
	-	Short-term	High flows	Sediment scour & shear stress	Francoeur and Biggs 2006
	+	Short- or mid-term	Low flows	Accumulation	Sabater et al. 2018
Seston	-	Short-term	Short-term drying	Lack of immigration	Sommer et al. 2004
	-	Mid-term	High flows	Export & dilution	Sommer et al. 2004
	+	Short-term	High flows	Immigration	Stevenson 1990*
	+	Short-term	High flows	Suspension	Peipoch et al. 2025

**Mechanism previously hypothesized, but not demonstrated, in the literature for the listed producer or group*

***Mechanism documented for a different producer and hypothesized for listed producer or group.*

Table 2.2: Information on metrics used as predictor variables for modeling monthly biomass of different stream producers. For models with two predictor variables, only one high-flow variable and one low-flow variable were used, never two high-flow variables or two low-flow variables. Predictor variables were created for short-term (7d, 14d, 30d), mid-term (90d), and long-term (180d) timeframes. Short-term drying refers to 7-, 14-, or 30-day timeframes. Seasonal drought refers to 90- or 180-day timeframes.

Predictor Variables	Flow Category	Hydrologic Scenario	Metric Description	Unit	Range
max	High	Extreme high flow	Max instantaneous flow	$m^3 s^{-1}$	1.44 – 154.61
min	Low	Extreme low flow	Min instantaneous flow	$m^3 s^{-1}$	0.91 – 7.67
sd	Variation	Steady flows	Variation in instantaneous flows	$m^3 s^{-1}$	0.08 – 19.45
state.low	Low	Extreme low flows/ drought	Proportion of time below the 7Q10*, what is considered low by state policy (≤ 1.28 m3 s–1)	—	0 – 1
x.low	Low	Extreme low flows/drought	Proportion of time under the lowest tributary 10th percentile (P10) of flows in the historic record (P10: ≤ 1.42 m3 s–1)	—	0 – 1
low	Low	Low flows	Proportion of time under the lowest daily 25th percentile (P25) of flows in the historic record (≤ 2.78 m3 s–1)	—	0 – 1
below.avg	Low	Low flows	Proportion of time under the mean daily mean flow (P50) in the historic record (≤ 9.94 m3 s–1)	—	0 – 1
above.avg	High	High flows	Proportion of time over the daily 50th percentile (P50) in the historic record (≥ 501 m3 s–1)	—	0 – 1
high	High	High flows	Proportion of time over the largest daily 75th percentile of flows (P75) in the historic record (≥ 29.68 m3 s–1)	—	0 – 1
x.high	High	Extreme high flows	Proportion of time over the largest daily 95th percentile (P95) of flows in the historic record (≥ 104.04 m3 s–1)	—	0 – 1
standard.spate	High	Extreme high flow event(s)	Standardized measure of the largest change in daily flow	—	0 – 1

**7Q10 is the 7-day mean flow that occurs, on mean, once every 10 years*

Table 2.3: Chemical and physical properties of the Middle Oconee River during the sampling period from June 2016 to August 2018. Time between sampling events varied as sampling occurred during all biomass sampling events, but also opportunistically. However, we were unable to collect samples from February 2018 – May 2018. We took the mean of samples taken from above and below the Hunnicutt tributary on the same date. SD = standard deviation.

Variable	Mean (SD)	Range	n
Turbidity (NTU)	23.3 (46.2)	6 .09 – 354.5	58
NH4 (ppm)	0.022 (0.012)	0.002 – 0.054	23
NO3 (ppm)	0.879 (0.17)	0.528 – 1.203	23
SRP (ppm)	0.006 (0.003)	0 – 0.011	23
TN (ppm)	1.180 (0.723)	0.860 – 4.285	23
TP (ppm)	0.018 (0.017)	0.001 – 0.063	23
DO (mg/L)	8.40 (2.80)	3.17-15.32	34
pH	7.92 (0.46)	6.64 - 9	32
Conductivity (μS/cm)	95.5 (21.5)	66.7 – 141.9	32
Temperature (C°)	20.16 (6.7)	5.9 – 28.8	36

Table 2.4: Top models (ΔAIC < 2) predicting mean and maximum biomass of Podostemum, filamentous algae, biofilm (Chl-*a*) for the entire reach. AFDM is measured in g m^{-2} for benthic producers and g L-1 for seston. Biofilm Chl-*a* is measured in mg m^{-2}. An increase in the metric 'min.180' indicates a less severe minimum, so a positive coefficient estimate indicates a negative effect of low flows. Timeframes: short-term (7d, 14d, 30d), mid-term (90d), long-term (180d). Predictor variables are scaled, and dominant variables are in bold text.

Top Models	R^2	High Flow Coefficient Estimate	High Flow Standard Error	Low Flow Coefficient Estimate	Low Flow Standard Error	ΔAIC	AIC wt.
Podostemum (AFDM)							
mean ~ above.avg.180 + min.180	0.87	48.63	7.94	30.90	8.24	—	0.82
max ~ above.avg.7 + **min.180**	0.76	- 488.39	133.83	826.65	124.75	—	0.52
Filamentous algae, *Rhizoclonium* (AFDM)							
mean ~ x.high.180 + **min.180**	0.73	6.74	2.12	7.96	2.17	—	0.33
mean ~ above.avg.7 + **min.180**	0.71	- 6.66	2.28	12.80	2.13	1.18	0.18
mean ~ above.avg.180 + **min.180**	0.70	6.29	2.29	7.72	2.37	1.92	0.18
max ~ x.high.180 + **min.180**	0.73	67.15	20.26	71.19	20.74	—	0.34
max ~ above.avg.7 + **min.180**	0.70	- 64.60	22.20	118.98	20.70	1.83	0.14
Biofilm (Chl-*a*)							
mean ~ standard.spate.90 + **x.low.90**	0.88	- 4.97	1.19	10.86	1.14	—	0.53
max ~ standard.spate.30 + **x.low.90**	0.86	- 47.95	21.83	167.18	20.51	—	0.17
max ~ standard.spate.90 + **x.low.90**	0.86	- 44.42	20.34	179.04	19.53	0.05	0.17
Biofilm (AFDM)							
mean ~ above.avg.7 + low.7	0.44	41.04	16.64	40.58	14.94	—	0.03
mean ~ **max.90** + min.7	0.43	- 65.44	19.92	25.84	19.60	0.16	0.03
mean ~ above.avg.7 + low.90	0.42	44.32	17.21	39.83	15.48	0.62	0.02

mean ~ **max.90** + state.low.180	0.41	- 46.30	16.90	16.21	15.41	0.85	0.02
mean ~ **max.90** + x.low.180	0.41	- 46.85	16.85	15.72	15.36	0.91	0.02
mean ~ **max.90** + min.14	0.40	- 65.95	23.15	22.20	22.69	1.02	0.02
mean ~ **max.90** + low.180	0.40	- 48.66	16.71	14.22	15.38	1.13	0.02
mean ~ above.avg.7 + low.30	0.40	41.66	17.26	37.92	15.48	1.15	0.02
mean ~ max.90 + low.7	0.39	- 41.77	19.40	15.05	17.73	1.28	0.02
max ~ above.avg.7 + state.low.180	0.45	1154.82	361.10	692.68	323.38	—	0.11
max ~ above.avg.7+ x.low.180	0.44	1139.58	362.94	671.85	325.07	0.30	0.10
max ~ above.avg.7 + low.180	0.40	1112.12	377.58	569.61	341.42	1.74	0.05
Seston (AFDM)							
mean ~ above.avg.90 + min.180	0.48	0.73	0.29	0.75	0.29	—	0.08
max ~ above.avg.90 + min.180	0.59	0.96	0.33	1.13	0.33	—	0.25
max ~ x.high.180 + min.180	0.55	0.92	0.36	0.92	0.36	1.78	0.10

Table 2.5: Support for flow ecology hypotheses for each primary producer. Y indicates that the hypothesis was supported, and N indicates the hypothesis was not supported. P indicates that there was partial support for the hypothesis: the direction matched, but the timeframe did not. An increase in the metric 'min.180' indicates a less severe minimum flow, and thus a negative effect of low flows. Timeframes as in Table 2.4.

Producer	Direction of Predicted Relationship	Predicted Time Frame (days)	Hydrologic Scenario	Hypothesis Supported for Mean Biomass (direction & metrics)	Hypothesis Supported for Maximum Biomass (direction & metric)
Podostemum	-	Mid- or long-term	Extreme low flows/drought	Y (+ min.180)	Y (+ min.180)
	-	Mid- or long-term	Low flows	Y (+ min.180)	Y (+ min.180)
	+	Mid- or long-term	High flows	Y (+ above.avg.180)	N
Filamentous algae	-	Mid-term	Low flows	P (+ min.180)	P (+ min.180)
	-	Short-term	Extreme high flow event(s)	Y (- above.avg.7)	Y (- above.avg.7)
	+	Mid-term	High flows	P (+ x.high.180) P (+ above.avg.180)	P (+ x.high.180)
	+	Long-term	Extreme high flow event(s)	Y (+ x.high.180)	Y (+ x.high.180)
Biofilm (Chl-*a*)	-	Long-term	Extreme low flows/drought	N	N
	-	Short-term	High flows	P (- standard.spate.90)	Y (- standard.spate.30)
	+	Short- or mid-term	Low flows	Y (+ x.low.90)	Y (+ x.low.90)

FIGURES

Figure 2.1: Study site diagram (A) and aerial photo (B) of the Middle Oconee River at Ben Burton Park in Athens, Georgia. A small, run-of-the-river hydropower facility currently exists upstream, beyond the extent of the aerial photo. The small brown square on river right of (A) indicates a municipal water intake facility across from the tributary, Hunnicutt Creek. Transects begin at the downstream end of the reach with T1-T3 (lower shoal) below the tributary, and T4-T6 (run) and T7 (upper shoal) above the tributary. Transect 7 is on the river left side of a small island that bisects the full width of the river. Inset indicates the sampling design for each transect, stratified into 5 equal blocks with one randomly located, destructive sample (red dots) taken from each block, which results in a total of 35 samples across the entire reach.

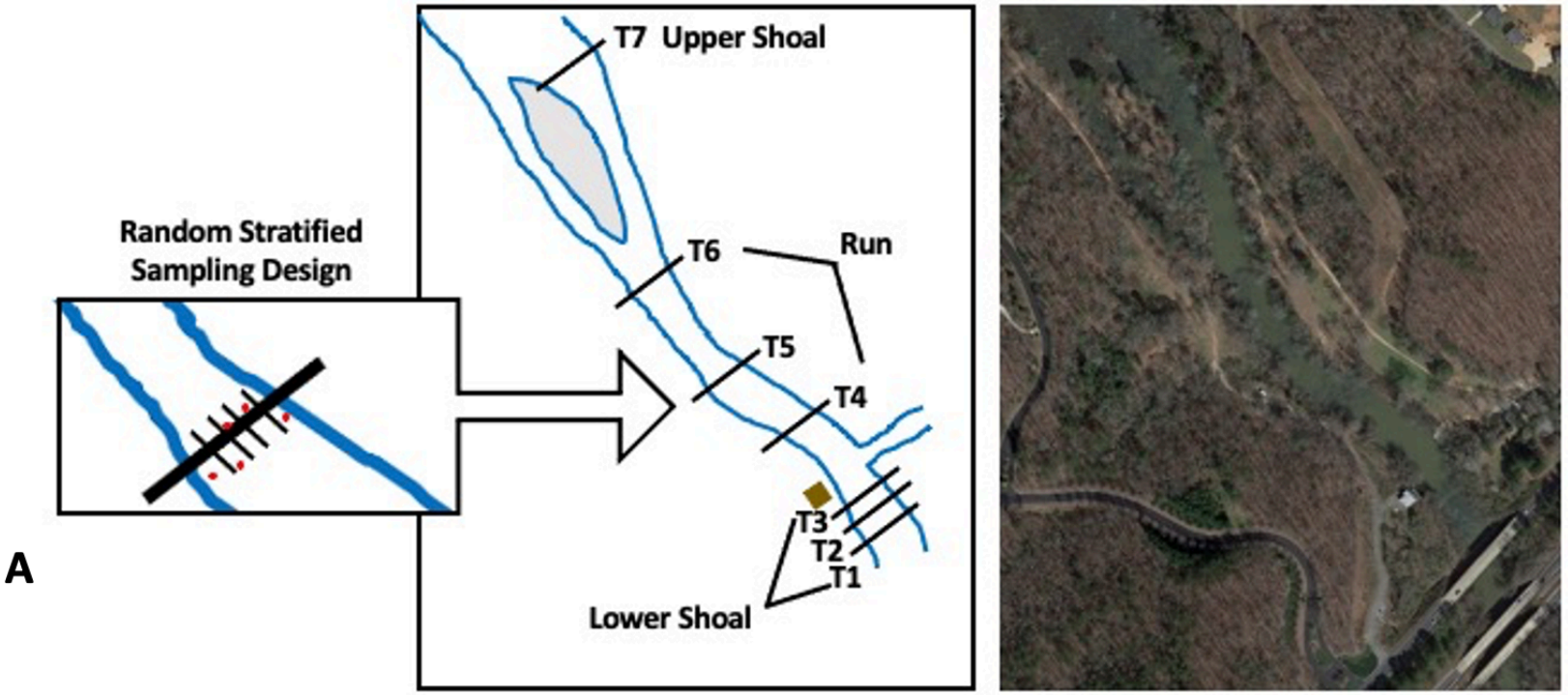
Random Stratified
Sampling Design
T7 Upper Shoal
T6
Run
T5
T4
T3
T2
T1
Lower Shoal
A
B
C

Figure 2.2: Daily mean discharge in the Middle Oconee River from USGS gage 02217500 from 01 January 2016 to 29 August 2018. This time window was used as the antecedent flow period for modeling producer biomass. The red lines indicate significant management-relevant thresholds: the state-declared low flow (bottom) and the highest 95th percentile of daily flows in the historic record (top), 1.28 and 104.04 $m^3 s^{-1}$ respectively.

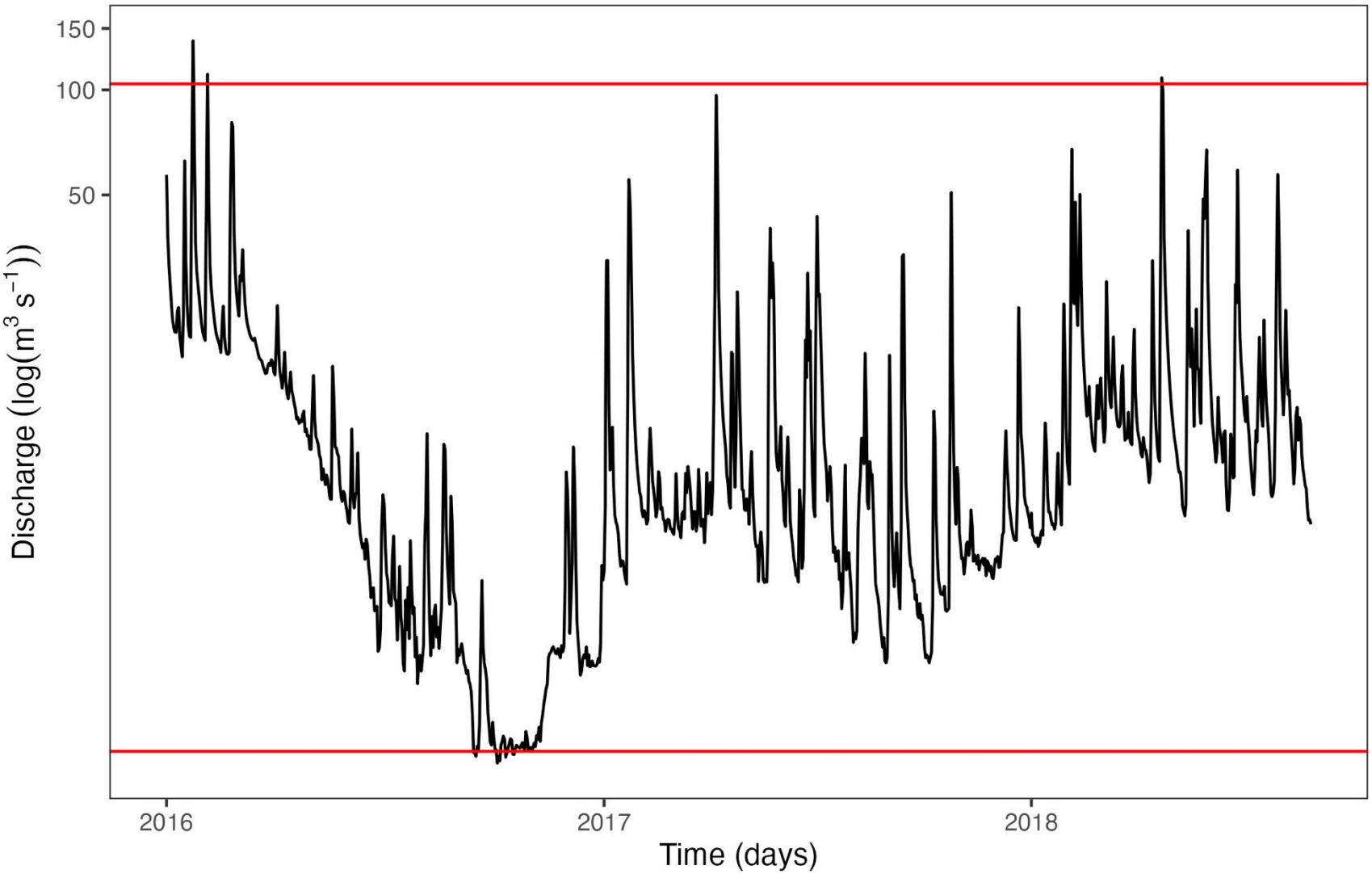
150
100
50
Discharge (log(m3 s−1))
2016
2017
2018
Time (days)

Figure 2.3: Monthly mean biomass of benthic producers over time by river segment (Year-Month). Units for AFDM are g m^{-2} whereas units for Chl-*a* are mg m^{-2}. The lower shoal and run both contained three transects with five blocks each (n = 15 per segment), while the upper shoal contained one transect with five blocks (n = 5) for a total of seven transects across the entire reach (n = 35). Only the lower shoal was sampled in June of 2017, producing19 total sampling events for that segment. All other segments have 18 total sampling events. Breaks in lines represent periods without sampling events.


Entire Reach
Lower Shoal
Run
Upper Shoal
Podostemum (AFDM)
Filamentous Algae (AFDM)
Biofilm (Chl-a)
Biofilm (AFDM)
Monthly Mean Biomass
Date
2016-07
2017-01
2017-07
2018-01
2018-07

Figure 2.4: Proportion of monthly mean AFDM of benthic producers over time by river segment. Lower shoal and Run: n = 15, Upper shoal: n = 5. Entire reach: n = 35. Only the lower shoal was sampled in June of 2017.

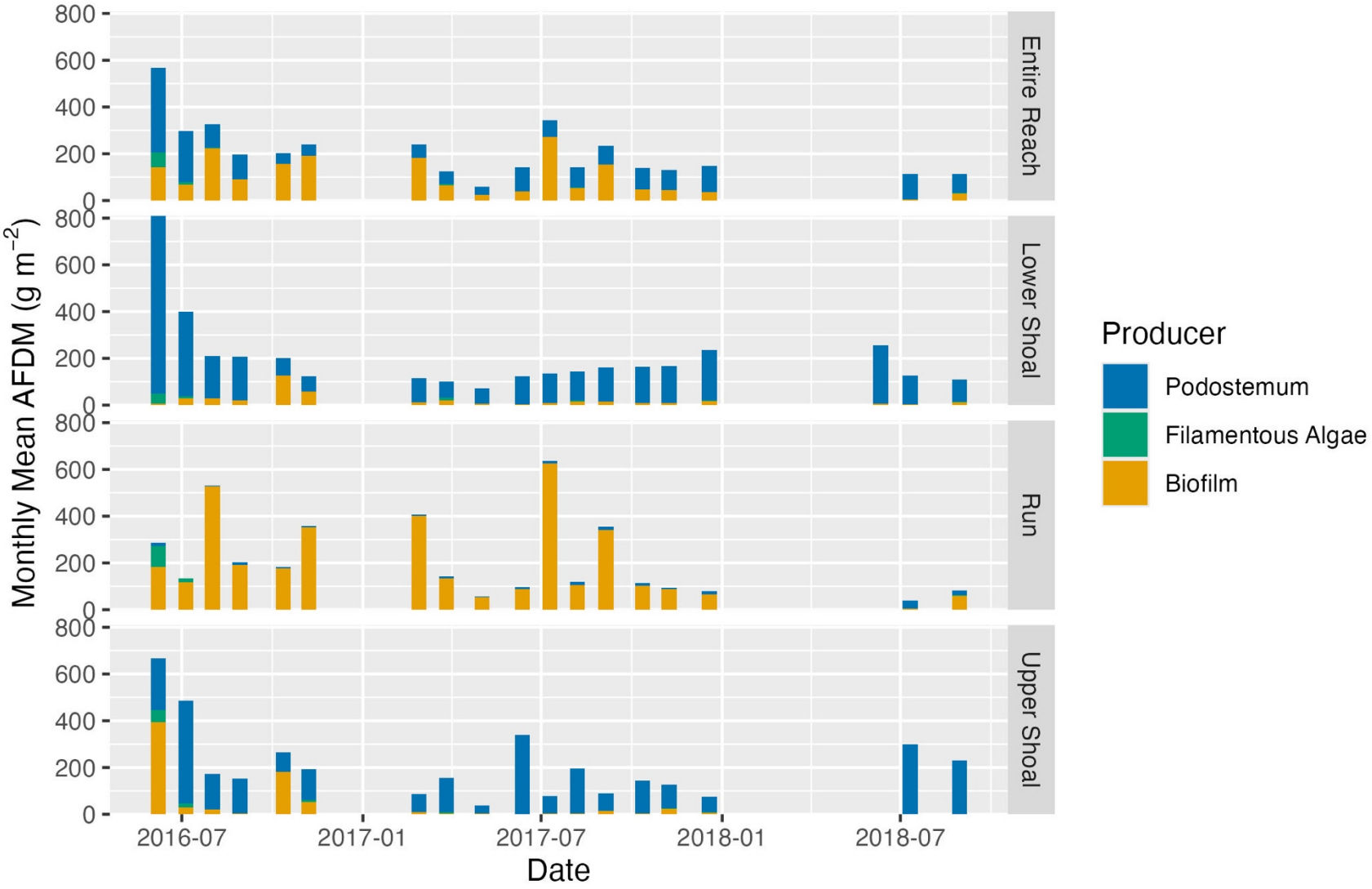
Monthly Mean AFDM (g m^{-2})
800
600
400
200
0
Entire Reach
Lower Shoal
Run
Upper Shoal
2016-07
2017-01
2017-07
2018-01
2018-07
Date
Producer
Podostemum
Filamentous Algae
Biofilm

Figure 2.5: Proportion of mean monthly AFDM from each benthic producer for all substrates across the entire reach (n = 18). BR.FR= bedrock or fixed rock, LR = large removable rock, SR = small removable rock, SS = soft sediment or sand. Mean biomass per substrate for all biomass types is displayed in Figure A2 with error bars indicating standard error of the mean (n = 18).

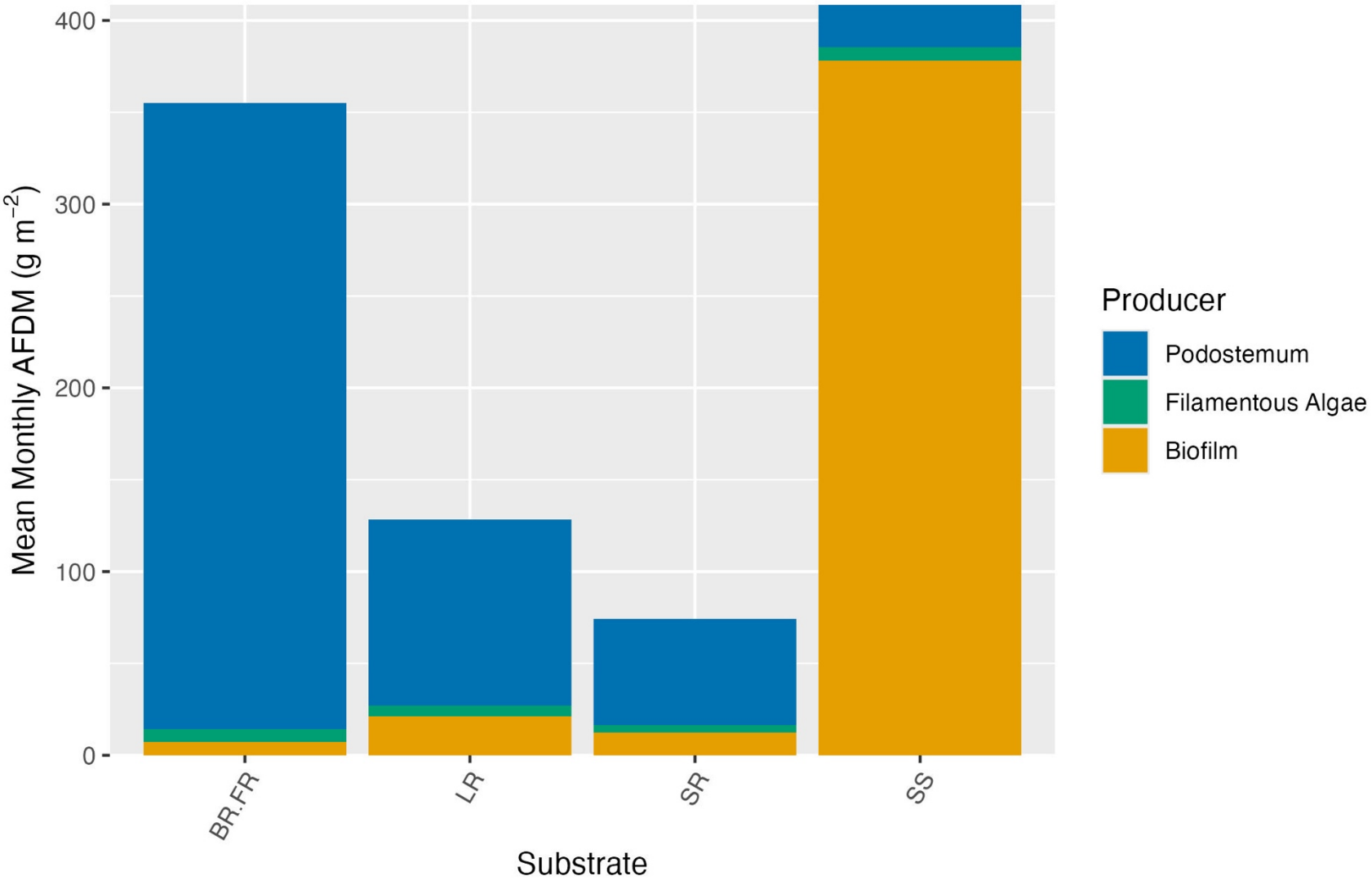
400
300
200
100
0
Mean Monthly AFDM (g m^{-2})
BR.FR
LR
SR
SS
Substrate
Producer
Podostemum
Filamentous Algae
Biofilm

Figure 2.6: Flow ecology relationships derived from the top models predicting monthly mean (A,C,E,G,I) and maximum (B,D,F,H,J) biomass across the entire reach. Relationships are projected from the first model listed for each producer in Table 2.4. Each model is represented by two plots, representing the biomass response (blue lines) to each of the two predictor variables in each model, while the other model variable is held constant. Shading indicates the confidence interval. Parameter estimates in the equations are for unscaled predictor variables, in contrast to the parameter estimates in Table 2.4, which are for scaled predictor variables. Biomass measured as AFDM is per g m^{-2} whereas biomass measured as Chl-*a* is per mg m^{-2}. Largest change in flow is a standardized variable while minimum flow is a measure of discharge in m^3 s^{-1}. Predictor variables for a proportion of time above or below a certain flow threshold have been converted into percentages. Full descriptions of predictor variables can be found in Table 2.2.

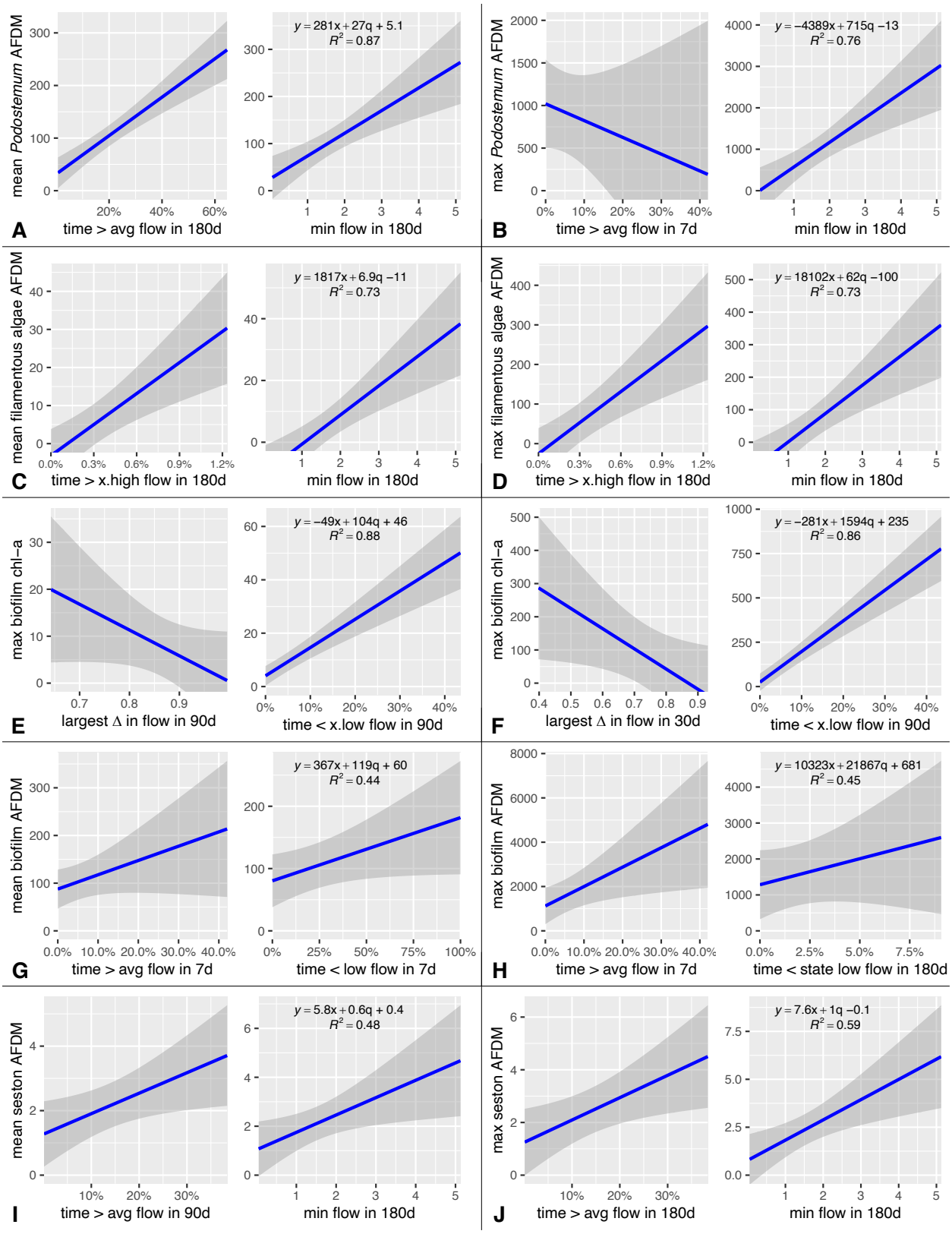
mean Podostemum AFDM
y = 281x + 27q + 5.1
R² = 0.87
time > avg flow in 180d
min flow in 180d
A
max Podostemum AFDM
y = −4389x + 715q −13
R² = 0.76
time > avg flow in 7d
min flow in 180d
B
mean filamentous algae AFDM
y = 1817x + 6.9q −11
R² = 0.73
time > x.high flow in 180d
min flow in 180d
C
max filamentous algae AFDM
y = 18102x + 62q −100
R² = 0.73
time > x.high flow in 180d
min flow in 180d
D
max biofilm chl−a
y = −49x + 104q + 46
R² = 0.88
largest Δ in flow in 90d
time < x.low flow in 90d
E
max biofilm chl−a
y = −281x + 1594q + 235
R² = 0.86
largest Δ in flow in 30d
time < x.low flow in 90d
F
mean biofilm AFDM
y = 367x + 119q + 60
R² = 0.44
time > avg flow in 7d
time < low flow in 7d
G
max biofilm AFDM
y = 10323x + 21867q + 681
R² = 0.45
time > avg flow in 7d
time < state low flow in 180d
H
mean seston AFDM
y = 5.8x + 0.6q + 0.4
R² = 0.48
time > avg flow in 90d
min flow in 180d
I
max seston AFDM
y = 7.6x + 1q −0.1
R² = 0.59
time > avg flow in 180d
min flow in 180d
J

REFERENCES

Allan, J. David., M. M. Castillo, and K. A. Capps. 2021. Stream ecology: Structure and function of running waters. Third. Springer.

Alnoee, A. B., P. S. Levi, A. Baattrup-Pedersen, and T. Riis. 2021. Macrophytes enhance reach-scale metabolism on a daily, seasonal and annual basis in agricultural lowland streams. Aquatic Sciences 83:11.

Arnon, S., A. I. Packman, C. G. Peterson, and K. A. Gray. 2007. Effects of overlying velocity on periphyton structure and denitrification. Journal of Geophysical Research: Biogeosciences 112:1–10.

Asaeda, T., and D. H. Son. 2000. Spatial structure and populations of a periphyton community: A model and verification. Ecological Modelling 133:195–207.

Battin, T. J., K. Besemer, M. M. Bengtsson, A. M. Romani, and A. I. Packmann. 2016. The ecology and biogeochemistry of stream biofilms. Nature Reviews Microbiology 14:251–263.

Bernhardt, E. S., J. B. Heffernan, N. B. Grimm, E. H. Stanley, J. W. Harvey, M. Arroita, A. P. Appling, M. J. Cohen, W. H. McDowell, R. O. Hall, J. S. Read, B. J. Roberts, E. G. Stets, and C. B. Yackulic. 2018. The metabolic regimes of flowing waters. Limnology and Oceanography 63:S99–S118.

Bernhardt, E. S., P. Savoy, M. J. Vlah, A. P. Appling, L. E. Koenig, R. O. Hall, M. Arroita, J. R. Blaszczak, A. M. Carter, M. Cohen, J. W. Harvey, J. B. Heffernan, A. M. Helton, J. D. Hosen, L. Kirk, W. H. McDowell, E. H. Stanley, C. B. Yackulic, and N. B. Grimm. 2022. Light and flow regimes regulate the metabolism of rivers. Proceedings of the National Academy of Sciences of the United States of America 119:e2121976119.

Biggs, B. J. 1996a. Patterns in benthic algae of streams. Pages 31–56 in M. L. Bothwell, editor. Agal Ecology: Freshwater Benthic Ecosystems. Academic Press.

Biggs, B. J. F. 1996b. Hydraulic habitat of plants in streams. Regulated Rivers: Research & Management 12:131–144.

Biggs, B. J. F., V. I. Nikora, and T. H. Snelder. 2005. Linking scales of flow variability to lotic ecosystem structure and function. River Research and Applications 21:283–298.

Biggs, B. J. F., and H. A. Thomsen. 1995. Disturbance of stream periphyton by perturbations in shear stress: time to structural failure and differences in community resistance. Journal of Phycology 31:233–241.

Biggs, B. J., D. G. Goring, and V. I. Nikora. 1998. Subsidy and stress responses of stream periphyton to gradients in water velocity as a function of community growth form. Journal of Phycology. 34:598–607.

Biggs, B. J., R. A. Smith, and M. J. Duncan. 1999. Velocity and sediment disturbance of periphyton in headwater streams: Biomass and metabolism. Journal of the North American Benthological Society 18:222–241.

Blaszczak, J. R., C. B. Yackulic, R. K. Shriver, and R. O. Hall. 2023. Models of underlying autotrophic biomass dynamics fit to daily river ecosystem productivity estimates improve understanding of ecosystem disturbance and resilience. Ecology Letters 26:1510–1522.

Bowden, W. B., J. M. Glime, and T. Riis. 2017. Macrophytes and bryophytes. Page Methods in Stream Ecology: Third Edition. Third. Academic Press.

Burkholder, J. M. 1996. Interactions of benthic algae with their substrata. Page in R. J. Stevenson, M. L. Bothwell, R. L. Lowe, and J. H. Thorpe, editors. Algal Ecology. Academic Press, San Diego.

Burnham, K. P., and D. R. Anderson. 2002. Model selection and multimodel inference: a practical information-theoretic approach. Page The Journal of Wildlife Management. 2nd edition. New York.

Burrows, R. M., L. Beesley, M. M. Douglas, B. J. Pusey, and M. J. Kennard. 2020. Water velocity and groundwater upwelling influence benthic algal biomass in a sandy tropical river: implications for water-resource development. Hydrobiologia 847:1207–1219.

Cardinale, B. J. 2011. Biodiversity improves water quality through niche partitioning. Nature 472:86–91.

Carter, A. M., H. E. Lowman, J. R. Blaszczak, C. C. Barbosa, M. DeSiervo, C. L. Torrens, M. R. Dunkle, S. M. Collins, I. Oleksy, L. R. Katona, and R. O. Hall. 2024. Exceptions to the heterotrophic rule: Prevalence and drivers of autotrophy in streams and rivers. Ecosystems 2024:1–17.

Core Writing Team, H. L. J. R. 2023. IPCC, 2023: Climate change 2023: Synthesis report. Contribution of working groups I, II and III to the sixth assessment report of the Intergovernmental Panel on Climate Change.

Dahm, C. N., M. A. Baker, D. I. Moore, and J. R. Thibault. 2003. Coupled biogeochemical and hydrological responses of streams and rivers to drought. Freshwater Biology 48:1219–1231.

Davis, J. L., M. C. Freeman, and S. W. Golladay. 2020. Identifying life-history traits that promote occurrence for four minnow (*Leuciscidae*) species in intermittent Gulf Coastal Plain streams. Southeastern Naturalist 19:103–127.

Dosdogru, F., L. Kalin, R. Wang, and H. Yen. 2020. Potential impacts of land use/cover and climate changes on ecologically relevant flows. Journal of Hydrology 584:124654.

Ellison, A. M. 2019. Foundation species, non-trophic interactions, and the value of being common. iScience 13:254–268.

Francoeur, S. N., and B. J. F. Biggs. 2006. Short-term effects of elevated velocity and sediment abrasion on benthic algal communities. Hydrobiologia 561:59–69.

Grubaugh, J. W., and J. B. Wallace. 1995. Functional structure and production of the benthic community in a Piedmont river: 1956-1957 and 1991-1992. Limnology and Oceanography 40:490–501.

Hart, D. D., B. J. Biggs, V. I. Nikora, and C. A. Flinders. 2013. Flow effects on periphyton patches and their ecological consequences in a New Zealand river. Freshwater Biology:1588–1602.

Hart, D. D., and C. M. Finelli. 1999. Physical-biological coupling in streams: The pervasive effects of flow on benthic organisms. Annual Review of Ecology and Systematics 30:363–395.

Hill, B. H., and J. R. Webster. 1984. Productivity of *Podostemum ceratophyllum* in the New River, Virginia. American Journal of Botany 71:130–136.

Hill, W. R., B. J. Roberts, S. N. Francoeur, and S. E. Fanta. 2011. Resource synergy in stream periphyton communities. Journal of Ecology 99:454–463.

Hosen, J. D., K. S. Aho, A. P. Appling, E. C. Creech, J. H. Fair, R. O. Hall, E. D. Kyzivat, R. S. Lowenthal, S. Matt, J. Morrison, J. E. Saiers, J. B. Shanley, L. C. Weber, B. Yoon, and P. A. Raymond. 2019. Enhancement of primary production during drought in a temperate watershed is greater in larger rivers than headwater streams. Limnology and Oceanography 64:1458–1472.

Hutchens, J. J., J. Bruce Wallace, and E. D. Romaniszyn. 2004. Role of *Podostemum ceratophyllum* Michx. in structuring benthic macroinvertebrate assemblages in a southern Appalachian river. Journal of the North American Benthological Society 23:713–727.

Katz, R. A., M. C. Freeman, and K. Tierney. 2015. Evidence of population resistance to extreme low flows in a fluvial-dependent fish species. Canadian Journal of Fisheries and Aquatic Sciences 72:1776–1787.

Kendrick, M. R., A. E. Hershey, and A. D. Huryn. 2019. Disturbance, nutrients, and antecedent flow conditions affect macroinvertebrate community structure and productivity in an Arctic river. Limnology and Oceanography 64:S93–S104.

Klausmeier, C. A., E. Litchman, and S. A. Levin. 2004. Phytoplankton growth and stoichiometry under multiple nutrient limitation. Limnology and Oceanography 49:1463–1470.

Kominoski, J. S., and A. D. Rosemond. 2012. Conservation from the bottom up: Forecasting effects of global change on dynamics of organic matter and management needs for river networks. Freshwater Science 31:51–68.

Lake, P. S. 2003, July 1. Ecological effects of perturbation by drought in flowing waters. John Wiley & Sons, Ltd.

Lytle, D. A., and N. L. Poff. 2004. Adaptation to natural flow regimes. Trends in Ecology & Evolution 19:94–100.

Manning, D. W. P., A. D. Rosemond, J. P. Benstead, P. M. Bumpers, J. S. Kominoski, D. W. P. Manning, A. D. Rosemond, J. P. Benstead, P. M. Bumpers, and J. S. 2020 Kominoski. 2020. Transport of N and P in U.S. streams and rivers differs with land use and between dissolved and particulate forms. Ecological Applications 30:e02130.

Matthaei, C. D., J. J. Piggott, and C. R. Townsend. 2010. Multiple stressors in agricultural streams: interactions among sediment addition, nutrient enrichment and water abstraction. Journal of Applied Ecology 47:639–649.

McKay, S. K. 2014, September 23. Informing flow management decisions in the Middle Oconee River. University of Georgia.

Mosisch, T. D. 2001. Effects of desiccation on stream epilithic algae. New Zealand Journal of Marine and Freshwater Research 35:173–179.

Mulholland, P. J., G. Ronnie Best, C. C. Coutant, G. M. Hornberger, J. L. Meyer, P. J. Robinson, J. R. Stenberg, R. E. Turner, F. Vera-Herrera, and R. G. Wetzel. 1997. Effects of climate change on freshwater ecosystems of the south-eastern United States and the Gulf of Mexico. Hydrological Processes 11:949–970.

Murdock, J. N., and W. K. Dodds. 2007. Linking benthic algal biomass to stream substratum topography. Journal of Phycology 43:449–460.

Nelson, D. J., and D. C. Scott. 1962. Role of detritus in the productivity of a rock-outcrop community in a Piedmont stream. Limnology and Oceanography 7:396–413.

O'Donnell, B., and E. R. Hotchkiss. 2022. Resistance and resilience of stream metabolism to high flow disturbances. Biogeosciences 19:1111–1134.

Paerl, H. W., and J. Huisman. 2008. Climate: Blooms like it hot. Science 320:57–58.

Pahl, J. P. 2009. Effects of flow alteration on the aquatic macrophyte *Podostemum ceratophyllum* (riverweed); local recovery potential and regional monitoring strategy.

Palmer, M., and A. Ruhi. 2019. Linkages between flow regime, biota, and ecosystem processes: Implications for river restoration. Science 365.

Parker, J. D., D. E. Burkepile, D. O. Collins, J. Kubanek, and M. E. Hay. 2007. Stream mosses as chemically-defended refugia for freshwater macroinvertebrates. Oikos 116:302–312.

Parker, S. P., W. B. Bowden, and M. B. Flinn. 2016. The effect of acid strength and postacidification reaction time on the determination of chlorophyll a in ethanol extracts of aquatic periphyton. Limnology and Oceanography: Methods 14:839–852.

Peipoch, M., M. Daniels, and S. H. Ensign. 2025. Concentration–discharge relationships of chlorophyll describe the origin and fluxes of river algae across ecoregions. Freshwater Science 44:143–158.

Poff, N. L., B. D. Richter, A. H. Arthington, S. E. Bunn, R. J. Naiman, E. Kendy, M. Acreman, C. Apse, B. P. Bledsoe, M. C. Freeman, J. Hendriksen, R. B. Jacobson, J. G. Kennen, D. M. Merritt, J. H. O'keeffe, J. D. Olden, K. Rogers, R. E. Tharme, and A. Warner. 2010. The ecological limits of hydrologic alteration (ELOHA): A new framework for developing regional environmental flow standards. Freshwater Biology 55:147–170.

Poff, N. L., and J. K. H. Zimmerman. 2010. Ecological responses to altered flow regimes: a literature review to inform the science and management of environmental flows. Freshwater Biology 55:194–205.

Power, M. E., M. S. Parker, and W. E. Dietrich. 2008. Seasonal reassembly of a river food web: Floods, droughts, and impacts of fish. Ecological Monographs 78:263–282.

Power, M. E., and A. J. Stewart. 1987. Disturbance and recovery of an algal assemblage following flooding in an Oklahoma stream. American Midland Naturalist 117:333.

R Core Team. 2025. R: A language and environment for statistical computing. Vienna, Austria.

Rack, L. 2025. Quantifying streamflow needs for ecosystems in the context of water planning and management. Doctoral Dissertation, University of Georgia, Athens, GA.

Rahimi, L., C. Deidda, and C. De Michele. 2021. Origin and variability of statistical dependencies between peak, volume, and duration of rainfall-driven flood events. Scientific Reports 11:5182.

Reisinger, A. J., J. L. Tank, E. J. Rosi-Marshall, R. O. Hall, and M. A. Baker. 2015. The varying role of water column nutrient uptake along river continua in contrasting landscapes. Biogeochemistry 125:115–131.

Richter, B. D., A. T. Warner, J. L. Meyer, and K. Lutz. 2006. A collaborative and adaptive process for developing environmental flow recommendations. River Research and Applications 22:297–318.

Riis, T., and B. J. F. Biggs. 2001. Distribution of macrophytes in New Zealand streams and lakes in relation to disturbance frequency and resource supply - A synthesis and conceptual model. New Zealand Journal of Marine and Freshwater Research 35:255–267.

Roeder, D. R. 1977. Relationships between phytoplankton and periphyton communities in a central Iowa stream. Hydrobiologia 56:145–151.

Rosi-Marshall, E. J., and J. B. Wallace. 2002. Invertebrate food webs along a stream resource gradient. Freshwater Biology 47:129–141.

Rott, E., and J. D. Wehr. 2016. The spatio-temporal development of macroalgae in rivers. Pages 159–195 River Algae. Springer International Publishing, Cham.

Rüegg, J., C. C. Conn, E. P. Anderson, T. J. Battin, E. S. Bernhardt, M. Boix Canadell, S. M. Bonjour, J. D. Hosen, N. S. Marzolf, and C. B. Yackulic. 2020. Thinking like a consumer: Linking aquatic basal metabolism and consumer dynamics. Limnology and Oceanography Letters 6:1–17.

Sabater, S., F. Bregoli, V. Acuña, D. Barceló, A. Elosegi, A. Ginebreda, R. Marcé, I. Muñoz, L. Sabater-Liesa, and V. Ferreira. 2018. Effects of human-driven water stress on river ecosystems: a meta-analysis. Scientific Reports 8:11462.

Salmaso, N., and M. G. Braioni. 2008. Factors controlling the seasonal development and distribution of the phytoplankton community in the lowland course of a large river in Northern Italy (River Adige). Aquatic Ecology 42:533–545.

Sartory, D. P., and J. U. Grobbelaar. 1984. Extraction of chlorophyll a from freshwater phytoplankton for spectrophotometric analysis. Hydrobiologia 114:177–187.

Scott, M. C., G. S. Helfman, M. E. McTammany, E. F. Benfield, and P. V. Bolstad. 2002. Multiscale influences on physical and chemical stream conditions across blue ridge landscapes. Journal of the American Water Resources Association 38:1379–1392.

Sommer, T. R., W. C. Harrell, A. M. Solger, B. Tom, and W. Kimmerer. 2004. Effects of flow variation on channel and floodplain biota and habitats of the Sacramento River, California, USA. Aquatic Conservation 14:247–261.

Steinman, A. D., P. J. Mulholland, and W. R. Hill. 1992. Functional responses associated with growth form in stream algae. Journal of the North American Benthological Society 11:229–243.

Stevenson, R. J. 1990. Benthic algal community dynamics in a stream during and after a spate. Journal of the North American Benthological Society 9:277–288.

Stevenson, R. J., and E. F. Stoermer. 1982. Abundance patterns of diatoms on *Cladophora* in Lake Huron with respect to a point source of wastewater treatment plant effluent. Journal of Great Lakes Research 8:184–195.

Suren, A. M., and T. Riis. 2010. The effects of plant growth on stream invertebrate communities during low flow: A conceptual model. Journal of the North American Benthological Society 29:711–724.

Thomaz, S. M. 2021, December 6. Ecosystem services provided by freshwater macrophytes. Springer.

Vadeboncoeur, Y., and M. E. Power. 2017. Attached algae: The cryptic base of inverted trophic pyramids in freshwaters. Annual Review of Ecology, Evolution, and Systematics 48:255–279.

Vannote, Robin L.; Minshall, G. Wayne; Cummins, Kenneth W.; Sedell, James R.; Cushing, C. E. 1980. The river continuum concept. Canadian Journal of Fisheries and Aquatic Science 37:130–137.

Wehr, J. D., R. G. Sheath, and J. P. Kociolek. 2015. Freshwater algae of North America: Ecology and classification. Page (J. D. Wehr, R. G. Sheath, and J. P. Kociolek, Eds.) Freshwater Algae of North America: Ecology and Classification. 2nd edition. Elsevier Inc.

Wood, J., and M. Freeman. 2017. Ecology of the macrophyte *Podostemum ceratophyllum* Michx. (Hornleaf riverweed), a widespread foundation species of eastern North American rivers. Aquatic Botany 139:65–74.

Wood, J. L., J. W. Skaggs, C. Conn, and M. C. Freeman. 2019. Water velocity regulates macro-consumer herbivory on the benthic macrophyte *Podostemum ceratophyllum* Michx. Freshwater Biology 64:2037–2045.

AUTHOR CONTRIBUTIONS

Author C. C. Conn developed, supervised, and carried out all field work, lab processing, and analyses, and wrote the manuscript with input from all co-authors. Co-author P. M. Bumpers helped to plan, supervise, and carry out field work and lab processing. Co-authors A. D. Rosemond, M. C. Freeman, S. K. McKay, and S. J. Wenger contributed to the conception of the presented idea and secured funding. All co-authors contributed to the study design.

All co-authors agree that the work may be included in this thesis or dissertation.

CHAPTER 3

PRIMARY PRODUCER FUNCTIONAL DIVERSITY AND CONTRIBUTION TO STREAM PRODUCTIVITY [2]

[2] Conn, C., A. D. Rosemond, S. J. Wenger. To be submitted to a peer-reviewed journal.

ABSTRACT

Primary producers are an essential component of the stream environment and productivity a key aspect of global carbon cycling. However, a mechanistic understanding of how distinct producers differentially contribute to stream productivity is lacking. We investigated how producer identity and light availability regulate mass-specific gross primary productivity (GPP) and the effect on producer contribution to overall stream productivity. We conducted laboratory incubations of common producers found in a mid-sized temperate river in Athens, GA – the macrophyte *Podostemum ceratophyllum*, benthic biofilms, filamentous algae, and seston. We quantified GPP rates under laboratory conditions from field-collected producers across levels of photosynthetically active radiation (PAR) and found varying productive capacities, reflecting functional types with distinct mass specific GPP-light relationships. We applied GPP estimates to known areal biomass estimates for producer types over a moderately large spatial and temporal scale (i.e., approximately 11,100 m^2 and 11 monthly time steps) and found that stream community GPP was driven to a large extent by producer-specific responses to antecedent flow conditions. Given the contrasting productive capacities and relative contributions of different producers to overall stream productivity, we demonstrate that shifts in environmental conditions are able to influence stream function through distinct pathways and with disproportionate effects, depending on which producer groups are impacted. This necessitates an approach to managing ecosystem function and associated services that is more mechanistically aware and requires continued research to connect these mechanisms across scales and in other systems.

INTRODUCTION

Primary producers are a critical component of stream ecosystems, providing a basal energy resource for food webs and habitat complexity for numerous other organisms (Cardinale et al. 2011, Wood and Freeman 2017, Vadeboncoeur and Power 2017, Kendrick et al. 2019). Primary production is important in nearly all lotic systems, even those that are largely heterotrophic (Thorp and Delong 2002, Carter et al. 2024) and productivity is inextricably linked to other important stream processes, such as nutrient uptake (Johnson and Tank 2009, Hanrahan et al. 2018, Myrstener et al. 2021, Reisinger et al. 2021, Schlenker et al. 2024). Prior research has long documented patterns in primary producer standing stocks and quantified instantaneous metabolic rates with laboratory incubations and *in situ* chambers (e.g., Steinman and McIntire 1986, Rosemond 1993, Bott et al. 1997). Much of this research has occurred in small, headwater streams where producers are often less abundant and less structurally diverse, resulting in a heavy emphasis on stream biofilms (Battin et al. 2016). More recent research has elucidated patterns in whole stream metabolism for small and large streams (Dodds et al. 2013, Appling et al. 2018, Savoy et al. 2019, Bernhardt et al. 2022). However, much less research has linked these scales to provide a mechanistic understanding of how whole-stream metabolic patterns arise through space and time.

Gross primary productivity (GPP) provides a measure of how much inorganic carbon is fixed from the atmosphere by autotrophs within a given system. Ecosystem respiration (ER) is a measure of both autotrophic and heterotrophic metabolic activity, and the difference between the two is expressed as net ecosystem productivity (NEP), or whole stream metabolism. Primary productivity is largely controlled by abiotic factors: light (e.g., Boix Canadell et al. 2021), flow (Bernhardt et al. 2022), nutrient availability (e.g., Schlenker et al. 2024), and temperature (e.g.,

Nakano et al. 2022). Research has also demonstrated that primary producer (hereafter referred to as 'producer') biomass and diversity changes in response to antecedent conditions, such as hydrologic disturbance (Cardinale et al. 2006, Bernhardt et al. 2022, Peipoch et al. 2025, Conn et al. Ch.2) and herbivory (Power 1992b, Wood et al. 2019). This creates a complex web of dynamic interactions in which producers are shaped by top-down and bottom-up controls (Rosemond et al. 1993) and in turn, they directly and indirectly affect other stream biota (Tonkin et al. 2014, Rüegg et al. 2020) and the surrounding aquatic (Jones et al. 1994, Dodds and Biggs 2002) and terrestrial environments (Kautza and Sullivan 2016).

In comparison to forested headwater streams, mid-sized streams (here, loosely defined as 4^{th} – 6^{th} order) often have less canopy cover, which allows for an increase in primary production, and greater heterogeneity of the benthic substrata, which allows for a more diverse producer community. In addition to the algae-containing biofilms that typically dominate smaller streams, mid-sized systems can also support submerged macrophytes, filamentous algae, and suspended producers (of planktonic or benthic origins), all of which may be uniquely affected by antecedent conditions and differentially relied upon by the greater stream community. The Middle Oconee River in Athens, GA, a well-studied sixth order tributary of the Altamaha River, exemplifies this scenario, containing a common set of functionally and structurally diverse producers with unique responses to antecedent flow conditions and relative contributions to secondary production (Nelson and Scott 1962, Grubaugh and Wallace 1995, Pahl 2009, McKay 2014, Katz et al. 2015, Rack 2025, Conn et al. Ch.2). Among them, is the submerged macrophyte *Podostemum ceratophyllum* (hereafter "*Podostemum*"), which historically has had abundant populations across a large range of the eastern United States but is currently the subject of conservation concern due to declines in abundance (Wood and Freeman 2017). *Podostemum* plays a

foundational role in supporting the production of stream consumers, largely as complex habitat, and recent research from the Middle Oconee River has shown that spatial and temporal fluctuations in *Podostemum* biomass are driven by antecedent flow conditions (Conn et al. Ch.2). Conn et al. (Ch.2) documented *Podostemum* fluctuations relative to the biomass patterns of other morphologically distinct producer groups, namely filamentous algae and biofilms, that are differently relied upon by stream consumers and have distinct responses to the same antecedent flow conditions. Concurrent work (Conn et al. Ch. 2) provides a strong foundation for studying the potential impacts of these producer-specific fluctuations on stream function.

In this study we ask how identity and light, both directly and indirectly, regulate a producer's contribution to stream productivity. To quantify differences in mass-specific gross primary productivity (GPP) relative to light availability, we conducted metabolic experiments under different light treatments in a controlled laboratory setting for morphologically distinct producers representative of the Middle Oconee River: *Podostemum*, benthic biofilms containing algae (hereafter "biofilm"), filamentous algae, and suspended producers in seston. To evaluate the influence of the stream environment, we collected *Podostemum* and biofilm specimens from contrasting ambient light environments (shade vs. sun), along with associated substrate for biofilm, and seston from locations differing relative to a first-order tributary. Filamentous algae were represented by two phylogenetically distinct taxa: a green alga (*Rhizoclonium* sp., Division Chlorophyta, Domain Eukarya) and a cyanobacterium (*Lyngbya* sp., Domain Bacteria). To estimate areal productivity and temporal and spatial variation in producer contribution, we incorporated biomass data from the Conn et al. (Ch.2) study. By integrating instantaneous productivity, an important functional effect trait (*sensu* Naeem and Wright 2003) of aquatic primary producers, with a longer-term biomass record, we evaluate the potential mechanisms

linking producer identity, biomass dynamics, and environmental variation to whole stream function.

METHODS

Site Description

We collected benthic organic material for laboratory experiments from a small segment (<200 m) of the Middle Oconee River at Ben Burton Park in Athens, Georgia. The Middle Oconee River is a sixth-order tributary of the Altamaha River that flows through the Piedmont physiographic province. Our study section was largely open canopy, comprised of a sandy run and downstream cobble and bedrock shoal with a first-order tributary between them. Numerous studies over the past 60 years have examined the benthic communities of the Middle Oconee River and found a range of primary producers in varying proportions (e.g., Nelson and Scott 1962, Pahl 2009). In the years prior to our study (2016-2018), the same river segment was found to support three main primary producer groups: a macrophyte *Podostemum ceratophyllum*, biofilms containing benthic algae, and filamentous algae including *Rhizoclonium* sp. (Conn et al. Ch. 2).

Sample Collection

The objective of the laboratory trials was to quantify mass-specific GPP rates of diverse primary producer types and assess how GPP varies over a range of light conditions. Accordingly, we collected the following samples of producers from the Middle Oconee River on 29 July and 03 August, 2020, from either high or low light areas of the stream as indicated by sun or shade: 1) *Podostemum* (sun), 2) *Podostemum* (shade), 3) rock biofilms (sun), 4) rock biofilms (shade), 5) filamentous algae of two types (chlorophyte dominated and cyanobacterial dominated), 6) soft substrate biofilm (sun), 7) soft substrate biofilm (shade), and 8) seston (samples from two time

periods and two locations within the stream reach; July/August and upstream/downstream) (Table 3.1). All of these samples were returned to the laboratory to quantify NEP and ER rates in 30 ml vials under otherwise controlled conditions. These measurements were made on triplicate samples of each producer type at each of five irradiance levels and at stream water temperatures from the day of collection. Given no substantial change in stream conditions (e.g., hydrologic event) between 29 July and 03 August 2020, collection date was only a considered factor for seston, not benthic samples. Although these measurements made under laboratory conditions may be different from rates that would be determined *in situ*, they allow for direct comparisons of mass-specific GPP functional traits across producer types.

We collected benthic samples from multiple substrates to reflect the range of primary producer groups found in Conn et al. (Ch. 2). Samples of *Podostemum* and biofilm on hard substrate were limited to small rocks (i.e., gravel) in an effort to maintain sample integrity with minimal disturbance while adhering to the size constraints of the 30ml vials used for the lab experiments. However, we were unable to collect enough filamentous algae from small rocks, so we removed filamentous algae samples from bedrock and cobbles.

We varied the number of samples we collected for each producer and substrate as needed to collect enough samples for multiple replicates under each light condition. The sampling method was tailored to the bed substrate and followed the substrate-specific methods used by Conn et al. (Ch.2). For small rock samples, we used a modified Surber sampler known as a t-sampler (Wood et al. 2019) to collect surface gravel from a 102-cm^2 area of the streambed, either with or without *Podostemum* (representing biofilm only), and placed the contents in a polyethylene bag. We collected separate samples of *Podostemum* or biofilm-only small rocks from both sunny and shady locations (i.e. the edges of the channel experiencing considerable tree

cover during leaf-on and at least partial cover during leaf-off) of the downstream shoal. For biofilm samples on sand and soft sediment (hereafter referred to as 'soft substrate'), we used a PVC pipe corer with an opening of 45-cm^2 to collect a sample volume of approximately 227-cm^3 in a polyethylene bag. For filamentous algae samples, we used a razor blade to collect material from either bedrock or cobble and then added a small amount of stream water to the polyethylene bag. We placed all benthic samples in coolers for transport to the lab. We also collected stream water from both above and below the first-order tributary in large, 20 L high-density polyethylene carboys, which we covered with light-blocking polyethylene bags during transport. Once at the lab, all benthic samples were placed in a refrigerator, and covered carboys were placed directly into a dark, temperature-controlled room set to the temperature of the stream as measured on the day of collection. All samples were refrigerated until the trials, which occurred within 96 hours of the collection date.

Laboratory Experiment

Over a period of six days, we conducted trials within a light and temperature-controlled laboratory at the University of Georgia in Athens, Georgia to evaluate the productivity rate of each sample type (i.e. producer from different stream light environments and/or substrate, or taxa) under a range of light conditions. We grouped trials into rounds of the same substrate or producer, and prepared samples by round to minimize the time each sample spent unrefrigerated and/or without stream water before the trials. To prepare soft substrate samples, we poured the sample into a bucket, added stream water from a carboy, elutriated the contents, and then took at least 20 subsamples with 60 ml brown (i.e. light blocking) high-density polyethylene bottles. We collected one additional large subsample using a 1 L brown Nalgene, which we returned to the refrigerator. We then took the small subsamples to the dark, temperature-controlled room

(hereafter referred to as the 'trial room'). For both filamentous algae samples, we took a portion of algae from the stream water, removed any associated debris, and then separated out subsamples (without water) for the trials, returning the remainder to the refrigerator. We took a portion of rocks from each small rock sample bag, varying the amount of *Podostemum* for *Podostemum* samples, and returned the remainder to the refrigerator.

While vial contents varied for the different rounds, the assembly process was largely the same for producers on rocks and filamentous algae, and likewise for soft substrate and stream water. Once in the trial room, we transferred each small rock sample or filamentous algae subsample into a 30 ml glass vial and created sets of 6-8 vials. Just before we took initial measurements, we filled each vial with stream water from a flask with a magnetic stirrer, which constantly elutriated the contents to keep the stream water homogenized. For subsamples of soft substrate and stream water, we first grouped empty vials into sets of 6-8 for a trial. We filled the vials with the subsample just before we took initial measurements. For vials with stream water only, we filled each from the flask with homogenized stream water, whereas for soft substrate, we filled each vial from the 60 ml subsample bottle after inverting the bottle 2-3 times to homogenize.

For each of the vials in a trial set (i.e. 6-8 vials experiencing the same light condition), we started the trial before taking measurements of the next vial. We used a YSI 5010 Dissolved Oxygen Instrument with a YSI 5100 BOD probe to take measurements of dissolved oxygen and temperature. To take measurements, we inserted the probe, turned on the propeller, recorded the time and the measurements of dissolved oxygen concentration (mg O_2 L^{-1}) and temperature (C). We then topped the vial off with either stream water or diluted soft substrate, depending upon the sample, and placed the vial into the water bath to begin the trial time. The water bath was set to

the stream temperature as measured on the date of sample collection, and the light level at the depth of the sample correlated to one of the following photosynthetic active radiation (PAR) levels (μmol m^{-2} s^{-1}): 0 (no light), 90, 224, 452, 941, or 1625 (full light). After an average of 31 minutes (median 30, range 29-40), we removed each vial from the water bath in the same order they were inserted, recorded the time, and took a final measurement of dissolved oxygen and temperature. All assembly and measurements began under red light, but once the lamps were turned on for the trials, all samples in-wait or post-trial were covered with light-blocking plastic.

We created experimental light treatments by placing either 0, 3, 7, 11, or 16 sheets of shade cloth between the water bath and a grow lamp, which was suspended at a constant height (Image B1). The water depth was insufficient to include a light sensor in the water bath, so we determined the light level experienced by the sample using the Beer-Lambert Law irradiance attenuation equation with surface light measurements taken with a LI-COR sensor, turbidity of the tap water within the water-bath equal to 0.14 NTU, and a sample depth of 2.54 cm (*Equation 1*). Dark light treatments were conducted without the use of the grow lamp.

Equation 1

$$PAR_z = PAR_0 \cdot e^{(-K_d \cdot z)}$$

For calculating the underwater light level for each sample, where:

- PAR_z = the light at the bottom of the water bath or river (μmol photons m^{-2} s^{-1}).
- PAR_0 = the measured surface light (μmol photons m^{-2} s^{-1}) at the location of the biomass sample
- z = the water depth (m) of the biomass sample
- K_d = the diffuse attenuation coefficient (m^{-1}), calculated as:

$$K_d = 1.0 + (0.02 \cdot \overline{NTU})$$

- $\overline{NTU}$ = the turbidity in Nephelometric Turbidity Units of the tap water or on the day of the biomass sampling event

Laboratory Processing

We quantified biomass as ash-free dry mass (AFDM) rather than using chlorophyll *a* as an indicator of photosynthetic activity because we ultimately wanted to express rates on a per-mass basis (Bowden et al. 2017) for all producer types. We measured the volume of liquid (ml) remaining in vials after the final measurements to use in calculating biomass of either seston or soft substrate. For soft substrate and a select number of vials of seston, we then filtered the measured liquid onto 0.7 µm glass fiber filters (GFFs) to determine ash free dry mass (AFDM). For vials with rocks or filamentous algae, we discarded the liquid after measuring the volume and further processed the filamentous algae or producer material on the rocks or to determine AFDM. If we could not process the rocks immediately following their removal from the vials, we refrigerated them in polyethylene bags in the interim. To process rocks, we first removed any *Podostemum* material with a razor blade and placed the material into a weigh-tin. We then brushed and rinsed the rocks, collected the resulting slurries, which we filtered onto 0.7 µm GFFs and placed in weigh-tins. For filamentous algae, we removed the algal material and placed into weigh-tins. For soft substrate, we filtered the contents of the vial onto 0.7 µm GFFs and placed into weigh-tins. All weigh-tins were pre-ashed, and all GFFs were pre-ashed (i.e., combusted at 500° C) and pre-weighed. To determine a representative AFDM (g ml^{-1}) of seston and soft substrate, we processed additional subsamples that were stored in the refrigerator. All producer material was dry-weighed within the tins, combusted at 500° C, and reweighed to determine AFDM (g for vial contents and g ml^{-1} for representative samples).

Calculating Mass-specific GPP

We used the software R for all data preparation and analysis (R Core Team 2025). We grouped producers into the following general categories: *Podostemum*, rock biofilm, filamentous algae, soft substrate biofilm, and seston. We also conducted analyses with the producers further separated into types: *Podostemum* on rocks from the shade, *Podostemum* on rocks from the sun, rock biofilm from the shade, rock biofilm from the sun, filamentous green algae *Rhizoclonium* sp., filamentous cyanobacterium *Lyngbya* sp., soft substrate (silt) from the shade, soft substrate (sand) from the sun, downstream seston from July 29, upstream seston from July 29, and downstream seston from August 3. To determine mass-specific producer productivity rates, we first calculated the change in dissolved oxygen (mg O^2 L^{-1} min^{-1}) for each vial per trial. For vials in the dark, this change was ecosystem respiration (ER). For vials under one of the five experimental light conditions, this value was net ecosystem productivity (NEP). Whether the functional rate of the vial was comprised of one or more different producers depended upon the sample type. For instance, functional rates for vials of rocks with *Podostemum* was comprised of contributions from *Podostemum* on the rock, biofilm on the rock, and seston from the stream water versus soft substrate, which was comprised of biofilm from the soft substrate sample and seston from the stream water used in dilution.

Once a change in dissolved oxygen was calculated for each vial per trial, vials from light trials (i.e., NEP values) were matched with an appropriate dark trial (i.e., ER value). At least one set of vials per producer type underwent a dark trial in addition to one light condition and therefore had both an NEP and corresponding ER value. Our methodology is consistent with Conn et al. (Ch.2) in that we assume soft substrate and stream water to be homogenized. Thus, for soft substrate and stream water vials, once we had a set of vials that underwent a

corresponding dark trial, we used the mean ER of those vials as the ER value for the vials under the remaining light conditions. We then matched each rate with the appropriate producer masses, at which point we separated out any biofilm and/or seston included in the vial to isolate the producer of interest. For all vials except those containing soft substrate and stream water, AFDM of the producer of interest was directly weighed from the vial contents. Per our assumption of homogeneity, we used an average AFDM from representative subsamples for most stream water vials and some soft substrate vials. However, when available, we used the most precise values possible, regardless of the assumption of homogeneity. We then used *Equations 2-5* to calculate GPP for the producer of interest for each vial under a specific light condition.

Equation 2

$$GPP_S = \frac{(NEP - ER) \times V}{AFDM}$$

For calculating GPP of seston, where:

- GPP_S = mass-specific GPP contribution of seston for vial (mg O_2 g^{-1} h^{-1})
- NEP = Δ DO from light run of current vial (mg O_2 L^{-1} h^{-1})
- V = volume of stream water collected from vial (L)
- ER = Δ DO from corresponding dark run of the vial or Δ DO from the dark run of another subsample undergoing the same light treatment (mg O_2 L^{-1} h^{-1})
- $AFDM$ = AFDM of seston taken directly from the vial or mean AFDM from representative subsamples of the same sample scaled to the vial volume (g)

Equation 3

$$GPP_i = \frac{\left((NEP - ER) \times V\right) - \left((NEP_S - ER_S) \times V_{ml}\right)}{AFDM_i}$$

For calculating GPP of rock biofilm or filamentous algae, where:

- GPP_i = mass-specific GPP contribution of producer i for vial (mg O_2 g^{-1} h^{-1})
- NEP = Δ DO from light run of vial (mg O_2 L^{-1} h^{-1})
- V = volume of stream water collected from vial (L)
- ER = Δ DO corresponding dark run for vial (mg O_2 L^{-1} h^{-1})
- NEP_S = Mean NEP for seston from the same stream water sample for the same light treatment or NEP for seston from the stream water subsample undergoing the same trial (mg O_2 ml^{-1} h^{-1})
- ER_S = Mean NEP for seston from the same stream water sample or NEP for seston from the stream water subsample undergoing the same trial (mg O_2 ml^{-1} h^{-1})
- V_{ml} = volume of stream water collected from vial (ml)
- $AFDM_i$ = AFDM of the producer i (g)

Equation 4

$$GPP_{SS} = \frac{\big((NEP - ER) \times V\big) - \big((NEP_S - ER_S) \times P\big)}{AFDM - (\overline{AFDM}_S \times P)}$$

For calculating GPP of soft substrate biofilm, where:

- GPP = mass-specific GPP contribution of biofilm for vial (mg O_2 g^{-1} h^{-1})
- NEP = Δ DO from light run of current vial (mg O_2 L^{-1} h^{-1})
- ER = Δ DO from corresponding dark run of the vial or Δ DO from the dark run of another subsample from the same field sample (mg O_2 L^{-1} h^{-1})
- V = volume of stream water collected from vial (L)
- NEP_S = NEP for seston from the same subsample undergoing the same trial scaled to a vial or mean NEP for seston from the same stream water sample for the same light treatment scaled to a vial (mg O_2 h^{-1})

- ER_S = ER for seston from the same subsample undergoing the same trial scaled to a vial or mean ER for seston from the same sample under the same light treatment scaled to a vial (mg O_2 h^{-1})
- P = proportion of stream water based on sample dilution
- $AFDM$ = AFDM of biofilm and stream water taken directly from the vial or mean AFDM from representative subsamples of the same field sample scaled to the vial volume (g)
- $AFDM_S$= Mean AFDM of seston in a vial of the same stream water sample (g)

Equation 5

$$GPP_{PC} = \frac{\left((NEP - ER) \times V\right) - \left((\overline{NEP}_{BA+S} - \overline{ER}_{BA+S}) \times AFDM_{BA}\right)}{AFDM_{PC}}$$

For calculating GPP of *Podostemum* on rocks, where:

- GPP_{PC} = mass-specific GPP contribution of *Podostemum* for vial (mg O_2 g^{-1} h^{-1})
- NEP = Δ DO from light run of vial (mg O_2 L^{-1} h^{-1})
- ER = Δ DO from corresponding dark run (mg O_2 L^{-1} h^{-1})
- V = volume of stream water collected from vial (L)
- $\overline{NEP}_{BA+S}$ = Mean mass-specific NEP for vials of rock biofilm and seston from the same stream light environment under the same light treatment (mg O_2 g^{-1} h^{-1})
- $\overline{ER}_{BA+S}$ = Mean mass-specific ER for vials of rock biofilm and seston from the same stream light environment (mg O_2 g^{-1} h^{-1})
- $AFDM_{BA}$ = AFDM of filtered biofilm from the vial (g)
- $AFDM_{PC}$ = AFDM of *Podostemum* picked off rock from the vial (g)

Multiple vials with soft substrate and seston produced negative GPP values. There are multiple scenarios that could result in negative values, the most likely of which are that the assumption of homogeneity was invalid at such a small scale (i.e. averaged AFDM and/or ER was inappropriate) or respiration increased under light. Some soft substrate and seston vials with exact measurements of AFDM and/or ER (i.e. no assumption of homogeneity necessary) still produced negative values for GPP, suggesting that in at least some cases respiration rates did increase under light. Because the possible scenarios resulting in negative GPP values consistently require extremely low rates of productivity, we considered the GPP rates in those vials to be negligible and replaced them with zeros for further calculations.

We calculated a mean GPP from the individual vials (or averaged across samples, in the case of soft substrate) of each producer group and type for each light treatment. We also calculated a mean GPP per producer group and type across light treatments. For *Podostemum* and rock biofilm, the unit of replication was an individual rock out of the many rocks from multiple field samples in a given stream light environment. For filamentous algae, a replicate was a subsample from one of the two field samples corresponding to either *Rhizoclonium* sp. or *Lyngbya* sp. However, each of the soft substrate field samples – four from each stream light environment – was considered a replicate, thus soft substrate vials were averaged by field sample before averaging by producer type or group.

Evaluating the Effects of Light and Producer Type on Mass-specific GPP

To evaluate the direct effect of varying irradiance and indirect, antecedent mediation of stream light level on gross primary productivity, along with substrate and taxon, we conducted ordinary least squares linear regression (Table 3.1). We predicted mass-specific GPP for all producers by group or type and/or experimental light treatment (n = 121). We also conducted a regression analysis for each producer group predicting mass-specific GPP by type and/or

experimental light treatment (n ~ 30 per producer). For models predicting GPP by a producer category and experimental light treatment, we included an interaction term. We ranked models using the Akaike information criterion (AIC) (Burnham and Anderson 2002) and included all models with Δ AIC ≤ 2 as "competitive models" for evaluating the role of the light and type. We considered a predictor to be a significant driver of GPP when the variables were present in competitive models. We also qualitatively assessed the shape of the relationship between experimental light and mass-specific GPP for each producer group and type and compared the magnitude and variability of GPP rates between producer groups or types at each light level.

Calculating Areal Productivity and Assessing Producer Contribution to Segment GPP in the Middle Oconee River

To illustrate producer contribution to stream areal productivity, we calculated mean GPP per producer(mg O_2 g^{-1} h^{-1}) per segment (i.e. upstream run or downstream shoal) over a three-year period of variable flow conditions. We used biomass samples taken from the same stream reach from 2016-2018 (Conn et al. Ch.2). To align the categories in the biomass study with our producer types, we separated biomass of the producer biofilm into soft substrate biofilm and rock biofilm, the latter corresponding to biofilm from bedrock, fixed rock, large removable rock, and small removable rock. We assigned blocks 2-4 (central channel) of the biomass study transects as representative of a sunny light environment and blocks 1-5 as representative of a shady light environment (Figure 3.2). We excluded transect seven from the contribution illustration because our sample collection occurred only in the run and downstream shoal. We also excluded sampling events after July 2017 as no light measurements were available for the sample locations. The processing notes from the biomass study indicated whether each filamentous algae

sample was the chlorophyte or the cyanobacterium and later identified samples of both types as *Rhizoclonium* sp. and *Lyngbya* sp., so we assigned them accordingly.

We assigned each sample to a light condition of either shade or sun, and calculated a light level experienced by each sample using the Beer-Lambert Law irradiance attenuation equation (*Equation 5*). Once a sample light level was calculated, we matched each biomass sample to the mass-specific GPP rate corresponding to its assigned type at a light level that was closest to the light level of the sample. This process included the following assumptions:

- Mass-specific GPP rates assigned to each producer group and type remain representative over time even with potential changes, such as community composition or producer quality
- Mass-specific GPP rates on small rocks are the same as for larger hard substrates
- Mass-specific GPP rates are the same in both segments
- All samples within blocks 1 and 5 of the biomass study are shaded
- Instantaneous light levels measured at the biomass sample location are representative of the location's general light conditions over time

After each sample was assigned a mass-specific productivity rate (mg O_2 g^{-1} h^{-1}), we calculated an areal productivity rate (mg O_2 m^{-2} h^{-1}) and converted the rate into g C m^{-2} day^{-1} (*Equation 6*).

Equation 6

$$GPP_C = (R_{GPP} \cdot B) \times CF_{t\,\&\,m} \times CF_{PQ}$$

For calculating sample GPP in g C m^{-2} day^{-1}, where:

- GPP_C = areal gross primary productivity (g C m^{-2} day^{-1})
- R_{GPP} = mass-specific GPP rate (mg O_2 g $AFDM^{-1}$ h^{-1})

- B = sample biomass (g AFDM m^{-2})
- $CF_{t\ \&\ m}$ = time and mass conversion factor, calculated as:

$$CF_{time} = \frac{24\ h\ day^{-1}}{1000\ mg\ g^{-1}} = 0.024$$

- CF_{PQ} = metabolic conversion factor using a photosynthetic quotient (PQ) of 1.2 (Bott 2007) and calculated as:

$$CF_{PQ} = \frac{12\ g\ C\ mol\ C^{-1}}{32\ g\ O_2\ mol\ O_2{}^{-1} \times 1.2\ mol\ O_2\ mol\ C^{-1}} = 0.3125$$

After assigning each sample an areal productivity rate, we calculated a mean GPP (g C m^{-2} day^{-1}) per producer for each segment and a total GPP (g C m^{-2} day^{-1}) per segment for each of the 13 sampling events. We considered the proportion of total GPP from each producer's mean GPP as the 'producer contribution'. We then quantified producer contribution to total GPP relative to producer contribution to total AFDM (quantified as the proportion of total AFDM from each producer's mean AFDM), which we refer to as the 'relative GPP contribution' (*Equation 7*).

Equation 7

For calculating the relative GPP contribution for each producer, where:

$$C_i = \frac{\left(\frac{GPP_i}{\sum_{j=1}^{n} GPP_j}\right)}{\left(\frac{B_i}{\sum_{j=1}^{n} B_j}\right)}$$

- C_i= relative GPP contribution for producer i
- GPP_i= Areal GPP (g C m^{-2} day^{-1}) of producer i
- B_i= Areal biomass (g AFDM m^{-2}) of producer i
- $\sum_{j=1}^{n} GPP_j$= Total areal GPP of all n producers in the community
- $\sum_{j=1}^{n} B_j$= Total areal biomass of all n producers in the community

We interpreted the relative GPP contribution in relationship to the 1:1 proportionality line, where:

- $C_i > 1$ indicates a disproportionately high functional contribution. The producer's contribution to stream GPP exceeds its structural presence.
- $C_i \approx 1$ indicates a proportional functional contribution. The producer's contribution to GPP is proportional to its structural presence.
- $C_i < 1$ indicates a disproportionately low functional contribution. The producer's contribution to GPP falls short of its structural presence.

For data visualization, we applied a log-plus-one transformation to the index value. This transformation shifted the proportionality line from 1 to ln(2) ≈ 0.693. While the transformation changed the numerical value, the conceptual meaning remained the same: values above, on, or below the new line still indicated greater than, proportional to, or less than expected relative GPP contribution, respectively.

RESULTS

We found that rock biofilm and filamentous algae had consistently higher mass-specific GPP than *Podostemum* and soft substrate biofilm across all light levels, while seston was highly

variable (Figures 3.2, 3.3, B1). When producers were separated by type, *Podostemum* and soft substrate biofilm's GPP remained substantially lower than that of rock biofilm, filamentous algae, and some types of seston across all light levels (Figures 3.4, 3.5, B2). We found that an interactive effect of experimental light level and producer type was the best predictor of mass-specific GPP for global models – benthic producers and all producers (i.e. including seston) – and for all group-specific models with the exception of soft substrate (Table 3.2). Patterns for mean areal GPP were reversed for some producer groups relative to patterns for mean mass-specific GPP, especially when rates were separated by segment, and on average, the lower shoal was more productive than the run (Table 3.3).

Mean mass-specific GPP varied across light levels within and between producer groups (Figures 3.6-3.11). While *Podostemum* and rock biofilm producer groups exhibited positive GPP-PAR relationships, mean GPP decreased under full light conditions for samples from the shade while consistently increasing with PAR for samples from the sun (Figures 3.6 and 3.7). For both groups, samples from the sun exhibited higher maximums of mean GPP, consistently elevated values across all light levels, and stronger positive relationships with PAR (Figures 3.6 and 3.7). The filamentous green algae *Rhizoclonium* exhibited a similar GPP-PAR relationship as *Podostemum* and rock biofilm from the sun, while the filamentous cyanobacterium *Lyngbya* was similar to *Podostemum* and rock biofilm from the shade (Figure 3.8). However, the contrast between *Rhizoclonium* and *Lyngbya* was more pronounced. *Rhizoclonium* had substantially higher mean GPP values, reached its maximum at higher PAR levels, and showed greater variability around the means compared to *Lyngbya*. In contrast, soft substrate biofilm and seston producer groups both exhibited negative GPP-PAR relationships (Figures 3.9-3.11). For soft substrate biofilm, this negative GPP-PAR relationship occurred across all stream light

environments/substrates (Figure 3.9). For seston, the negative GPP response to PAR was variable across producer types (and/or subsets). Some types, such as August downstream seston, exhibited a positive relationship, and the magnitude of the means and PAR level at which the maximum occurred also varied across types (Figure 3.10 and 3.11).

The top model for *Podostemum* and rock biofilm included an interaction between PAR and the stream light environment while the top model for filamentous algae included an interaction between PAR and taxon. The top model, and only competitive model, for soft substrate excluded PAR. Soft substrate biofilm was best predicted by stream light environment, which was associated with substrate. While the top model predicting seston included an interaction between PAR and the sample type, the models predicting GPP by stream position and collection date were also competitive (i.e., within 2 AIC of the top model). Rock biofilm was the only producer group with a top model with an explanatory power above 50% (Adj. $R^2 = 0.63$), though both global top models had an explanatory power near 40% (Adj. $R^2 = 0.37$ for all producers and 0.41 for benthic producers) (Table 3.2). All other top models had an explanatory power of less than 25% with soft substrate biofilm being the only producer group with a top model with less than or equal to 10% (Adj. $R^2 = 0.24$ for *Podostemum*, 0.23 for filamentous algae, 0.10 for soft substrate and 0.15 for seston).

The ranking of producers by areal GPP was largely opposite the ranking of producers by mass-specific GPP, which also differed between segments (Table 3.4). Soft substrate, which had the lowest mass-specific GPP and areal GPP in the lower shoal, had the highest areal GPP in the run. Similarly, *Podostemum*, which had the second lowest mass-specific GPP, had the highest areal GPP in the lower shoal and the reach as a whole. Filamentous algae, which had the highest mass-specific GPP, also had a relatively high areal GPP rate– the second highest areal GPP in

the run and the reach as a whole while never ranking the lowest. The disparity between mean productivity rates, as measured by the normalized range ratio, was smaller for overall areal GPP than mass-specific GPP (1.08 and 2.14 respectively). However, when areal GPP was considered by segment, the disparity between the highest and lowest productivity rate was larger for lower shoal areal GPP than mass-specific GPP (2.14 to 2.69 respectively).

When areal GPP was calculated for the study section of the Middle Oconee River, rock biofilm and filamentous algae demonstrated a consistently high relative GPP contribution across sampling events and river segments (Figure 3.12). Filamentous algae, when present, typically had the highest relative contribution of GPP. In contrast, soft substrate consistently had the lowest relative GPP contribution, with only one data point near the proportionality line. *Podostemum*'s relative GPP contribution varied across segments: it was lower (near or below the proportionality line) in the lower shoal across sampling events, but more often high in the run, though to a lesser extent than filamentous algae and rock biofilm.

DISCUSSION

Our results suggest that producers vary in their contribution to stream productivity, reflecting differences in mass specific GPP-light relationships and in this system, biomass dynamics driven by producer-specific responses to antecedent flow conditions. When producers were grouped broadly by morphology and also when subdivided by stream light environment or taxon, we observed contrasting responses to varying irradiance in terms of magnitude, direction, peak, and overall shape of the photosynthesis-irradiance (PI) curve (e.g., saturation, photoinhibition, continuous light-limitation). Overall, the differences between producers in GPP-light relationships was consistent with expectations based on prior literature. Light availability in the stream environment, in addition to irradiance, was an important predictor of overall mass-

specific GPP and of mass-specific GPP for a particular producer group (with the exception of soft substrate biofilm). Interestingly, when mass-specific GPP rates were incorporated into a two-year biomass dataset, high mass-specific GPP rates did not correspond to high biomass, thus productive capacity did not uniformly determine contribution to overall stream productivity. Given the role of antecedent flow conditions in determining biomass patterns in this system and the potentially disproportionate contribution of *Podostemum* to areal GPP, these results implicate producer-specific variability as a mechanism by which overall stream function could be altered.

Determinants of Mass-specific GPP

While light is a fundamental requirement for photosynthesis, producers differ in their capacities to convert light into energy (as measured by GPP). Consequently, there is no universal optimal level of irradiance, nor a consistent relationship with irradiance for all producers to maximize productivity (Yang et al. 2020). However, light availability is a consistent constraint of GPP (Bernhardt et al. 2022). Further, greater specificity of benthic light conditions (i.e., factoring in light attenuation of incident surface light) can improve stream GPP predictions (Kirk et al. 2021). Thus, while light availability is limited by the seasonal photoperiod and extent of canopy cover, and then further decreases via water-column attenuation, our laboratory trials indicate that producers also have fundamentally different capacities and limits to their productivity. These relationships were not necessarily generalizable within a producer group. In both global and group-specific regression analyses PAR and 'type' (representative of distinctions in stream light environment or taxon) were important predictors of mass-specific GPP.

For both rock biofilm and *Podostemum*, stream light environment appeared to affect the capacity to increase productivity with increasing irradiance, though more data, especially additional light levels, is necessary to confirm these trends. Rock biofilm and *Podostemum*

samples from the sun became more productive with increasing irradiance while samples from the shade appeared to exhibit saturation and/or photoinhibition - reaching a maximum, after which GPP leveled off or slightly decreased. For *Podostemum*, which was the only single-species producer of the groups, samples from the sun are likely more indicative of an ultimate capacity for GPP, but even so, these results suggest that responses to environmental disturbance, such as decreasing riparian vegetation, could have short-term counterintuitive effects on stream productivity (e.g., producers conditioned to shade may not capitalize on the increased light availability).

Podostemum had lower rates of GPP than rock biofilm and filamentous algae across all light levels, which is consistent with general expectations based on the physiology of vascular plants in comparison to algae (Allan et al. 2021). For vascular plants, however, *Podostemum* is highly productive, and we documented GPP rates much higher than those previously recorded by Hill and Webster (1984) in the New River, VA. This is unsurprising given the relative lack of macroinvertebrates or detritus on our small rock samples compared to the larger substrates used in the Hill and Webster (1984) recirculating chambers, and to what is found in-stream in the Middle Oconee River.

Filamentous algae exhibited a similarly divergent response to irradiance: *Rhizoclonium* GPP exhibited no saturation while *Lyngbya* exhibited photoinhibition at higher irradiance. Given their phylogenetic difference – *Rhizoclonium* sp. (Chlorophyta) and *Lyngbya* sp. *(*a filamentous cyanobacterium) – it is not surprising that the two exhibited distinct responses to irradiance. These results align with prior research showing that *Rhizoclonium* has a wide tolerance range of light levels (Aroca et al. 2020) and *Lyngbya* an affinity for lower light (Bridgeman and Penamon 2010). Because some species of *Lyngbya* produce cyanotoxins (Carmichael et al. 1997,

Lajeunesse et al. 2012), their ability to reach maximum GPP at a lower light level is uniquely relevant to ecosystem and human health. While many filamentous green algae are adapted to moderate-to high light conditions, *Lyngbya* may pose a health concern even under low light conditions, such as streams where riparian buffers remain intact or their downstream reservoirs. Interestingly, LeRoy et al. (2023) found that even dramatic alterations to canopy cover do not necessarily shift stream algal species composition. For a species like *Rhizoclonium*, increased light could release constraints and boost GPP, whereas for rock biofilms and *Podostemum* from the shade, the initial response may be limited.

Soft substrate biofilm and seston were the only two groups to exhibit inverse relationships with irradiance and also the two groups with the least predictive models. Soft substrate biofilm was also the only producer group for which PAR was not in the top models predicting mass-specific GPP. Prior research has documented lower rates of GPP in sand and soft sediment in comparison to hard substrates (Hoellein et al. 2009) and attributed this reduction to increased instability (Atkinson et al. 2008): fine sediments are commonly disturbed, even mobile under low-flow conditions, and materials can be periodically, if not entirely, buried. Marcarelli et al. (2015) confirmed that the lower rate of GPP in sand is due not only to lower standing stocks, but also lower productivity rates. The only predictor in the top model for sand and soft substrate, stream light environment, was also associated with substrate – sand in the sun vs. silt in the shade. While biofilms from both sand and soft sediment consistently had low GPP rates in comparison to other producers, our findings are similar to those of Hoellein et al. (2009) who found that sand had higher GPP rates than that of fine benthic organic matter (FBOM). While FBOM refers specifically to the organic matter, it is typically associated with silt over

sand and our silt samples had a higher mean g AFDM ml^{-1} than that of sand samples, though more data would be needed to confirm this trend as ±1 SD ranges overlapped.

In contrast to soft substrate, the negative overall relationship between seston and PAR did not hold for all types –individual samples varying in both date and location relative to the first-order tributary. Samples exhibited differences in magnitude, light level at which maximum occurred, and the overall direction and shape of the relationship. Depending upon the light level and sample, seston samples exhibited low to no GPP as well as high GPP, with the GPP of certain samples occasionally surpassing even the GPP of filamentous algae, and at other times on par with both rock biofilms and/or filamentous algae. These findings are simultaneously consistent with the Conn et al. (Ch.2) biomass study where no detectable Chl-*a* was found in the water column of the same study reach, and the findings of Reisinger et al. (2015, 2021) where the water column was found to significantly contribute to ecosystem function, both stream metabolism and nutrient uptake, in multiple mid-sized rivers. The potentially high magnitude of seston GPP is also consistent with physiological differences between phytoplankton and other benthic algae, such as a higher surface area to volume ratio (Steinman et al. 1992b, Lange et al. 2016). While the top model for seston included both PAR and sample, all single predictor models describing the attributes of the sample (i.e., sample, collection date, and stream position) were competitive. Interestingly both downstream locations had an overall positive relationship with PAR, though considerable variation in magnitude. These differences between samples are likely indicative of the high turnover rate of suspended producers in the water column and given that the two samples exhibiting a positive relationship were downstream, inputs from the upstream tributary.

Producer Contribution to Stream Productivity and Potential Implications

Our primary producer groupings are coarse distinctions in morphology – vascular plants, multicellular filaments, prostrate algal/microbial assemblages, or unicellular phytoplankton – and associated substrate – hard, soft, or free-floating. These differences in growth form and attachment to particular substrates (or lack thereof) reflect distinctions in localized habitats and susceptibility to disturbance, which influence producer biomass and are also linked to physiological determinants of productivity. For example, individual biofilm assemblages are indisputably unique in their biotic constituents (Battin et al. 2016), and those on soft substrate are particularly susceptible to flow disturbance in ways that differ from biofilms on hard substrate, and both types distinct from mats of filamentous algae. Thus, while further subdivision based on stream light environment or taxon might best predict the GPP-light relationship, the biomass of many broader producer groupings can be reliably predicted by abiotic factors operating at larger temporal and spatial scales.

General relationships between growth form and disturbance susceptibilities are relatively established in the literature (Biggs and Thomsen 1995, Biggs et al. 1998, Riis and Biggs 2001, 2003b, Francoeur and Biggs 2006, Suren and Riis 2010), though seldom empirically validated for a diverse producer community such as this, even less frequently at scales correlating to environmental controls and/or management action. In this system, however, quantifiable differences in the responses of these producer groups to antecedent high and low flow conditions were documented in three years immediately prior to this study (Conn et al. Ch.2). This provides a unique opportunity to assess the relative contributions of different producers to stream productivity in the context of already established relationships with antecedent flow conditions and with a producer of disproportionate ecological importance and conservation concern.

When mass-specific GPP rates were incorporated into the two-year biomass data set from the same river reach, areal GPP rates did not exhibit the same patterns across producers as mass-specific GPP rates (i.e., the same producers that had high GPP did not have high biomass, and vice versa). Our findings from the laboratory trials indicate that producers have distinct mass-specific GPP, which for most broad groups and divisions of type, were relative to instantaneous light availability. However, these small-scale laboratory trials did not incorporate the full range of abiotic and biotic factors that are known to limit biomass accrual – herbivory, water column attenuation (via water depth and turbidity), or hydrologic disturbance, for example (Francoeur and Biggs 2006). In some instances, high production may be realized despite a lack of biomass – herbivores can exert top-down control that limits producer biomass accumulation, yet carbon is still transferred to the next trophic level, increasing biomass of consumers (e.g., Suren and Riis 2010). The decoupling of biomass and productivity highlights the importance of identifying the physiological and ecological mechanisms through which producers differentially contribute to stream productivity.

While rock biofilm and filamentous algae, and at some points seston, had substantially higher rates of mass-specific productivity, *Podostemum* and soft substrate biofilm were the overall two biggest contributors to stream productivity across time and space due to high biomass (seston was not included in the comparison). Given this high GPP contribution despite low productivity rates, soft substrate biofilm and to a lesser extent *Podostemum* were relatively inefficient in their contributions: their influence was largely a factor of biomass accrual and not high GPP. In contrast, rock biofilm, and especially filamentous algae (when present) had a high relative GPP contribution: their contribution to stream productivity was disproportionate relative to their contribution to overall biomass. Notably, *Podostemum* and rock biofilm consistently

dominated different segments, and filamentous algae and *Podostemum* both experienced periods of high biomass in the summer of 2016 while rock biofilm appeared to peak in the fall of 2016. Together, these differences in relative GPP contribution imply that shifts in environmental conditions – such as flow variability or disturbance – could have disproportionate effects on stream productivity and ecosystem functioning, depending on which producer groups are most impacted.

Given contrasting contributions, shifts in environmental conditions could influence stream function via different pathways (i.e., producers), and different mechanisms (e.g., flow or temperature acting on biomass and/or productivity). For example, in this illustration, increased duration and severity of low flow events, which *Podostemum* is negatively affected by, could have dramatic effects on stream metabolism given *Podostemum*'s disproportionate contribution to GPP and to secondary production via the provisioning of complex habitat (Wood and Freeman 2017). Given the current conservation concern around *Podostemum*, this may be an increasingly plausible scenario. While the resulting balance of changes to GPP and ER would ultimately affect stream metabolism are outside of the scope of this study, given *Podostemum*'s foundational role, the impact could be a fundamental shift across levels of production.

In contrast, increasing temperatures due to climate change could lead to even higher rates of GPP in *Rhizoclonium*, and while some species of the genus are moderately palatable in small amounts, herbivory decreases as dense algal mats form. This scenario is thus relevant to water management, as the water quality of the stream and most especially downstream reservoirs can be negatively affected if biomass accrues and the material is not consumed. Large amounts of microbial decomposition can lead to hypoxia. Further, when the filamentous algae contain

cytotoxins, increasing biomass presents additional health concerns for humans and wildlife (O'Neil et al. 2012, Gkelis et al. 2014, Paerl 2017).

While these results are specific to the Middle Oconee River, and serve as illustrative examples only, they highlight the importance of understanding the mechanisms underpinning stream function. Our study contains various assumptions (see Methods) and is also limited by the scale at which laboratory trials were conducted. Continued research is essential to predict how dynamics such as decoupling of biomass and productivity, varying contributions of different producers, and diverse environmental controls operate across scales and in different systems. Experimental research examining the effects of localized stimuli on producer function already exists in abundance for many taxa, as do *in situ* mesocosms of assorted temperate benthic communities, and high frequency stream metabolism data, which has been used to identify environmental drivers of large-scale patterns in stream metabolism. Linking these scales offers an opportunity to evaluate how these mechanisms propagate from local processes to overall stream function. These linkages are critical for understanding stream ecosystem functioning under increasing global change and in the context of different management strategies.

TABLES

Table 3.1: Predictor variables for regression analysis of mass-specific GPP. PAR is a discrete numerical variable describing the experimental treatment of the sample. All other predictor variables are factors describing the producer category or stream environment of the sample. Collection date was only considered as a factor for water samples.

Predictor Variable	Metric Description	Unit	Categories
PAR	Photosynthetic active radiation level of experimental light treatment	μmol m^{-2} s^{-1}	(1) PAR 90 (2) PAR 224 (3) PAR 452 (4) PAR 941 (5) PAR 1625
Producer	General producer group of sample	—	(1) PC - *Podostemum* (2) BA – rock biofilm (3) FA – filamentous algae (4) SS – soft substrate biofilm (5) WC - seston
Type	Specific subset of producer group of sample	—	(1) *Podostemum* from shade or (2) sun (3) Rock biofilm from shade or (4) sun (5) Filamentous green alga or (6) blue-green algae (7) Soft substrate biofilm from shade or (8) sun (9) Seston from above or (10) below tributary in July or (11) seston from below tributary in August
Stream light for PC or BA	Stream light environment of sample	—	(1) Shade – river edge with tree cover (2) Sun – open-canopy central channel
Taxa	Taxon of filamentous algae sample	—	(1) Green alga *Rhizoclonium* (2) Cyanobacterium *Lyngbya*
Stream light for SS	Stream light environment and substrate of biofilm sample	—	(1) Silt biofilm from shade (2) Sand biofilm from sun
Sample	Sample with unique stream position and collection date	—	(1) Upstream July seston (2) Downstream July seston (3) Downstream August seston
Stream position	In-stream location of water sample relative to tributary	—	(1) Upstream = above tributary (2) Downstream = below tributary
Collection date	Water sample collection date	—	(1) 29 July 2020 (2) 03 August 2020

Table 3.2: Mean areal gross primary productivity (g C m-2 day-1) of segment total GPP, producer mean GPP, and producer mean GPP by segment across 13 sampling events. Type is not a producer category for areal GPP as it was used to assign the mass-specific GPP rate for the calculation of areal GPP.

Level	Segment	Producer	Mean GPP	Standard Deviation	n
Overall Segment	Lower Shoal	All	5.27	7.31	19
Overall Segment	Run	All	3.27	4.7	18
Overall Producer	All	Rock biofilm	2.71	4.56	37
Overall Producer	All	Filamentous algae	1.08	1.03	37
Overall Producer	All	*Podostemum*	1.27	3.79	37
Overall Producer	All	Soft substrate biofilm	1.06	2.4	37
Producer by Segment	Lower Shoal	*Podostemum*	5.23	5.43	19
Producer by Segment	Lower Shoal	Rock biofilm	1.45	1.14	19
Producer by Segment	Lower Shoal	Filamentous algae	0.96	2.55	19
Producer by Segment	Lower Shoal	Soft substrate biofilm	0.06	0.15	19
Producer by Segment	Run	*Podostemum*	0.19	0.13	18
Producer by Segment	Run	Rock biofilm	0.71	0.79	18
Producer by Segment	Run	Filamentous algae	1.57	4.81	18
Producer by Segment	Run	Soft substrate biofilm	2.05	3.13	18

Table 3.3: All competitive models (ΔAIC < 2) predicting GPP (mg O2 g^{-1} h^{-1}) of all producers (i.e., including seston), benthic producers , *Podostemum*, rock biofilm, filamentous algae, soft substrate biofilm, and seston. 'Type' in the top models for all and benthic producers refers to the specific distinction between subsets of a producer group. The specific Type variable for each producer group is identified in the producer-specific models.

Competitive Models	n	Adj. R^2	PAR Range		Type Range		PAR × Type Range		ΔAIC	AIC wt
All Producers	164									
GPP ~ PAR + Type + PAR×Type		0.37	-0.012	0.039	-4.929	11.388	-0.017	0.034	—	1.00
Benthic Producers	121									
GPP ~ PAR + Type + PAR×Type		0.41	-0.001	0.039	-4.917	5.096	-0.006	0.034	—	1.00
Podostemum	30									
GPP ~ PAR + Stream light + PAR×Stream light		0.24	0.001	0.003	0.080	—	0.002	—	—	0.61
GPP ~ PAR		0.16	0.002	0.002	—	—	—	—	1.21	0.33
Rock Biofilm	30									
GPP ~ PAR + Stream light + PAR×Stream light		0.63	0.005	0.019	0.814	—	0.014	—	—	1.00
Filamentous Algae	29									
GPP ~ PAR + Taxon + PAR×Taxon		0.23	0.002	0.039	-3.351	—	0.037	—	—	0.74
Soft Substrate Biofilm	32									
GPP ~ Stream light		0.10	—	—	1.806	—		—	—	0.66
Seston	43									
GPP ~ PAR + Sample + PAR×Sample		0.15	-0.012	0.008	-8.218	8.099	-0.020	-0.040	—	0.28
GPP ~ Stream position		0.07	—	—	-7.693	—	—	—	0.31	0.24
GPP ~ Collection date		0.05	—	—	7.061	—	—	—	1.21	0.15
GPP ~ Sample		0.06	—	—	-9.936	-4.186	—	—	1.42	0.14

Table 3.4: Each producer's mean mass-specific and areal productivity rates. Mean mass-specific GPP is in units of g C g^{-1} day^{-1} while areal GPP is in units of g C m^{-1} day^{-1}. Mass-specific GPP is the mean of samples across all experimental light treatments for a given producer group. Areal GPP is the mean of means across sampling events for a given producer group. Type is not a producer category for areal GPP as it was used to assign the mass-specific GPP rate to biomass data of the Conn et al. (Ch.2) study to calculate areal GPP. Normalized range ratio: mass-specific GPP = 2.14, overall areal GPP = 1.08, run areal GPP = 1.65, and lower shoal = 2.68.

Producer	Mass-specific GPP	SD	Rank	Reach Areal GPP	SD	Rank	Run Areal GPP	SD	Rank	Lower Shoal Areal GPP	Rank	SD
Podostemum	1.42	1.03	**3**	2.71	4.56	**1**	0.19	0.13	**4**	5.23	**1**	5.43
Rock biofilm	6.15	5.24	**2**	1.08	1.03	**4**	0.71	0.79	**3**	1.45	**2**	1.14
Filamentous algae	10.31	15.42	**1**	1.27	3.79	**2**	1.57	4.81	**2**	0.96	**3**	2.55
Soft substrate biofilm	0.48	1.17	**4**	1.06	2.4	**3**	2.05	3.13	**1**	0.06	**4**	0.15

FIGURES

Figure 3.1: Study site diagram (A) and corresponding aerial photo (B) of the Middle Oconee River at Ben Burton Park in Athens, Georgia from the Conn et al. (Ch.2) study. This figure and the following description (modified) were taken from the original Conn et al. (Ch.2) manuscript to describe the data used in our assessment of producer contribution to productivity. A small, run-of-the-river hydropower facility currently exists upstream, beyond the extent of the aerial photo. The small brown square on river right of (A) indicates a municipal water intake facility across from a first-order tributary, Hunnicutt Creek. Transects begin at the downstream end of the reach with T1-T3 (lower shoal) below the tributary, and T4-T6 (run) and T7 (upper shoal) above the tributary. Transect 7 was not used in our study. Inset indicates the sampling design for each transect, stratified into 5 equal blocks with one randomly located, destructive sample (red dots) taken from each block, which results in a total of 35 samples across the entire reach. Shaded areas are assigned as B1 (river left) and B5 (river right), while sunny areas are assigned as the central channel B2 – B4.

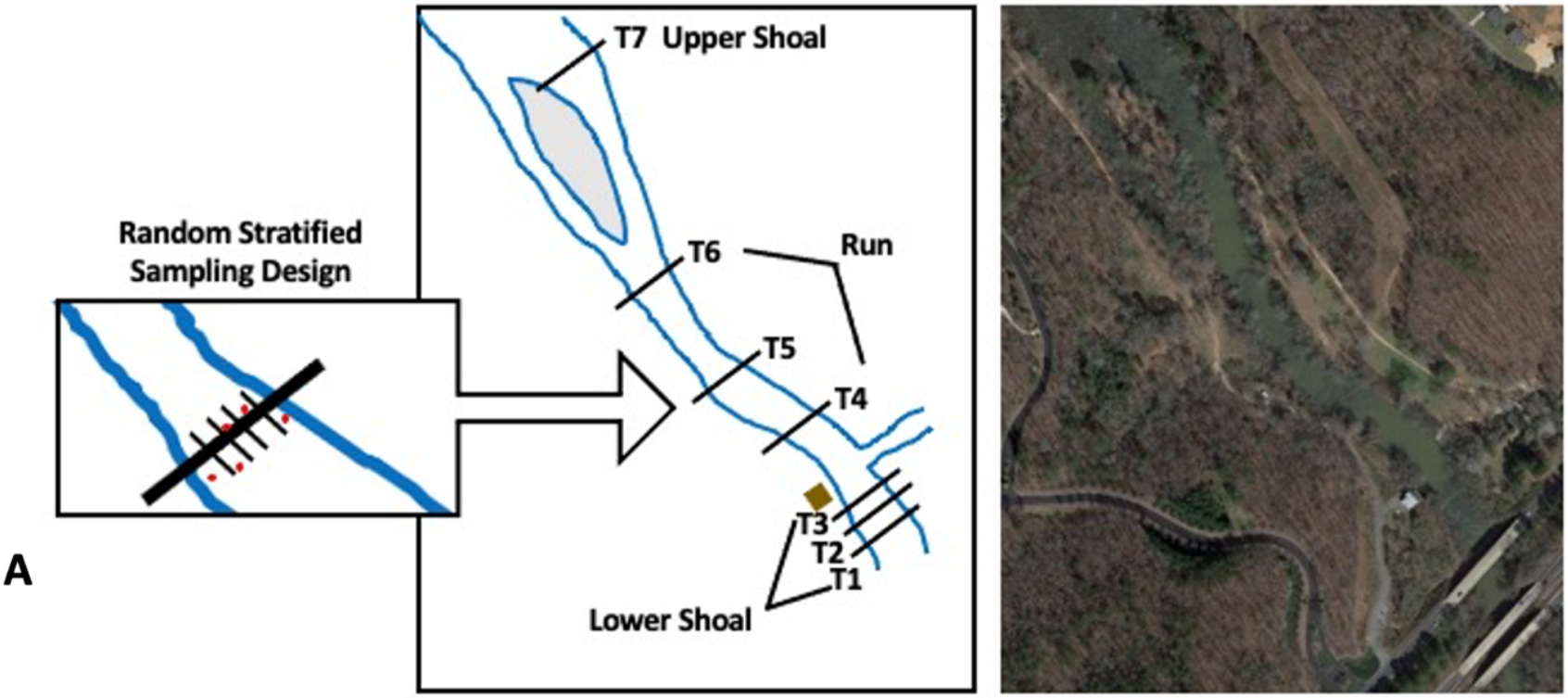
Random Stratified
Sampling Design
T7 Upper Shoal
T6
Run
T5
T4
T3
T2
T1
Lower Shoal
A
B
C

Figure 3.2: Mass-specific GPP across producer groups. Boxplots display GPP (mg O_2 g^{-1} h^{-1}) for all light levels combined (μmol photons m^{-2} s^{-1}) using a discontinuous y-axis. The top panel shows high-GPP values (190-200 mg O_2 g^{-1} h^{-1}), containing one filamentous algae outlier, while the bottom panel displays the remaining data (0-50 mg O_2 g^{-1} h^{-1}). Boxes represent the interquartile range (25th-75th percentiles) with median line; whiskers extend to 1.5×IQR.

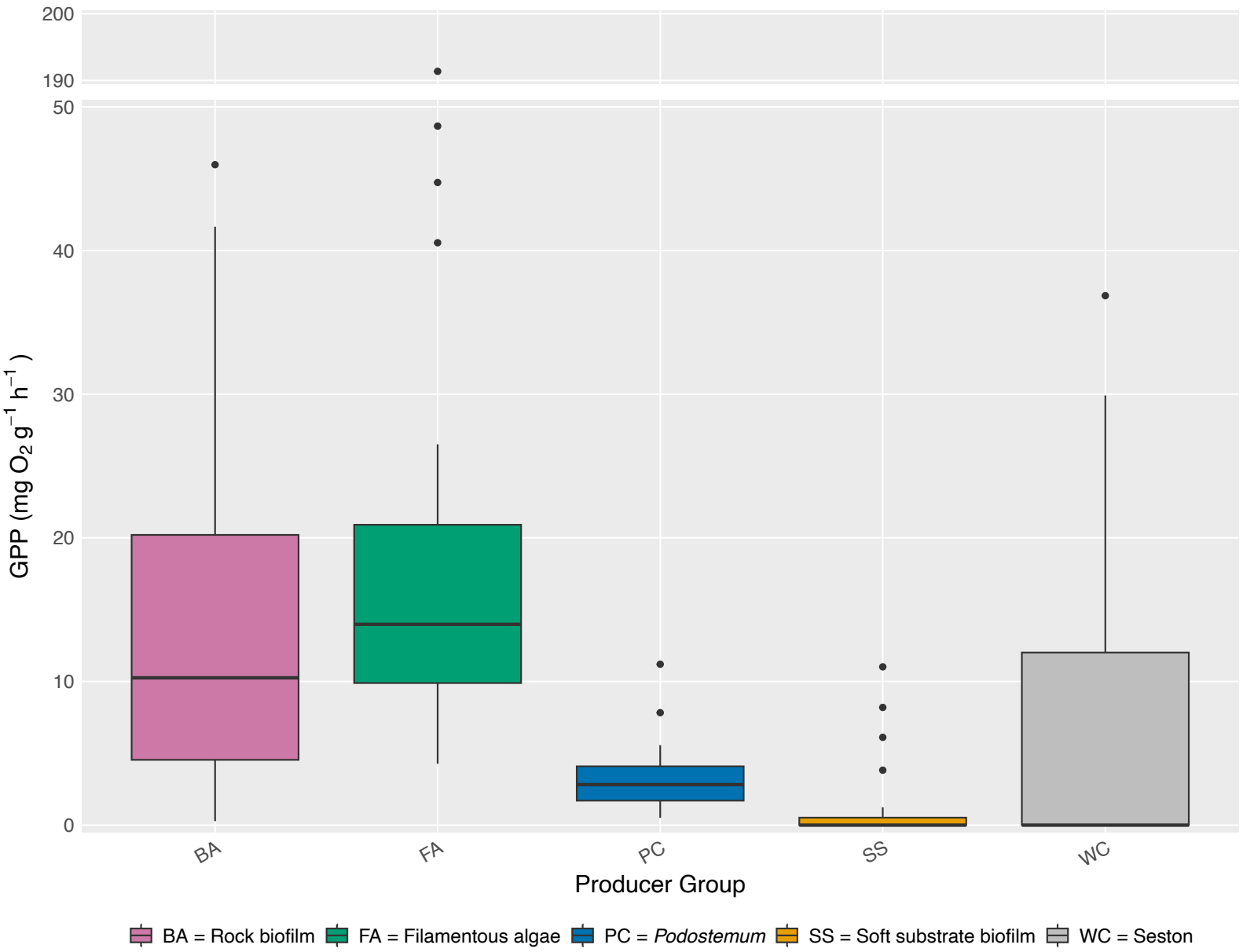
200
190
50
40
30
20
10
0
GPP (mg O2 g-1 h-1)
BA
FA
PC
SS
WC
Producer Group
BA = Rock biofilm
FA = Filamentous algae
PC = Podostemum
SS = Soft substrate biofilm
WC = Seston

Figure 3.3: Mass-specific GPP across producer groups by light treatment. Boxplots display GPP (mg O_2 g^{-1} h^{-1}) by experimental light treatment (μmol photons m^{-2} s^{-1}). Boxes represent the interquartile range (25th-75th percentiles) with median line; whiskers extend to 1.5×IQR. Sample sizes $\sim 30 \pm 2$ for all groups except seston. Seston sample size = 43

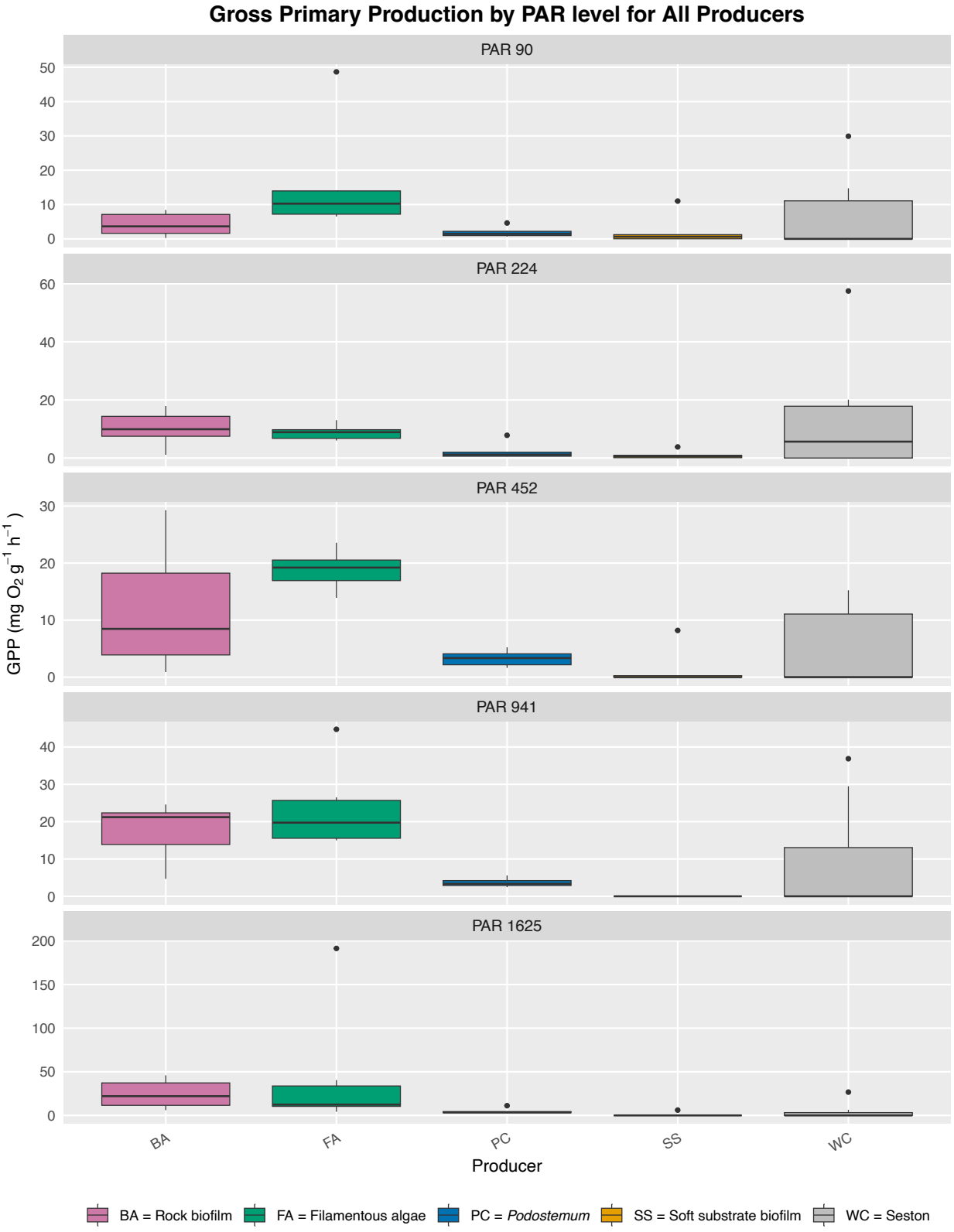
Gross Primary Production by PAR level for All Producers
PAR 90
PAR 224
PAR 452
PAR 941
PAR 1625
GPP (mg O2 g−1 h−1)
Producer
BA
FA
PC
SS
WC
BA = Rock biofilm
FA = Filamentous algae
PC = Podostemum
SS = Soft substrate biofilm
WC = Seston

Figure 3.4: Mass-specific GPP across producer types. Boxplots display GPP (mg O_2 g^{-1} h^{-1}) for all light levels combined (μmol photons m^{-2} s^{-1}) using a discontinuous y-axis. The top panel shows high-GPP values (190-200 mg O_2 g^{-1} h^{-1}), containing one *Rhizoclonium* outlier, while the bottom panel displays the remaining data (0-50 mg O_2 g^{-1} h^{-1}). Boxes represent the interquartile range (25th-75th percentiles) with median line; whiskers extend to 1.5×IQR.

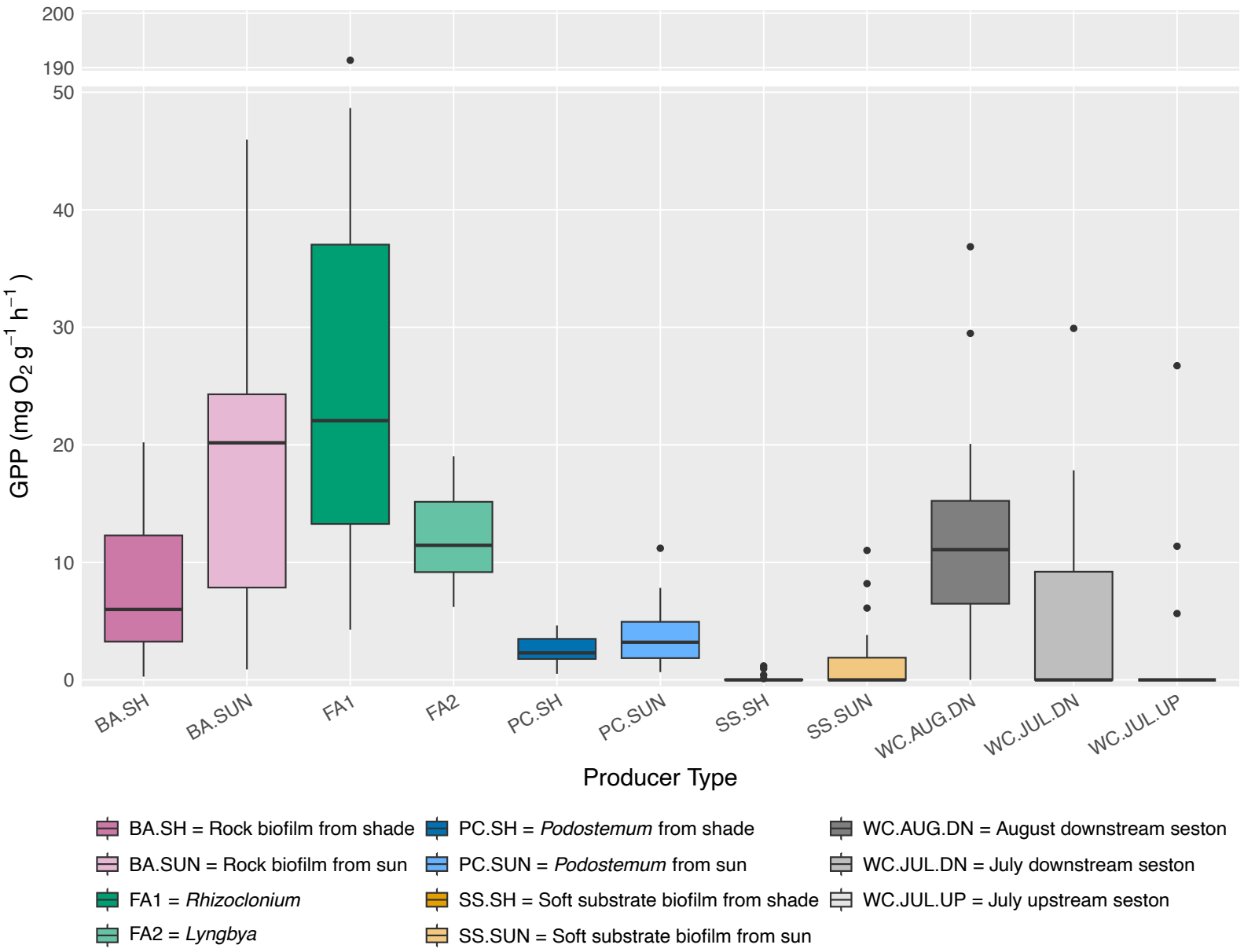
200
190
50
40
30
20
10
0
GPP (mg O2 g-1 h-1)
BA.SH
BA.SUN
FA1
FA2
PC.SH
PC.SUN
SS.SH
SS.SUN
WC.AUG.DN
WC.JUL.DN
WC.JUL.UP
Producer Type
BA.SH = Rock biofilm from shade
BA.SUN = Rock biofilm from sun
FA1 = Rhizoclonium
FA2 = Lyngbya
PC.SH = Podostemum from shade
PC.SUN = Podostemum from sun
SS.SH = Soft substrate biofilm from shade
SS.SUN = Soft substrate biofilm from sun
WC.AUG.DN = August downstream seston
WC.JUL.DN = July downstream seston
WC.JUL.UP = July upstream seston

Figure 3.5: Mass-specific GPP across producer types by light treatment. Boxplots display GPP (mg O_2 g^{-1} h^{-1}) by experimental light treatment (μmol photons m^{-2} s^{-1}). Boxes represent the interquartile range (25th-75th percentiles) with median line; whiskers extend to 1.5×IQR. Sample sizes $\sim 15 \pm 2$ for all producer types. Corresponding Figure B1 displays mass-specific gross primary productivity across producer groups by light treatment separated into high and low GPP rates.

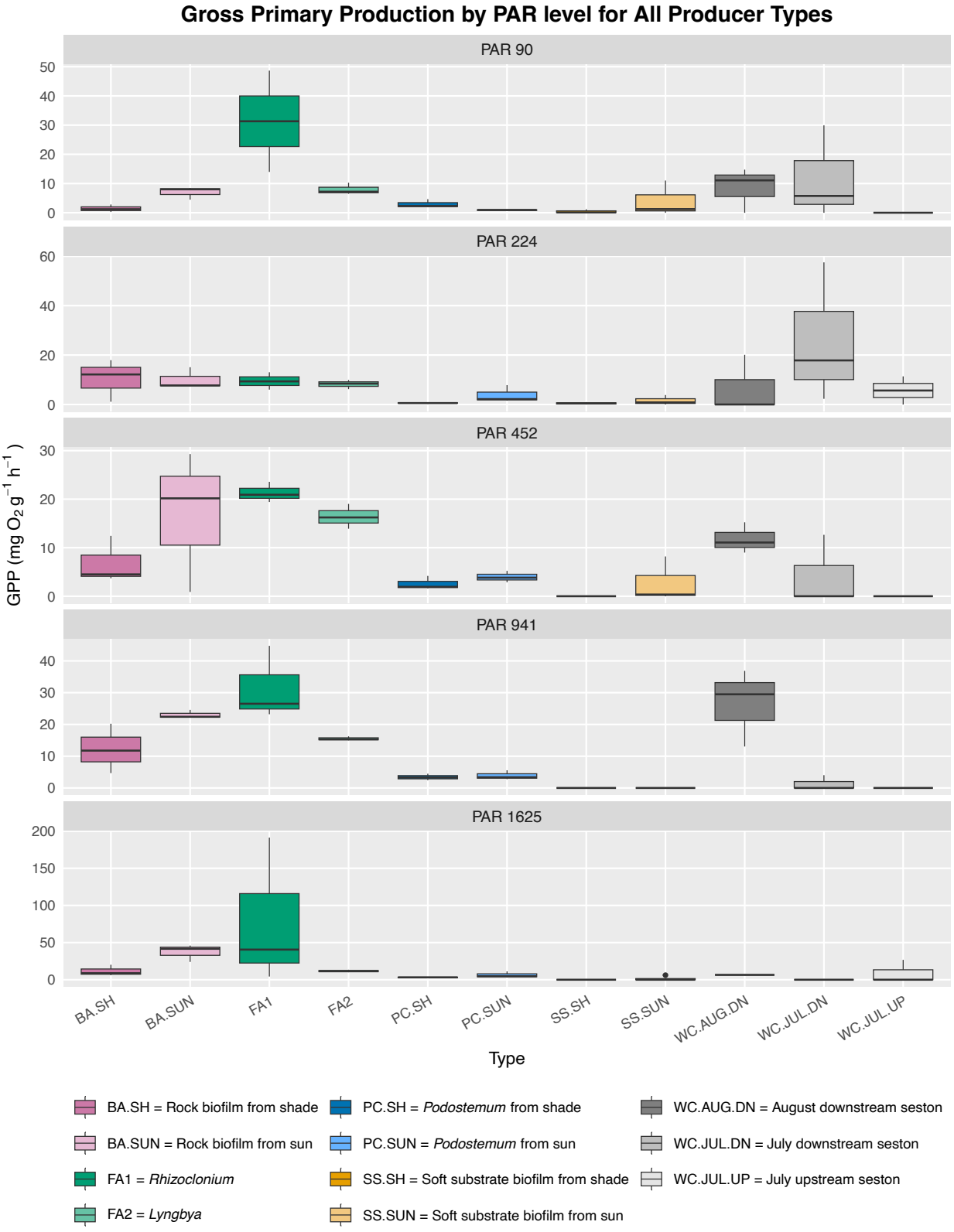
Gross Primary Production by PAR level for All Producer Types
PAR 90
PAR 224
PAR 452
PAR 941
PAR 1625
GPP (mg O2 g−1 h−1)
BA.SH
BA.SUN
FA1
FA2
PC.SH
PC.SUN
SS.SH
SS.SUN
WC.AUG.DN
WC.JUL.DN
WC.JUL.UP
Type
BA.SH = Rock biofilm from shade
BA.SUN = Rock biofilm from sun
FA1 = Rhizoclonium
FA2 = Lyngbya
PC.SH = Podostemum from shade
PC.SUN = Podostemum from sun
SS.SH = Soft substrate biofilm from shade
SS.SUN = Soft substrate biofilm from sun
WC.AUG.DN = August downstream seston
WC.JUL.DN = July downstream seston
WC.JUL.UP = July upstream seston

Figure 3.6: Mean (left) and sample (right) mass-specific GPP (mg O^2 $g^{-}1$ h^{-1}) by experimental light treatment (µmol m^{-2} s^{-1}) for *Podostemum* by group and type. Type for *Podostemum* is stream light environment – shade or sun. Left: Sample size for mean mass-specific GPP was consistent between types and across all light treatments (n = 3), as depicted in column 2. Right: Relationship between mass-specific productivity and experimental light treatment. Relationships are projected from linear models predicting GPP by PAR for all *Podostemum* data (row 1) or separated by stream light environment (rows 2-3). For both columns, shading indicates the confidence interval. Corresponding Figure B2 displays mass-specific gross primary productivity across producer types by light treatment separated into high and low GPP rates.

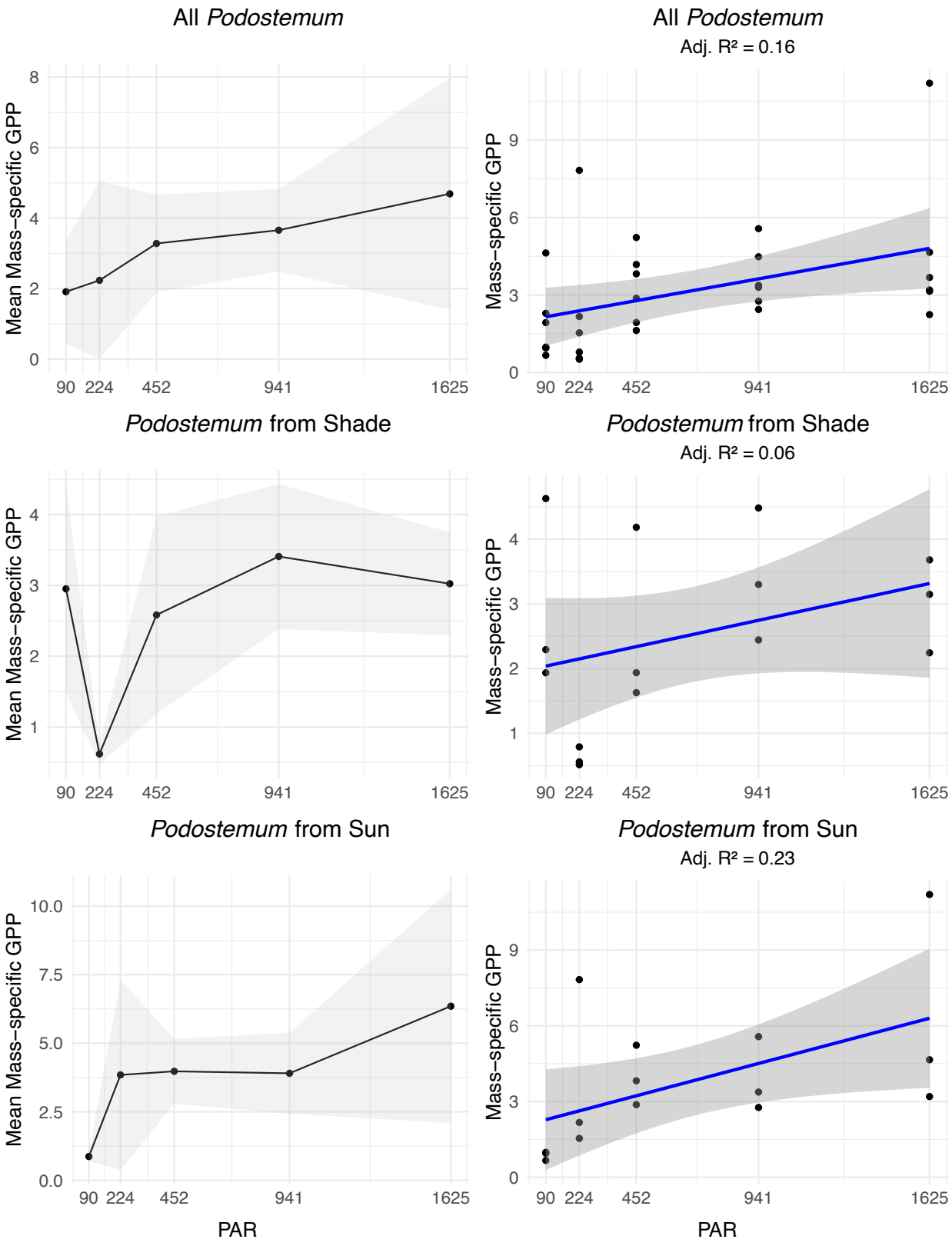
All *Podostemum*
Mean Mass−specific GPP
0
2
4
6
8
90 224 452 941 1625
All *Podostemum*
Adj. R² = 0.16
Mass−specific GPP
0
3
6
9
90 224 452 941 1625
Podostemum from Shade
Mean Mass−specific GPP
1
2
3
4
90 224 452 941 1625
Podostemum from Shade
Adj. R² = 0.06
Mass−specific GPP
1
2
3
4
90 224 452 941 1625
Podostemum from Sun
Mean Mass−specific GPP
0.0
2.5
5.0
7.5
10.0
90 224 452 941 1625
PAR
Podostemum from Sun
Adj. R² = 0.23
Mass−specific GPP
0
3
6
9
90 224 452 941 1625
PAR

Figure 3.7: Mean (left) and sample (right) mass-specific GPP (mg O^2 $g^{-}1$ h^{-1}) by experimental light treatment (μmol m^{-2} s^{-1}) for rock biofilm by group and type. Type for rock biofilm is stream light environment – shade or sun. Left: Sample size for mean mass-specific GPP was consistent between types and across all light treatments (n = 3), as depicted in column 2. Right: Relationship between mass-specific productivity and experimental light treatment. Relationships are projected from linear models predicting GPP by PAR for all rock biofilm (row 1) or separated by stream light environment (rows 2-3). For both columns, shading indicates the confidence interval.

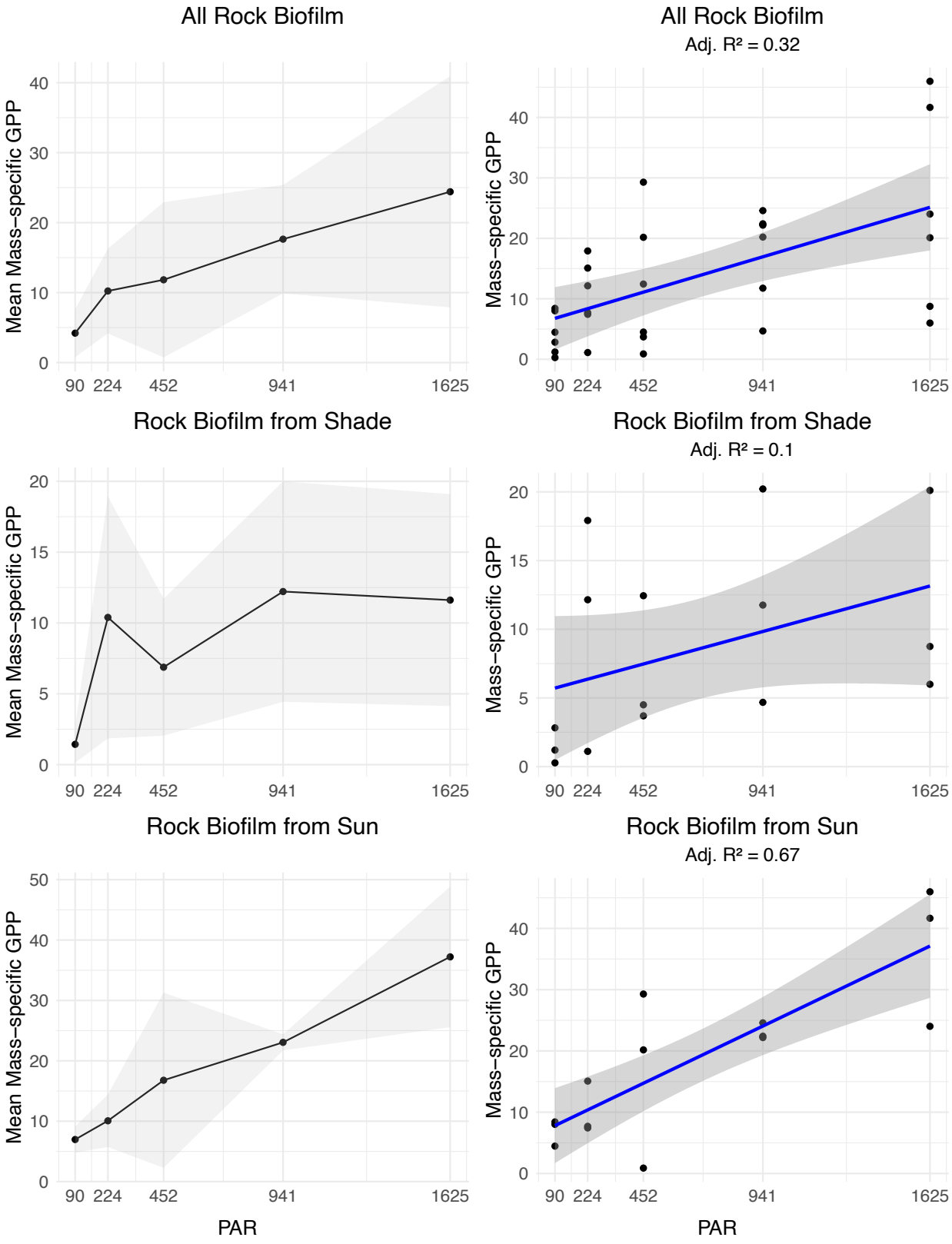
All Rock Biofilm
Mean Mass−specific GPP
0
10
20
30
40
90
224
452
941
1625
All Rock Biofilm
Adj. R² = 0.32
Mass−specific GPP
0
10
20
30
40
90
224
452
941
1625
Rock Biofilm from Shade
Mean Mass−specific GPP
0
5
10
15
20
90
224
452
941
1625
Rock Biofilm from Shade
Adj. R² = 0.1
Mass−specific GPP
0
5
10
15
20
90
224
452
941
1625
Rock Biofilm from Sun
Mean Mass−specific GPP
0
10
20
30
40
50
90
224
452
941
1625
PAR
Rock Biofilm from Sun
Adj. R² = 0.67
Mass−specific GPP
0
10
20
30
40
90
224
452
941
1625
PAR

Figure 3.8: Mean (left) and sample (right) mass-specific GPP (mg O^2 $g^{-}1$ h^{-1}) by experimental light treatment (μmol m^{-2} s^{-1}) for filamentous algae by group and type. Type for filamentous algae is taxon – *Rhizoclonium* or *Lyngbya*. Left: Sample size was consistent between types and across all light treatments (n = 3) except for PAR 90, where one *Rhizoclonium* data point was excluded, as depicted in column 2. Right: Relationship between mass-specific productivity and experimental light treatment. Relationships are projected from linear models predicting GPP by PAR for all filamentous algae (row 1) or separated by taxon (rows 2-3). For both columns, shading indicates the confidence interval.

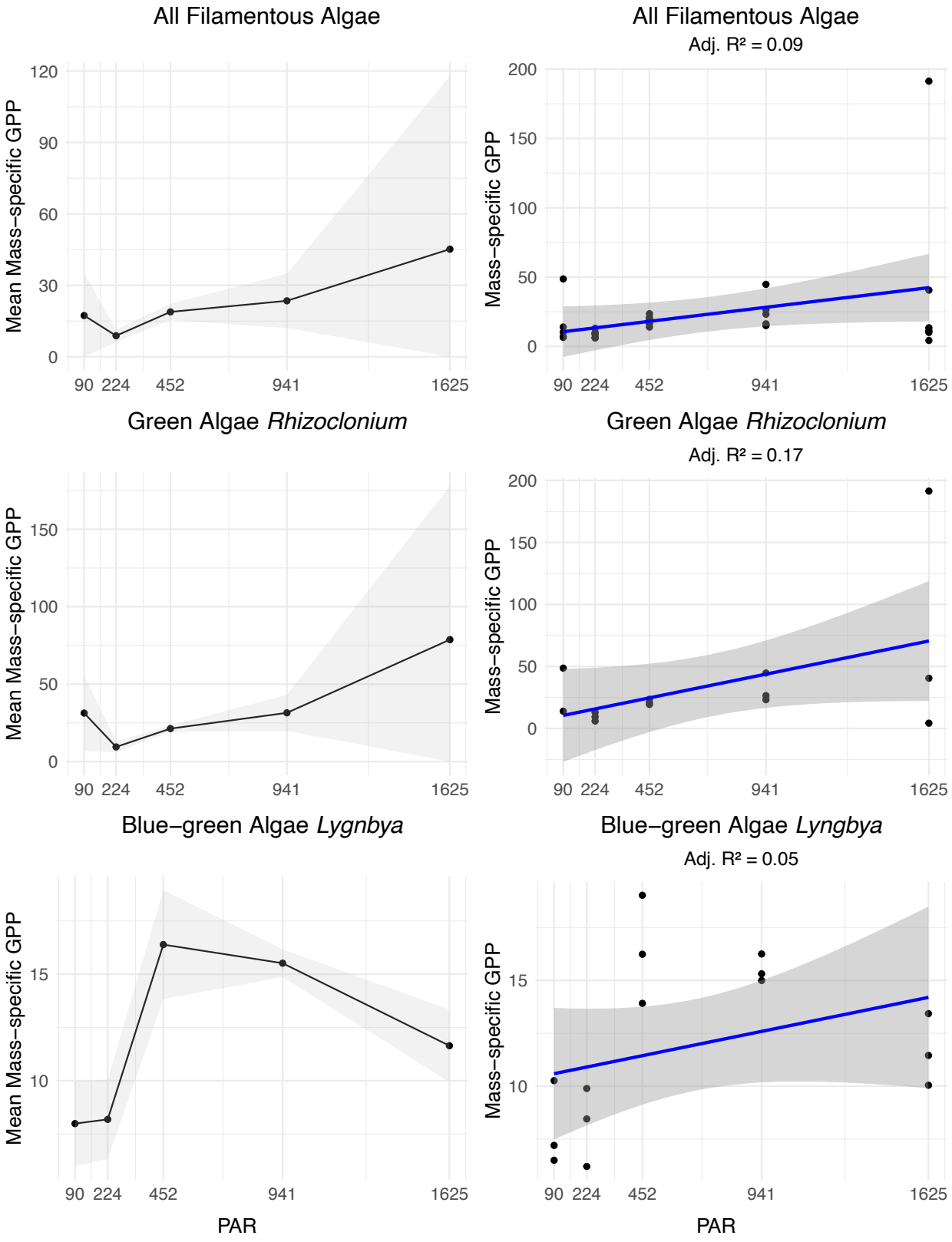
All Filamentous Algae
Mean Mass−specific GPP
120
90
60
30
0
90 224 452 941 1625
All Filamentous Algae
Adj. R² = 0.09
Mass−specific GPP
200
150
100
50
0
90 224 452 941 1625
Green Algae Rhizoclonium
Mean Mass−specific GPP
150
100
50
0
90 224 452 941 1625
Green Algae Rhizoclonium
Adj. R² = 0.17
Mass−specific GPP
200
150
100
50
0
90 224 452 941 1625
Blue−green Algae Lygnbya
Mean Mass−specific GPP
15
10
90 224 452 941 1625
PAR
Blue−green Algae Lyngbya
Adj. R² = 0.05
Mass−specific GPP
15
10
90 224 452 941 1625
PAR

Figure 3.9: Mean (left) and sample (right) mass-specific GPP (mg O^2 $g^{-}1$ h^{-1}) by experimental light treatment for soft substrate biofilm by group and type (μmol m^{-2} s^{-1}). Type for soft substrate biofilm is stream light environment, which was associated with substrate – silt from shade or sand from sun. Left: Sample size for mean mass-specific GPP was consistent between types and across all light treatments (n = 3) except PAR 1625 – full light – where one additional data point is included per type, as depicted in column 2. Silt biofilm from the shade produced negative values (which were zeroed) for PAR 452, 921, and 1625. Right: Relationship between mass-specific productivity and experimental light treatment. Relationships are projected from linear models predicting GPP by PAR for all soft substrate biofilm (row 1) or separated by stream light environment/substrate (rows 2-3). For both columns, shading indicates the confidence interval.

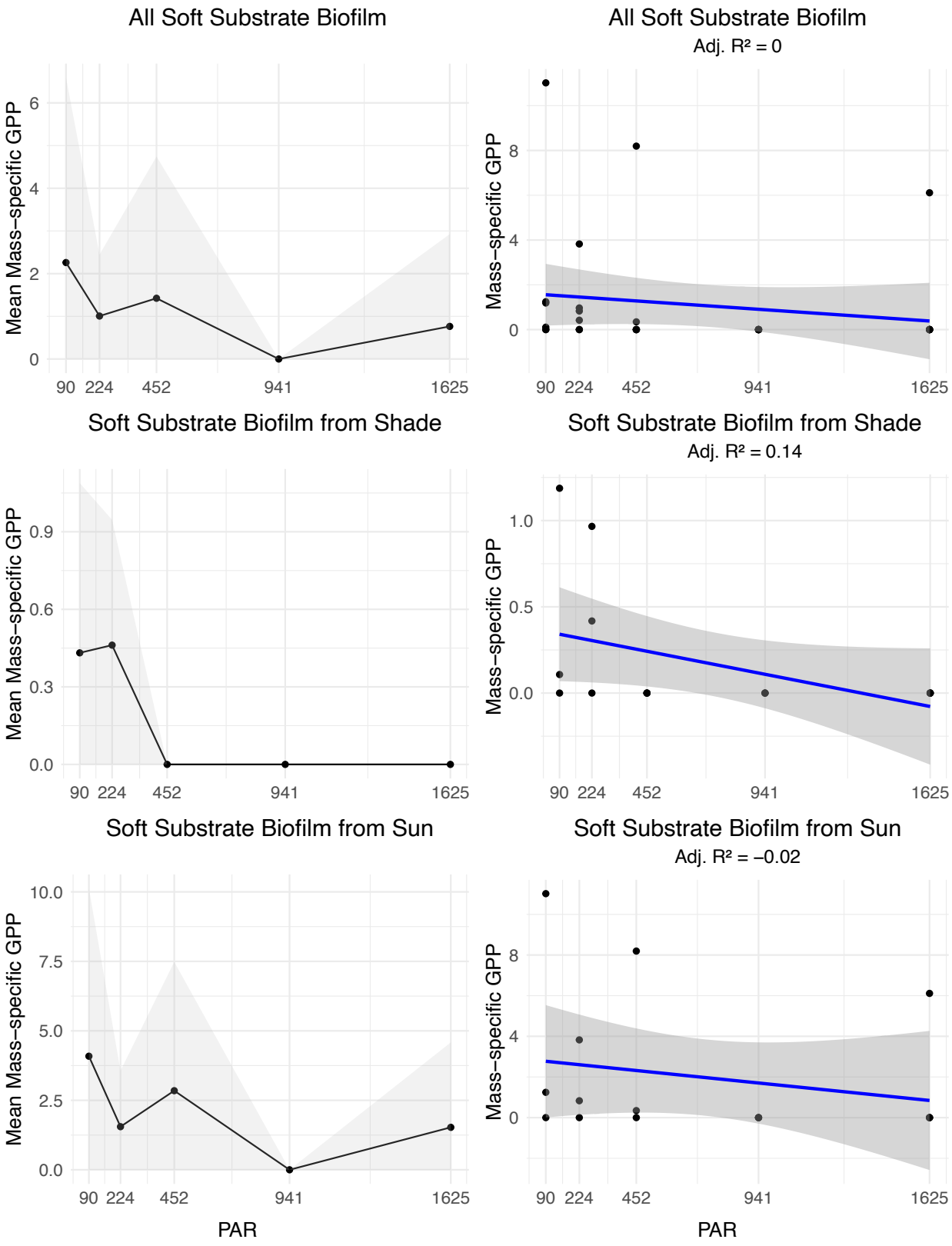
All Soft Substrate Biofilm
Mean Mass−specific GPP
0
2
4
6
90 224 452 941 1625
All Soft Substrate Biofilm
Adj. R² = 0
Mass−specific GPP
0
4
8
90 224 452 941 1625
Soft Substrate Biofilm from Shade
Mean Mass−specific GPP
0.0
0.3
0.6
0.9
90 224 452 941 1625
Soft Substrate Biofilm from Shade
Adj. R² = 0.14
Mass−specific GPP
0.0
0.5
1.0
90 224 452 941 1625
Soft Substrate Biofilm from Sun
Mean Mass−specific GPP
0.0
2.5
5.0
7.5
10.0
90 224 452 941 1625
PAR
Soft Substrate Biofilm from Sun
Adj. R² = −0.02
Mass−specific GPP
0
4
8
90 224 452 941 1625
PAR

Figure 3.10: Mean (left) and sample (right) mass-specific GPP (mg O^2 $g^{-}1$ h^{-1}) by experimental light treatment (μmol m^{-2} s^{-1}) for seston by group and type. Type for seston is sample – unique combination of collection date and stream position – July upstream, July downstream, August downstream. Left: Sample size was consistent across all types and light treatments (n = 3) except for PAR 1625, where July downstream seston only had one data point, as depicted in column 2. Right: Relationship between mass-specific productivity and experimental light treatment. Relationships are projected from linear models predicting GPP by PAR for all seston (row 1) or separated by sample (rows 2-4). For both columns, shading indicates the confidence interval.

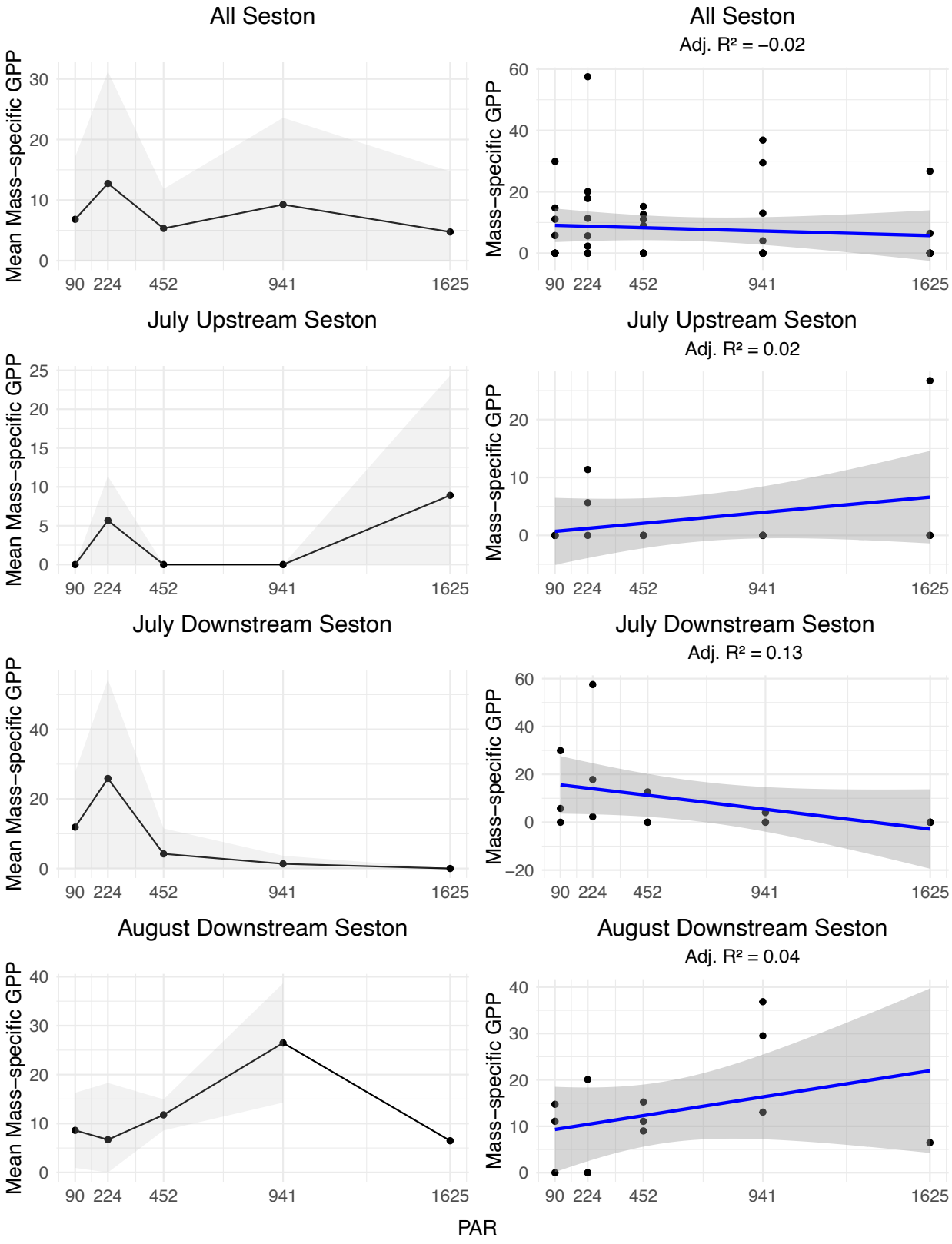
All Seston
Mean Mass−specific GPP
30
20
10
0
90 224 452 941 1625
All Seston
Adj. R² = −0.02
Mass−specific GPP
60
40
20
0
90 224 452 941 1625
July Upstream Seston
Mean Mass−specific GPP
25
20
15
10
5
0
90 224 452 941 1625
July Upstream Seston
Adj. R² = 0.02
Mass−specific GPP
20
10
0
90 224 452 941 1625
July Downstream Seston
Mean Mass−specific GPP
40
20
0
90 224 452 941 1625
July Downstream Seston
Adj. R² = 0.13
Mass−specific GPP
60
40
20
0
−20
90 224 452 941 1625
August Downstream Seston
Mean Mass−specific GPP
40
30
20
10
0
90 224 452 941 1625
August Downstream Seston
Adj. R² = 0.04
Mass−specific GPP
40
30
20
10
0
90 224 452 941 1625
PAR

Figure 3.11: Mean (left) and sample (right) mass-specific GPP (mg O^2 $g^{-}1$ h^{-1}) by experimental light treatment (μmol m^{-2} s^{-1}) for seston by group and subsets of date or stream position relative to a first-order tributary. Type for seston is sample –July upstream, July downstream, August downstream – which created two additional subsets – collection date (rows 2 & 3) and stream position (rows 4 & 5). Left: Sample size was consistent across all subsets and light treatments (n = 3) except for PAR 1625, where July downstream seston only had one data point, as depicted in column 2. Right: Relationship between mass-specific productivity and experimental light treatment. Relationships are projected from linear models predicting GPP by PAR for all seston (row 1) or separated by collection date (rows 2 & 3) and stream position (rows 4 & 5). For both columns, shading indicates the confidence interval.

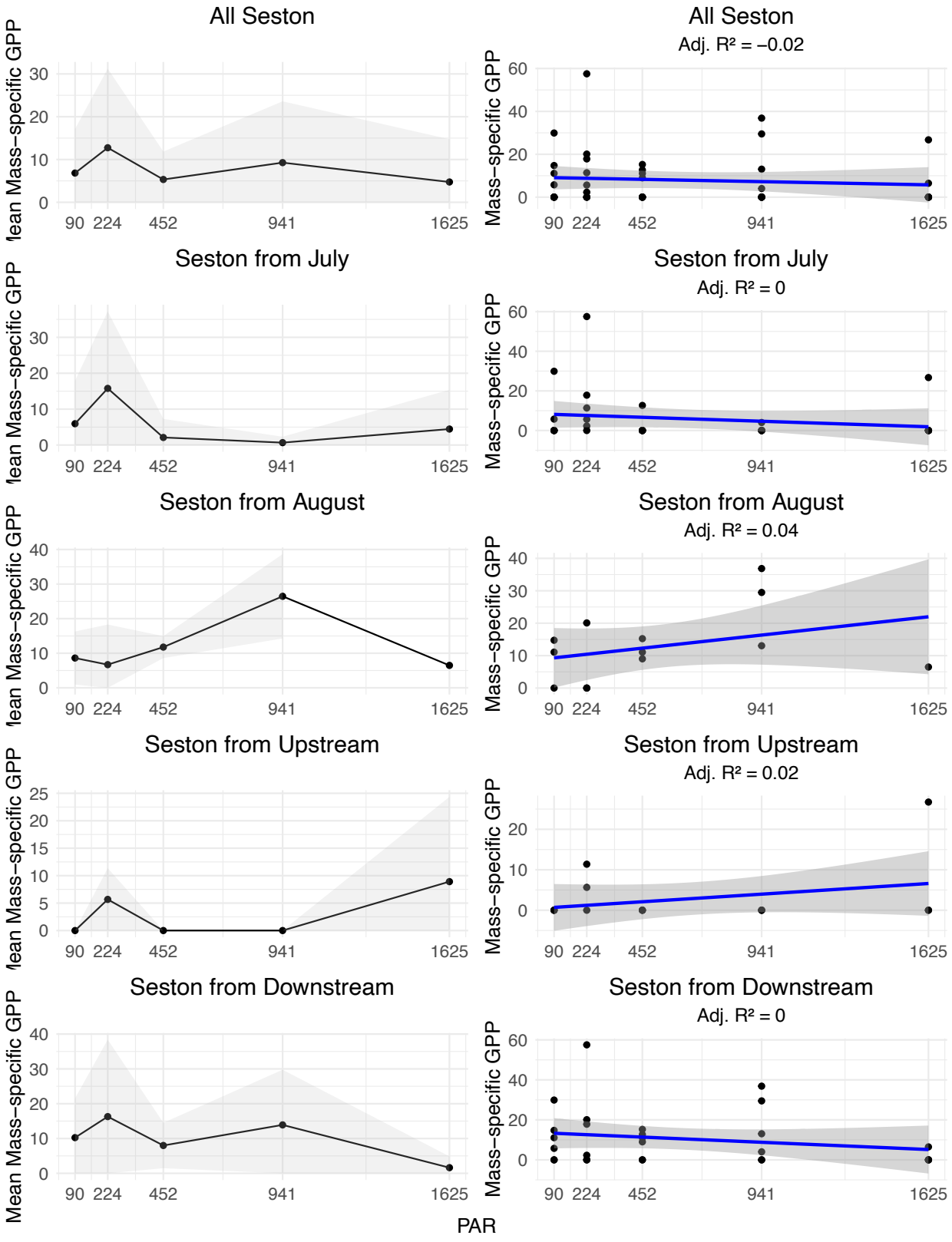
All Seston
Adj. R² = −0.02
Seston from July
Adj. R² = 0
Seston from August
Adj. R² = 0.04
Seston from Upstream
Adj. R² = 0.02
Seston from Downstream
Adj. R² = 0
Mean Mass−specific GPP
Mass−specific GPP
90 224 452 941 1625
PAR

Figure 3.12: Areal productivity (g C m^{-2} day^{-1}) (top), biomass (g AFDM m^{-2}) (middle), and relative GPP contribution (bottom) across 13 sampling events in the Middle Oconee River. Biomass data is from the Conn et al. (Ch.2) study. The relative GPP contribution (C_i) is unitless and $\log(1 + C_i)$ transformed. The dashed line in the relative GPP contribution plot (bottom) represents the proportionality line but at 0.693 due to the data transformation. If C_i is above the 1:1 line, the producer contributes more to total community productivity than would be expected based on its share of the total biomass. If C_i is on the 1:1 line, the producer's contribution to total community productivity is exactly proportional to its share of the total biomass. If C_i is below the 1:1 line, the producer contributes less to total community productivity than would be expected based on its share of the total biomass. Colors remain consistent across plots.

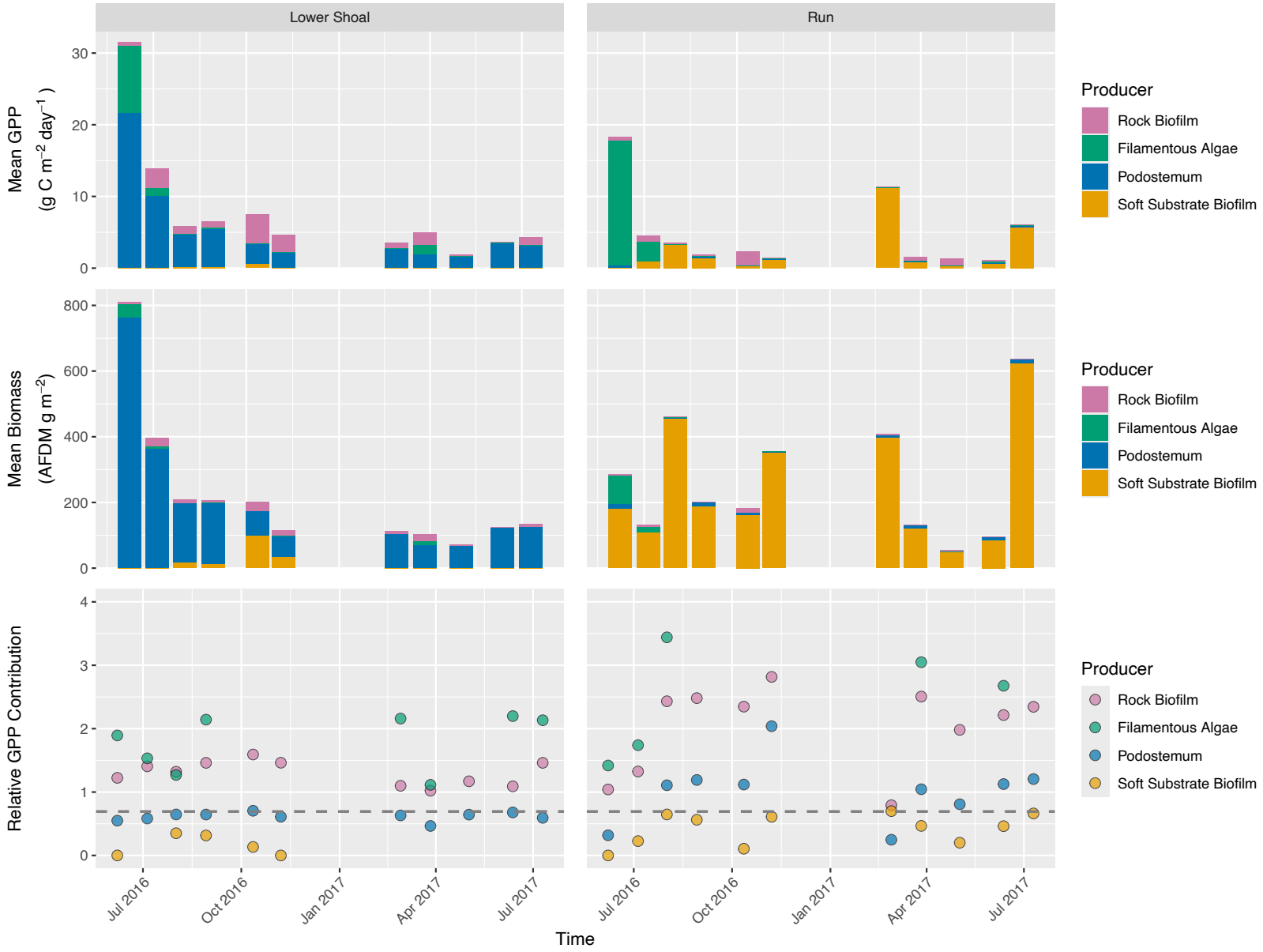
Lower Shoal
Run
Mean GPP
(g C m^{-2} day^{-1})
Mean Biomass
(AFDM g m^{-2})
Relative GPP Contribution
Producer
Rock Biofilm
Filamentous Algae
Podostemum
Soft Substrate Biofilm
Jul 2016
Oct 2016
Jan 2017
Apr 2017
Jul 2017
Time

REFERENCES

Allan, J. David., M. M. Castillo, and K. A. Capps. 2021. Stream ecology: Structure and function of running waters. Third. Springer.

Appling, A. P., J. S. Read, L. A. Winslow, M. Arroita, E. S. Bernhardt, N. A. Griffiths, R. O. Hall, J. W. Harvey, J. B. Heffernan, E. H. Stanley, E. G. Stets, and C. B. Yackulic. 2018. The metabolic regimes of 356 rivers in the United States. Scientific Data 2018 5:1 63:S99–S118.

Aroca, G. E., M. E. Ramírez, H. Robotham, and M. Avila. 2020. Morphological and reproductive studies on the green filamentous pest *Rhizoclonium*-like affecting *Agarophyton chilensis* commercial farms in southern Chile. Aquatic Botany 167:103291.

Atkinson, B. L., M. R. Grace, B. T. Hart, and K. E. N. Vanderkruk. 2008. Sediment instability affects the rate and location of primary production and respiration in a sand-bed stream. https://doi.org/10.1899/07-143.1 27:581–592.

Battin, T. J., K. Besemer, M. M. Bengtsson, A. M. Romani, and A. I. Packmann. 2016. The ecology and biogeochemistry of stream biofilms. Nature Reviews Microbiology 14:251–263.

Bernhardt, E. S., P. Savoy, M. J. Vlah, A. P. Appling, L. E. Koenig, R. O. Hall, M. Arroita, J. R. Blaszczak, A. M. Carter, M. Cohen, J. W. Harvey, J. B. Heffernan, A. M. Helton, J. D. Hosen, L. Kirk, W. H. McDowell, E. H. Stanley, C. B. Yackulic, and N. B. Grimm. 2022. Light and flow regimes regulate the metabolism of rivers. Proceedings of the National Academy of Sciences of the United States of America 119:e2121976119.

Bernot, M. J., D. J. Sobota, R. O. Hall, P. J. Mulholland, W. K. Dodds, J. R. Webster, J. L. Tank, L. R. Ashkenas, L. W. Cooper, C. N. Dahm, S. V. Gregory, N. B. Grimm, S. K.

Hamilton, S. L. Johnson, W. H. McDowell, J. L. Meyer, B. Peterson, G. C. Poole, H. M. Maurice Valett, C. Arango, J. J. Beaulieu, A. J. Burgin, C. Crenshaw, A. M. Helton, L. Johnson, J. Merriam, B. R. Niederlehner, J. M. O'Brien, J. D. Potter, R. W. Sheibley, S. M. Thomas, and K. Wilson. 2010. Inter-regional comparison of land-use effects on stream metabolism. Freshwater Biology 55:1874–1890.

Biggs, B. J. F., and H. A. Thomsen. 1995. Disturbance of stream periphyton by perturbations in shear stress: time to structural failure and differences in community resistance. Journal of Phycology 31:233–241.

Biggs, B. J., D. G. Goring, and V. I. Nikora. 1998. Subsidy and stress responses of stream periphyton to gradients in water velocity as a function of community growth form. Page Journal of Phycology.

Boix Canadell, M., L. Gómez-Gener, A. J. Ulseth, M. Clémençon, S. N. Lane, and T. J. Battin. 2021. Regimes of primary production and their drivers in Alpine streams. Freshwater Biology 66:1449–1463.

Bott, T. L. 2007. Primary Productivity and Community Respiration. Pages 663–690 in F. R. Hauer and G. A. Lamberti, editors. Methods in Stream Ecology. Elsevier, Cambridge.

Bott, T. L., J. T. Brock, A. Baattrup-Pedersen, P. A. Chambers, W. K. Dodds, K. T. Himbeault, J. R. Lawrence, D. Planas, E. Snyder, and G. M. Wolfaardt. 1997. An evaluation of techniques for measuring periphyton metabolisms in chambers. Canadian Journal of Fisheries and Aquatic Sciences 54:715–725.

Bowden, W. B., J. M. Glime, and T. Riis. 2017. Macrophytes and bryophytes. Page Methods in Stream Ecology: Third Edition. Third. Academic Press.

Bridgeman, T. B., and W. A. Penamon. 2010. *Lyngbya wollei* in Western Lake Erie. https://doi.org/10.1016/j.jglr.2009.12.003 36:167–171.

Burnham, K. P., and D. R. Anderson. 2002. Model selection and multimodel inference: a practical information-theoretic approach. Page The Journal of Wildlife Management. 2nd edition. New York.

Cardinale, B. J., H. Hillebrand, and D. F. Charles. 2006. Geographic patterns of diversity in streams are predicted by a multivariate model of disturbance and productivity. Journal of Ecology 94:609–618.

Cardinale, B. J., K. L. Matulich, D. U. Hooper, J. E. Byrnes, E. Duffy, L. Gamfeldt, P. Balvanera, M. I. O'Connor, and A. Gonzalez. 2011. The functional role of producer diversity in ecosystems. American Journal of Botany 98:572–592.

Carmichael, W. W., W. R. Evans, Q. Q. Yin, P. Bell, and E. Moczydlowski. 1997. Evidence for paralytic shellfish poisons in the freshwater cyanobacterium *Lyngbya wollei* (Farlow ex Gomont) comb. nov. Applied and environmental microbiology 63:3104–3110.

Carter, A. M., H. E. Lowman, J. R. Blaszczak, C. C. Barbosa, M. DeSiervo, C. L. Torrens, M. R. Dunkle, S. M. Collins, I. Oleksy, L. R. Katona, and R. O. Hall. 2024. Exceptions to the heterotrophic rule: Prevalence and drivers of autotrophy in streams and rivers. Ecosystems 2024:1–17.

Cummins, K. W. 1974. Structure and Function of Stream Ecosystems. BioScience 24:631–641.

Dodds, W. K., and B. J. F. Biggs. 2002. Water velocity attenuation by stream periphyton and macrophytes in relation to growth form and architecture. Journal of the North American Benthological Society 21:2–15.

Dodds, W. K., A. M. Veach, C. M. Ruffing, D. M. Larson, J. L. Fischer, and K. H. Costigan. 2013. Abiotic controls and temporal variability of river metabolism: multiyear analyses of Mississippi and Chattahoochee River data. Freshwater Science 32:1073–1087.

Francoeur, S. N., and B. J. F. Biggs. 2006. Short-term effects of elevated velocity and sediment abrasion on benthic algal communities. Advances in Algal Biology: A Commemoration of the Work of Rex Lowe:59–69.

Gkelis, S., T. Papadimitriou, N. Zaoutsos, and I. Leonardos. 2014. Anthropogenic and climate-induced change favors toxic cyanobacteria blooms: Evidence from monitoring a highly eutrophic, urban Mediterranean lake. Harmful Algae 39:322–333.

Grubaugh, J. W., and J. B. Wallace. 1995. Functional structure and production of the benthic community in a Piedmont river: 1956-1957 and 1991-1992. Limnology and Oceanography 40:490–501.

Hanrahan, B. R., J. L. Tank, A. F. Aubeneau, and D. Bolster. 2018. Substrate-specific biofilms control nutrient uptake in experimental streams. Freshwater Science 37:456–471.

Hill, B. H., and J. R. Webster. 1984. Productivity of *Podostemum ceratophyllum* in the New River, Virginia. American Journal of Botany 71:130–136.

Hoellein, T. J., J. L. Tank, E. J. Rosi-Marshall, and S. A. Entrekin. 2009. Temporal variation in substratum-specific rates of N uptake and metabolism and their contribution at the stream-reach scale. https://doi.org/10.1899/08-073.1 28:305–318.

Johnson, L. T., and J. L. Tank. 2009. Diurnal variations in dissolved organic matter and ammonium uptake in six open-canopy streams. https://doi.org/10.1899/08-107.1 28:694–708.

Jones, C. G., J. H. Lawton, and M. Shachak. 1994. Organisms as Ecosystem Engineers. Oikos 69:373.

Katz, R. A., M. C. Freeman, and K. Tierney. 2015. Evidence of population resistance to extreme low flows in a fluvial-dependent fish species. Canadian Journal of Fisheries and Aquatic Sciences 72:1776–1787.

Kautza, A., and S. M. P. Sullivan. 2016. The energetic contributions of aquatic primary producers to terrestrial food webs in a mid-size river system. Ecology 97:694–705.

Kendrick, M. R., A. E. Hershey, and A. D. Huryn. 2019. Disturbance, nutrients, and antecedent flow conditions affect macroinvertebrate community structure and productivity in an Arctic river. Limnology and Oceanography 64:S93–S104.

Kirk, L., R. T. Hensley, P. Savoy, J. B. Heffernan, and M. J. Cohen. 2021. Estimating Benthic Light Regimes Improves Predictions of Primary Production and constrains Light-Use Efficiency in Streams and Rivers. Ecosystems 24:825–839.

Lajeunesse, A., P. A. Segura, M. Gélinas, C. Hudon, K. Thomas, M. A. Quilliam, and C. Gagnon. 2012. Detection and confirmation of saxitoxin analogues in freshwater benthic *Lyngbya wollei* algae collected in the St. Lawrence River (Canada) by liquid chromatography-tandem mass spectrometry. Journal of chromatography. A 1219:93–103.

Lange, K., C. R. Townsend, and C. D. Matthaei. 2016. A trait-based framework for stream algal communities. Ecology and Evolution 6:23–36.

Leroy, C. J., S. M. Claeson, I. J. Garthwaite, M. A. Thompson, L. J. Thompson, B. K. Kamakawiwo'ole, A. M. Froedin-Morgensen, V. Mcconathy, J. M. Ramstack Hobbs, R. Stancheva, C. M. Albano, · Debra, and S. Finn. 2023. Canopy development influences early successional stream ecosystem function but not biotic assemblages 85:77.

Marcarelli, A. M., C. J. Huckins, and S. L. Eggert. 2015. Sand aggradation alters biofilm standing crop and metabolism in a low-gradient Lake Superior tributary. Journal of Great Lakes Research 41:1052–1059.

McKay, S. K. 2014, September 23. Informing flow management decisions in the Middle Oconee River. University of Georgia.

Myrstener, M., L. Gómez-Gener, G. Rocher-Ros, R. Giesler, and R. A. Sponseller. 2021. Nutrients influence seasonal metabolic patterns and total productivity of Arctic streams. Limnology and Oceanography 66:S182–S196.

Nakano, D., T. Iwata, J. Suzuki, T. Okada, R. Yamamoto, and M. Imamura. 2022. The effects of temperature and light on ecosystem metabolism in a Japanese stream. Freshwater Science 41:113–124.

Nelson, D. J., and D. C. Scott. 1962. Role of detritus in the productivity of a rock-outcrop community in a Piedmont stream. Limnology and Oceanography 7:396–413.

O'Neil, J. M., T. W. Davis, M. A. Burford, and C. J. Gobler. 2012. The rise of harmful cyanobacteria blooms: The potential roles of eutrophication and climate change. Harmful Algae 14:313–334.

Paerl, H. W. 2017. Controlling cyanobacterial harmful blooms in freshwater ecosystems. Microbial biotechnology 10:1106–1110.

Pahl, J. P. 2009. Effects of flow alteration on the aquatic macrophyte *Podostemum ceratophyllum* (riverweed); local recovery potential and regional monitoring strategy.

Palmer, M. A., and C. M. Febria. 2012. The Heartbeat of Ecosystems. Science 336:1393–1394.

Peipoch, M., M. Daniels, and S. H. Ensign. 2025. Concentration–discharge relationships of chlorophyll describe the origin and fluxes of river algae across ecoregions. Freshwater Science 44:143–158.

Power, M. E. 1992. Hydrologic and trophic controls of seasonal algal blooms in northern California rivers. Hydrobiologia 125:385–410.

R Core Team. 2025. R: A language and environment for statistical computing. Vienna, Austria.

Rack, L. 2025. Quantifying streamflow needs for ecosystems in the context of water planning and management. Doctoral Dissertation, University of Georgia, Athens, GA.

Reisinger, A. J., J. L. Tank, R. O. Hall, E. J. Rosi, M. A. Baker, and L. Genzoli. 2021. Water column contributions to the metabolism and nutrient dynamics of mid-sized rivers. Biogeochemistry 153:67–84.

Reisinger, A. J., J. L. Tank, E. J. Rosi-Marshall, R. O. Hall, and M. A. Baker. 2015. The varying role of water column nutrient uptake along river continua in contrasting landscapes. Biogeochemistry 125:115–131.

Riis, T., and B. J. F. Biggs. 2001. Distribution of macrophytes in New Zealand streams and lakes in relation to disturbance frequency and resource supply - A synthesis and conceptual model. New Zealand Journal of Marine and Freshwater Research 35:255–267.

Riis, T., and B. J. F. Biggs. 2003. Hydrologic and hydraulic control of macrophyte establishment and performance in streams. Limnology and Oceanography 48:1488–1497.

Rosemond, A. D. 1993. Interactions among irradiance, nutrients, and herbivores constrain a stream algal community. Oecologia 94:585–594.

Rosemond, A. D., P. J. Mulholland, and J. W. Elwood. 1993. Top-down and bottom-up control of stream periphyton: effects of nutrients and herbivores. Ecology 74:1264–1280.

Rüegg, J., C. C. Conn, E. P. Anderson, T. J. Battin, E. S. Bernhardt, M. Boix Canadell, S. M. Bonjour, J. D. Hosen, N. S. Marzolf, and C. B. Yackulic. 2020. Thinking like a consumer: Linking aquatic basal metabolism and consumer dynamics. Limnology and Oceanography Letters 6:1–17.

Savoy, P., A. P. Appling, J. B. Heffernan, E. G. Stets, J. S. Read, J. W. Harvey, and E. S. Bernhardt. 2019. Metabolic rhythms in flowing waters: An approach for classifying river productivity regimes. Limnology and Oceanography 64:1835–1851.

Schlenker, A., M. Brauns, P. Fink, and M. Weitere. 2024. Beyond biomass: Resource effects on primary production and consumer nutrient assimilation in streams. Freshwater Biology 69:1353–1363.

Steinman, A. D., and C. D. McIntire. 1986. Effects of current velocity and light energy on the structure of periphyton assemblage in laboratory streams. Journal of Phycology 22:352–361.

Steinman, A. D., P. J. Mulholland, and W. R. Hill. 1992. Functional responses associated with growth form in stream algae. Journal of the North American Benthological Society 11:229–243.

Suren, A. M., and T. Riis. 2010. The effects of plant growth on stream invertebrate communities during low flow: A conceptual model. Journal of the North American Benthological Society 29:711–724.

Thorp, J. H., and M. D. Delong. 2002. Dominance of autochthonous autotrophic carbon in food webs of heterotrophic rivers. Oikos 96:543–550.

Tonkin, J. D., R. G. Death, and J. Barquín. 2014. Periphyton control on stream invertebrate diversity: is periphyton architecture more important than biomass? Marine and Freshwater Research 65:818.

Vadeboncoeur, Y., and M. E. Power. 2017. Attached algae: The cryptic base of inverted trophic pyramids in freshwaters. Annual Review of Ecology, Evolution, and Systematics 48:255–279.

Wood, J., and M. Freeman. 2017. Ecology of the macrophyte *Podostemum ceratophyllum* Michx. (Hornleaf riverweed), a widespread foundation species of eastern North American rivers. Aquatic Botany 139:65–74.

Wood, J. L., J. W. Skaggs, C. Conn, and M. C. Freeman. 2019. Water velocity regulates macro-consumer herbivory on the benthic macrophyte *Podostemum ceratophyllum* Michx. Freshwater Biology 64:2037–2045.

Yang, X., L. Liu, Z. Yin, X. Wang, S. Wang, and Z. Ye. 2020. Quantifying photosynthetic performance of phytoplankton based on photosynthesis–irradiance response models. Environmental Sciences Europe 32:1–13.

AUTHOR CONTRIBUTIONS

Author C. C. Conn conceived of the presented idea, developed the study design, conducted all experiments and lab-processing, developed the code and conducted all analyses, and wrote the manuscript with input from all co-authors. Co-authors A. D. Rosemond and S. J. Wenger contributed to the conception of the presented idea and interpretation of results. Co-author A. D. Rosemond contributed to the experimental design, and co-author S. J. Wenger contributed to the analytical design. All co-authors contributed to the interpretation of the results and writing of the manuscript.

All co-authors agree that the work may be included in this thesis or dissertation.

CHAPTER 4

HYDRAULIC MODEL DECISIONS AND HYDROLOGIC REPRESENTATION INFLUENCE UNDERSTANDING OF HOW STREAMFLOW AFFECTS HABITAT PROVISIONING[3]

[3] Conn, C. C., T. A. Keys, M. C. Freeman, S. K. McKay. To be submitted to a peer-reviewed journal.

ABSTRACT

Hydraulic models are integral to modern river management, yet determining the appropriate level of representational and computational detail required to inform decision-making remains a critical challenge. Using a site on the Middle Oconee River in Athens, Georgia, we evaluated how key decisions in hydraulic model design (varying data input resolution, sampling design, and dimensionality) and hydrologic representation (varying hydrologic metrics) influence ecological inferences about fish habitat provisioning. To assess these effects, we computed three habitat metrics representing ecologically-relevant habitat types for focal fish taxa: total wetted habitat, proportion shallow-fast habitat, and a Shannon-Weiner habitat diversity index. Higher resolution models consistently outperformed simpler models, but the sensitivity of different habitat metrics to change in model complexity varied, influencing the relative risk and value of the increased modeling investment. A complementary approach using both time-weighted and targeted discharge statistics provided the most accurate and comprehensive depiction of how streamflow variability affects habitat provisioning, although targeted metrics alongside traditional central tendency statistics yielded substantial gains in ecological insight. In this context, model complexity and hydrologic representation strongly influenced ecological understanding for the less common shallow-fast habitat type. These results underscore that the appropriate level of representational and computational detail should be guided by the project objectives and risk tolerance; for sensitive or rare habitats, investing in greater model complexity may be warranted to capture critical flow ecology dynamics.

INTRODUCTION

As water managers seek to balance societal needs and the requirements for aquatic ecosystem integrity, they increasingly rely upon integrated modeling — a framework that combines multiple models across disciplines and scales — to inform the decision-making

process (Borsuk et al. 2004, Uusitalo et al. 2015, Larsen et al. 2016). Integrated modeling is especially useful in the context of environmental flows (eflows) (i.e., the quantity, timing, and quality of water flows required to sustain freshwater ecosystems and our reliance on them) as it provides a formal structure for linking complex ecological and geophysical processes to allow managers to forecast the ecological outcomes of potential eflow scenarios (Gregory and Keeney 2002, Addison et al. 2013, Davis et al. 2015, Dietze et al. 2018, Poff 2018, Harris et al. 2024). However, while forecasting can decrease the uncertainty around the outcomes of different management actions, accurately capturing real-world complexity can lead to increasing model complexity, and with it, decreasing tractability (due to limitations in resources) and interpretability (Turner and Carpenter 2017). For these reasons, model development often presents challenging trade-offs between simplicity/complexity and resolution/accuracy (Larsen et al. 2016). Thus, water managers must assess the payoff of a modeling investment relative to the need for information, complexity, and/or confidence in predictions. Ideally, one would invest in the least complex model to adequately capture ecological complexity and make the right conclusions about the merits of water management actions (Uusitalo et al. 2015, Larsen et al. 2016, Turner and Carpenter 2017).

Complexity arises in multiple aspects of the modeling and interpretive process including analytical methods (e.g., data and model resolution), physical processes (e.g., flow variability), ecological outcomes (e.g., multiple species, multiple metrics), and management actions (e.g., extraction rates) (Richter et al. 2006, Poff et al. 2010b, 2016, Schultz et al. 2010). Each of these aspects represents a decision point that affects key model attributes, as described by Shultz et al. (Schultz et al. 2010) — the tractability, interpretability, specificity, and validation potential of the model. For a model to be useful, it must not be so complex that it is too costly, and thus not

tractable, or uninterpretable, and thus not useful in decision-making. However, it must be complex enough to accurately represent the system or systems of interest, providing an appropriate level of specificity, and to be reasonably validated. While the modeling process is intended to decrease uncertainty around decision-making, each modeling decision-point carries the risk of structural uncertainty, which could lead to inaccurate model predictions or the accumulation of systematic error propagating through the model. Model evaluation, preferably against real-world data, is an important tool for understanding and reducing structural uncertainty, and validation potential scales with a model's representational detail. As more processes and patterns are represented, there is more opportunity to test the replication of those processes and patterns (Larsen et al. 2016). These complex interactions between accuracy, complexity, uncertainty, and risk underscore the need to understand how modeling choices affect ecological inference. This information is crucial for both adequately managing decision uncertainty (Uusitalo et al. 2015) and ensuring the resulting information is adequately salient (i.e., relevant to the decision at hand) (Brauman et al. 2021).

In this study, we address how common aspects of model complexity interact and potentially affect ecological inference about aquatic habitat provisioning. We do so by constructing integrated hydraulic-habitat models of fish communities in response to variation in stream flow. First, we examine the role of hydraulic model complexity on ecological inference relative to fish habitat metrics. Second, we study how different approaches for assessing hydrologic variability could alter understanding of habitat provisioning. These two aspects of complexity (i.e., model and physical) often arise in environmental flow analyses, and we hope this study helps managers prioritize investments in modeling to most effectively inform flow management decisions.

METHODS

We conducted two studies with data from a Piedmont river in the southeastern United States to determine how ecological inference varies with hydraulic model complexity and selection of hydrologic metric (Table 4.1). We used high resolution hydraulic models to predict ecological outcomes for three fish habitat types: deep-fast, shallow-fast, and shallow-slow. In study 1, we varied the data resolution (i.e., 5, 9, and 17 cross-sections), sampling design (i.e., evenly space vs. bed-slope stratified cross-sections), and hydraulic model resolution (i.e., one vs. two dimensions) to assess the effect of model complexity on ecological inference. In study 2, we varied the hydrologic metric (i.e., mean discharge, median discharge, annual 7Q10, annual 30Q2, and 30% of mean annual flow) and conducted an effectiveness analysis to assess the effect of metric choice on ecological inference. We used R to compute habitat metrics and analyze ecological outcomes in both studies (R Core Team 2022).

Middle Oconee River

The Middle Oconee River is a sixth-order tributary of the Altamaha River with a watershed area of roughly 641 km^2 in northeast Georgia (Figure 4.1). While there are no major impoundments within the main channel, there is an intake near Athens, GA for the off-channel Bear Creek Reservoir, which provides municipal water for four surrounding counties. The current water permit allows for a maximum water withdrawal of 60 million gallons per day (MGD) (Georgia EPD Permit Number 078-0304-05) subject to meeting minimum flow criteria. While withdrawal rates as of 2012 (Campana et al.) were typically less than 20 MGD, the permitted rates represent a substantial portion of river flow with the proportion increasing dramatically during the late summer months when discharge is at its lowest. A streamflow gage downstream of the intake has provided discharge data for long-term streamflow monitoring since

1938 (U.S. Geological Survey Gage number 02217500). Using the flow data and other ecological field data, researchers have studied benthic communities and hydrologic patterns in this river for more than 60 years (Nelson & Scott, Grubaugh and Wallace, Katz and Freeman, McKay et al., Bhattacharjee et al, McDowell, Wood et al., Rack, Conn et al. Ch.2). Thus, the Middle Oconee River provides a unique study site with a long-term flow record in a well-studied ecological landscape. In addition, Bhattacharjee et al. (2019) measured channel geometry using 17 transects (Figure 1) over a 0.46 km reach of the river to model variation in water depths and velocities in relation to discharge. This field data and a LiDAR model provided the basis for assessing the effects of model complexity and hydrologic representation on ecological inference.

Study 1: Hydraulic Model Complexity

In Study 1, we addressed two research questions: (1) How does input data resolution, sampling design, and hydraulic model dimensionality affect habitat outcomes? and (2) Does model resolution change inference about the ecology of the system? To answer these questions, we evaluated habitat outcomes for 10 steady-state hydraulic models, which varied in input data resolution, sampling design, and dimensionality. Input data resolution refers to the use of 5, 9, or 17 cross-sections of elevational data (i.e., differences in sampling density), while sampling design refers to the selection of evenly spaced or bed-slope stratified placement for the models using 5 or 9 cross-sections. A 1-dimensional (1D) and a 2-dimensional (2D) model were developed for each level of input data resolution and sampling design. We then computed three habitat metrics — total wetted area, proportion shallow-fast habitat, and habitat diversity — for all ten hydraulic models to evaluate the effect on habitat outcomes and ecological inference.

Hydraulic Model Development

We first processed the topographic and bathymetric data collected for the hydraulic models. We used a previously developed digital elevation model (DEM), converted from high resolution LiDAR data collected in 2015, as floodplain topography. However, because traditional LiDAR does not penetrate water, we developed a 2D representation of channel bathymetry from surveyed channel cross sections. In 2013, Bhattacharjee et al. (2019) surveyed 17 cross-sections along a 0.46 km study reach using an RTK-GPS. We merged these two data sets using a spline approach to interpolate the measured cross sections, as illustrated by Merwade et al. (2008). The resulting 2D representation was then mosaicked on top of the floodplain LiDAR raster dataset to create a seamless DEM. The final 2D terrain surfaces have a spatial resolution of 4 ft (~1.22 m), which is consistent with the LiDAR-derived DEM for the site.

We repeated this data merger and interpolation process to create four additional bathymetric maps of the system, which varied the input data resolution to the hydraulic models. For the first geometry, we removed alternating cross-sections until only 9 remained. For the next geometry, we removed the same number of cross-sections but did so strategically, in areas with the least change in bed slope (referred to here as bed slope stratified). For the third geometry, we removed every third cross-section until only 5 cross-sections remained. For the final geometry, we reduced input data resolution to 5 cross sections using the bed slope stratification method. This process created 5 data resolution levels: 17 cross-sections, 9 evenly selected cross-sections, 9 bed-slope stratified selected cross-sections, 5 evenly selected cross-sections, and 5 bed-slope stratified selected cross-sections.

Once the 5 geometries were developed, we conducted one- and two-dimensional steady state simulations in HEC-RAS for each geometry (US Army Corps of Engineers 2019). We used

a steady state 1D HEC-RAS model previously developed by Bhattacharjee et al. (2019) based on all 17 cross sections. Bhattacharjee et al. calibrated their model by iteratively adjusting the Manning's roughness value for the channel and floodplains for each cross section such that model results matched observed water surface levels. We developed a steady state 2D HEC-RAS model using the same roughness values as the calibrated 1D model at each cross section. For each of the 10 simulations (5 geometries with both 1d and 2d runs), we conducted 79 steady-state simulations for a range of flows between 0.28 m^3/s to 566.33 m^3/s (the range of observed flows at the gage). Finally, we exported the resulting depth and velocity raster datasets from HEC-RAS and classified them into categories as specified in Table 4.2.

Habitat Assessment

We used three ecologically-relevant habitat types developed by Bhattacharjee et al. (2019) to evaluate ecological outcomes (Table 4.2). These habitat types, and their representative taxa, correspond to fish habitat suitability criteria developed by Bain et al. (1995) and subsequently used to evaluate habitat availability in relation to flow for southeastern US fishes (Bowen et al. 1998). Notably, shallow-fast habitat is the rarest and supports a more speciose fish assemblage, so any effects on shallow-fast habitat are considered of particular ecological interest. Remaining habitat, designated as 'other', was incorporated into total wetted area estimates.

We calculated habitat area for the HEC-RAS depth and velocity raster datasets using the 'raster' package in R statistical software (R Core Team, 2019). For each depth dataset, we classified pixels as either shallow or deep based on the designated habitat criteria value (Table 2). Similarly, each pixel in the corresponding velocity raster dataset was classified as either slow or fast. Once the depth and velocity rasters were classified, we separated each class (i.e., shallow vs. deep and slow vs. fast) into its own raster dataset such that cells meeting that criteria were

assigned a value of 1 while those that did not were assigned a value of 0. Because habitat suitability for a given representative species differs, deep-fast and shallow-fast habitat types have different velocity threshold values and required the creation of two separate "fast" datasets for each velocity dataset. We then added together the corresponding datasets (e.g., shallow-slow = shallow + slow) to calculate suitability for each habitat type, which resulted in each cell having a value of either 0, 1, or 2. Cells with a value of 0 represent pixels that contain neither corresponding datasets while cells with a value of 1 contain only one of the datasets, and cells with a value of 2 contain both of the corresponding datasets. We then reclassified the rasters such that pixels with a value of 0 or 1 were listed as null. And finally, we calculated areas for each fish habitat type using the 'area' function and calculated the total wetted area by adding the remaining habitat categorized as 'other' with the total area of the three specific fish habitat types.

To evaluate ecological outcomes more thoroughly, we developed a Shannon-Wiener habitat diversity metric using each habitat type as 'species', which provides a measure of how wetted area is distributed between the different habitat types. We calculated dimensionless diversity for each discharge using *Equation 1*.

Equation 1

$$S_j = -\sum_i p_{ij} ln(p_{ij})$$

Where :

- S_j = the Shannon diversity index at a given flow condition j
- j = flow condition (specific discharge)
- i = habitat type (shallow-fast, deep-fast, shallow-slow, other)
- p_{ij} = proportion of habitat type i t flow condition j

The diversity index has a potential minimum of 0 when one habitat is present and all others are absent and a maximum of 1.386 when all habitat types are equally represented. We used the following bins to interpret the index:

- 0-0.5: Low diversity (one type dominates)
- 0.5-1.0**:** Moderate diversity
- 1.0-1.386**:** High diversity (types are relatively even; theoretical max = 1.386)

We applied the ten hydraulic-habitat models over a range of river discharges to develop habitat rating curves depicting the availability of each habitat type (e.g., Figure 4.2) and established the highest resolution model as a benchmark (i.e., 2D-17XS model scenario). To evaluate the effects of model complexity — dimensionality, sampling density (input data resolution, sampling design (bed-slope stratification) — we calculated the percent difference of habitat values at each discharge for all model scenarios (i.e. remaining 9 model scenarios) in comparison to the benchmark. We assessed model performance for accuracy (systematic bias), precision (prediction variability), error severity (magnitude of extreme deviations), and discharge-specific error patterns (magnitude and distribution relative to discharge).

Study 2: Hydrologic Representation

Environmental flow analyses often center on a small number of streamflow targets such as a minimum flow threshold or a central tendency statistic like a mean or median. Historically, these flows are the focus of hydraulic simulations and other flows are neglected. In Study 2, we asked how metric selection affects habitat outcomes and their resulting ecological implications. We used the same three ecologically relevant habitat metrics developed in study 1 (total wetted area, proportion of shallow-fast habitat, and habitat diversity) calculated from only the highest resolution hydraulic model — the 2D HEC-RAS model developed with data from all 17 cross

sections. In addition to evaluating habitat at specific discharge values, we conducted a magnitude-frequency analysis to calculate a time-weighted average of habitat over the entire range of flows used in study 1 (79 values between 0.28 $m^3 s^{-1}$ to 566.33 $m^3 s^{-1}$).

To evaluate how the selection of different stream flow metrics informs ecological inference, we compared total wetted area, the proportion of shallow-fast habitat, and habitat diversity at the following discharges: mean (4.75 $m^3 s^{-1}$), median (9.91 $m^3 s^{-1}$ with 10^{th} and 90^{th} percentiles of 4.16 and 26.05), annual 7Q10 (1.27 $m^3 s^{-1}$), and annual 30Q2 (4.39 $m^3 s^{-1}$). All four metrics are commonly used to provide environmental flow recommendations, i.e., target flows used in environmental regulations (Richter et al. 1996, Annear et al. 2004, Risley et al. 2008). While mean and median discharge are integrative metrics estimating typical flow conditions, 7Q10 (the lowest discharge that occurs over 7 consecutive days with a 10-year recurrence interval) and 30Q2 (the lowest discharge that occurs over 30 consecutive days within a two-year recurrence interval) are threshold metrics representing minimum flow tolerances. Because of the differences in the recurrence interval, 7Q10 represents a rarer event (10% chance in a given year) whereas 30Q2 is relatively common (50% chance of it occurring in a given year). Both of these metrics have been used in the State of Georgia to regulate water withdrawal amounts (Peterson et al. 2011, Gotvald 2017).

We then used a magnitude-frequency analysis to estimate the amount of habitat across the entire range of the flow regime. We calculated a frequency distribution of all discharge values (frequency curve in Bhattacharjee et al. 2019)(Figure 4.3) and a habitat rating curve for all three habitat types from the HEC-RAS simulations. The product of the amount of habitat (i.e., magnitude) and probability of occurrence (i.e., frequency) provides a relative measure of the time-weighted amount of habitat (i.e., the magnitude-frequency curve in Figure 4.3). The area

under this curve is the total amount of a given habitat type provided by the entire flow regime over the 60-year simulation period (Bhattacharjee et al. 2019). Unlike the other habitat metrics at specific discharges thresholds, time-weighted average provides a measure of habitat that incorporates duration. We extended the time-weighted approach by calculating habitat frequency percentiles, which identify the smallest 10% (10^{th} percentile) and largest 10% (90^{th} percentile) of habitat areas regardless of discharge. This contrasts with flow exceedance percentiles, which describe habitat conditions at specific discharge frequencies. We then evaluated hydrologic metrics by assessing their: (1) redundancy or systematic differences in habitat predictions, (2) complementary value, (3) differential sensitivity across habitat types, and (4) consequences for environmental flow recommendations and associated management risks.

RESULTS

Two dimensional models performed better across all habitat metrics when ecological metrics from alternative models were compared to those of the highest resolution model scenario (2D-17XS) as a benchmark. One dimensional models were specifically more prone to extreme overprediction (Figure 4.4). For all metrics and for all aspects of model complexity, the largest model error consistently occurred at the upper and lower extremes of discharge (Figure 4.5).

For predicting total wetted area (Figure 4.4), model dimensionality appeared to affect both precision & accuracy. When compared to 1D models, 2D models exhibited less median-bias and thus more accuracy on average as well as less variability and fewer large errors, especially those of more extreme overprediction. The most extreme overpredictions of 1D models occurred at high flows (max = 31.20 % at 368.12 m^3 s^{-1}) and the most extreme underpredictions at low flows (max = 30.96% at 0.28 m^3 s^{-1}) (Figure 4.5). In contrast, 2D models were most prone to extreme underpredictions, which occurred at low flows (max of 29.05% at 0.28 m^3 s^{-1}), though

there were 2D models that produced smaller overpredictions at low and high flows (max of 8.68 at 0.28 m^3 s^{-1}). For both 1D and 2D models, reducing sampling density increased median-bias and variability, decreasing accuracy and precision. However, sampling design based on bed slope stratification mitigated losses in accuracy and precision in both 1D and 2D models, though it was not enough to overcome the increased errors of overprediction in 1D models (Figure 4.4). Notably, the highest resolution model scenario (2D-17XS) estimated systematically more wetted area than all other scenarios.

We found similar patterns in model performance predicting shallow-fast habitat (Figure 4.4). Again, dimensionality affected both accuracy and precision, with 2D models exhibiting less median-bias and variability than 1D models. The 1D models exhibited a much greater tendency toward over-prediction in comparison to 2D models, most notably extreme overpredictions with decreasing sample density. For 1D models, overprediction was frequent across discharges, and extreme overpredictions exceeded 400% difference from the benchmark at high flows (max = 418.76% at 283.17 m^3s^{-1}) (Figure 4.5). However, the highest flows produced underpredictions in the 1D model. Even among 2D models, decreasing data input resolution affected the median and increased the risk of overprediction. For 2D models, stratification again reduced the effect of changes to sampling density, decreasing the risk of overprediction. However, this did not occur in 1D models. In fact, at some sampling densities, stratification appears to have compounded existing model error, resulting in more median-bias, greater variability, and the extreme > 400% overpredictions. Given the high percent differences from the benchmark, even for the second highest resolution model (2D- 9XS Strat), this metric appears the most sensitive to model simplification.

While other metrics exhibited larger systemic bias (e.g., wider IQR or more extreme outliers), the habitat diversity metric appeared to be the most difficult metric for models to predict with precision across discharges. Regardless of any aspect model complexity, models consistently produced both over- and under-predictions of habitat diversity across the range of discharges. Similar to model performance with the other two habitat metrics, 2D models predicted habitat diversity with greater accuracy and precision than 1D models, especially with respect to overprediction (Figure 4.34). However, unlike with other habitat metrics, changes in sampling density had no clear effect on either 1D or 2D models, nor did sampling design for 1D models. In contrast, stratification improved the overall precision of 2D models, reducing the variability around the mean, especially of overprediction, but it also introduced more extreme underpredictions. Regardless of dimension, models under- and over-predicted diversity at high and low flows. However, only non-stratified samples, both 1D and 2D, produced large errors at low flows, which were underpredictions (max = 64.24% at 0.28 $m^3 s^{-1}$).

Using the highest model resolution (2D-17XS), we examined how the choice of hydrologic metric could affect ecological inference. We computed habitat outcomes at common discharge thresholds used in environmental flow assessment – central tendencies percentiles, and low flow statistics – and compared the outcomes produced by those single-discharge metrics to time-weighted habitat outcomes (Table 4.3). We found that the central tendency hydrologic metrics – mean and median – provided similar estimates of total wetted habitat area as time-weighted average. However, both mean and median overestimated the provisioning of the rarer, shallow-fast habitat in comparison to the time-weighted average. For habitat diversity, median and time-weighted average provided similar estimates, while the diversity estimate for mean was lower, indicating a higher influence of lower diversity values at certain flow conditions.

Proportion of shallow-fast habitat differed between flow percentiles and time-weighted percentiles. The 10th and 90th percentiles of discharge showed a decrease from low to high flow (12.63% to 6.87%, respectively), whereas time-weighted percentiles showed the largest 10% of the habitat proportion occurred at high flows (26.05 – 356.79; Table 4.3). The median discharge estimated a higher proportion (15.58%) than either flow percentile, revealing a unimodal relationship between flow and shallow-fast habitat (Table 4.3). Further, the broad range of associated high flows from the time-weighted 90th percentile suggests a more complex, multi-modal relationship.

The habitat diversity estimate decreased from the 10th to 90th percentiles of flow (1.16 to 0.72, respectively) indicating a negative relationship with flow (Table 4.3). Similarly, the higher habitat diversity estimate was associated with lower discharges in the time-weighted percentiles. However, the habitat percentiles revealed a mismatch between habitat size and diversity: the larger habitat (i.e., 90th percentile of habitat) was associated with the lower diversity estimate, while the smaller habitat was linked to higher diversity.

The regulatory low flow metric 30Q2 uses a similar discharge threshold as the 10th percentile of flow, resulting in redundant values. In contrast, the 7Q10 metric represents extreme low flow and produced lower values than the 10th percentile of discharge across all three habitat outcomes. This indicates a continued decline in habitat quantity and diversity with more extreme low flows (Table 4.3). The proportion of shallow-fast habitat appeared particularly sensitive, with the estimate halving from 12.63 to 6.29.

DISCUSSION

Our findings illustrate that both hydraulic model complexity and hydrologic metric selection can significantly shape ecological understanding, especially for sensitive and less

common habitat types. Using the highest model resolution (2D-17XS) for the Middle Oconee River as a benchmark, we found that increasing model dimensionality combined with targeted field data collection strategies, such as stratified sampling, enhanced habitat predictions, consistently reduced the risk of overprediction and proved especially critical for accurately estimating certain habitat outcomes (i.e., proportion shallow-fast habitat). However, we found distinct limitations of even the highest resolution model in accurately and precisely predicting habitat provisioning under extreme low or high flows. In evaluating the outcomes from hydrologic metrics that represent discharge in different ways, we found distinct benefits to using time-weighted metrics, as well as complementary insights provided by targeted summary statistics in the presence of a complex, non-monotonic relationship between flow and proportion shallow-fast habitat. While these specific ecological responses to modeling choices are unique to the Middle Oconee River in Athens, GA, the general patterns provide insight into how differences in hydraulic model complexity and hydrologic representation may influence common management decisions, such as environmental flow recommendations.

In Study 1, we found that greater model dimensionality and informed field data collection (i.e. increased sampling density and transect stratification) improved model performance for all three habitat provisioning outcomes: (1) total wetted area, encompassing all unique combinations of water velocity and depth and thus habitat for all taxa, (2) the proportion of the less common, and therefore potentially higher management concern shallow-fast habitat, and (3) the Shannon-Wiener diversity index which quantifies the evenness and richness of hydraulic habitat types provisioned for of associated taxa. While greater model complexity generally improved model performance, there were instances in which increased data input resolution and/or stratification offered little benefit (e.g., performance of all higher-sampling density models in predicting

habitat diversity), or even reduced model performance (e.g., 1D stratified models in predicting the proportion shallow-fast habitat).

Overall, the metric total-wetted habitat was the least sensitive to variations in model complexity, whereas proportion shallow-fast habitat was the most sensitive to changes. However, across all configurations, 1D models exhibited a greater tendency toward overprediction, which could potentially lead to underestimation of the ecological risk associated with lower eflow thresholds (i.e., overestimating habitat provisioning at lower discharges). For total wetted habitat, incorporating stratification across models mediated the effects of decreased cross-section density (i.e., reduced data input resolution). However, when predicting the proportion of shallow-fast habitat, this same method introduced extreme overpredictions. Given that water managers are likely to prioritize the protection of this rarer habitat type, the results illustrate a case where investing in greater model complexity may be justified to obtain a more representative depiction of habitat provisioning to inform flow recommendations. An important distinction involves the risks posed by overpredictions, which are an essential consideration in water management because they help determine the appropriate 'Level of Effort' (LoE), including whether greater or reduced investments, including modeling investments, are justified (Schultz et al. 2010, Harris et al. 2023). Prior research confirms that shallow-fast habitat specifically is associated with higher risk in regard to models overpredicting available habitat due to ecological dynamics – predation and competition (Hayes et al. 2009).

Though total-wetted habitat estimates were affected by modeling decisions, the ecological consequences under non-extreme conditions (e.g., little habitat available to any taxa) are not as clearly interpretable as with specific habitat types. This demonstrates that the choice of ecological metric, alongside model complexity and hydrologic metric selection, determines how

salient a model is: whether the information produced is relevant to decision-makers (Brauman et al. 2021). If a hydraulic model were used to provide information about biota not specialized to depth-velocity combinations, then perhaps a general habitat metric might provide sufficient ecological insights to management recommendations such as eflows. Harris et al. (2023) specifically state that many restoration applications only require lower LoE, which encompasses both model inputs and ecological outcomes. However, whether a general habitat parameter could lead to ecological insights would likely depend upon the associated level of model complexity. In a case study of the Rio Grande, Harris et al. (2024) found a simple ecological metric (i.e., total area) offered minimal insight into habitat provided to the Silvery Minnow with 1D models, but the value was improved with higher model complexity. However, the overall results of their study suggest such an investment in model complexity is better applied to more affirmative ecological outcomes.

While it is important to know how model complexity affects ecological outcomes, these effects don't guarantee meaningful differences in management action. For example, in Study 1 our 1D models overestimated shallow-fast habitat, but if the discrepancy in habitat provisioning were not enough to warrant a change in management (e.g., water withdrawal strategy), there would be no practical effective gain from the investment in complexity. While this is knowledge gained in hindsight, considering the scale of the ecological response relative to the thresholds of management actions can indicate the level of accuracy and precision (representative detail) required from the model. Further, quantifying the level of uncertainty in the modeling process can also indicate whether model performance lies within an acceptable range. Given acceptable model performance, incorporating uncertainty quantification, such as sensitivity analysis, offers

a cost-effective way to improve decision-making in environmental flow management without increasing model complexity.

To effectively use habitat information for water management decision (e.g., eflow determinations), decision-makers must identify which aspects of the flow regime to manage: a choice that depends heavily on the specific hydrologic metrics selected to characterize the regime (McKay et al. 2016). Natural flow regimes are dynamic, and prior research indicates that managing multiple aspects of the natural hydrograph is necessary to maintain the structure and function of aquatic ecosystems (Poff et al. 1997b). It has long been established that not all flow events are equally relevant to the ecology of the system and that magnitude and frequency, specifically, are important aspects of flow to characterize to understand the 'effective' impact on a system (Wolman and Miller 1960). Effectiveness analysis offers a method for incorporating frequency and magnitude into the assessment of habitat provisioning (McKay et al. 2016, Bhattacharjee et al. 2019). Thus, in Study 2, we included time-weighted metrics derived from effectiveness analysis (i.e., magnitude frequency analysis) to examine how hydrologic representation shapes the ecological information available for interpretation.

We found that that time-weighted statistics provided the best understanding of typical provisioning of the less-common, shallow-fast habitat and of habitat diversity. However, a complementary approach**,** capturing the effects of both general and specific aspects of the flow record, provided the most thorough understanding of ecological outcomes, given the presence of a complex flow ecology relationship. While using time-weighted average offered little improvement in estimating total wetted habitat, it produced a more accurate estimate of the proportion of shallow-fast habitat, avoiding the overestimation associated with both mean and median metrics. Given the high likelihood that this habitat is a conservation priority, using a

time-weighted average could reduce uncertainty and the associated risks around the effects of eflow decisions by ensuring that they do not underestimate the amount of shallow-fast habitat provided.

None of the central tendency statistics revealed the nonlinear relationship between the proportion shallow-fast habitat and flow, nor did the use of flow or habitat percentiles alone, regardless of how flow variability was incorporated into the statistics (i.e., time-weighted vs. specific discharge thresholds). This relationship was most fully characterized by a complementary approach, using the central tendency statistic median and both time-weighted percentiles and percentiles of specific discharge thresholds. Using the 10^{th} and 90^{th} flow percentiles alongside the median indicated a unimodal relationship as habitat was higher at the median than at either percentile. However, adding the time-weighted percentiles revealed that it was a multi-modal relationship as the 90^{th} percentile of habitat occurred at higher flows than the peak at moderate flows. The use of one or the other percentiles (flow or habitat) would result in opposite ecological inferences (shallow fast decreases vs. increases, respectively, with increasing flow), while central tendency statistics alone could result in an overprediction of the proportion of shallow-fast habitat. Thus, a simple approach to characterizing the flow-ecology relationship could result in inappropriate eflow determinations. While the habitat outcomes and associated management risks of this relationship are specific to the Middle Oconee River, complex relationships are characteristic of ecological systems (Larsen et al. 2016, Dietze et al. 2018).

Notably, the time-weighted percentile statistics (i.e., 10% smallest amount of habitat), may be a simple method to assess habitat bottlenecks for populations that are habitat-limited. Similar to the concept of ecological bottleneck (Wiens 1977), a habitat bottleneck is as a limitation in critical habitat for one or more life stages that ultimately affects the adult population

level (Bovee et al. 1998). Where static hydraulic models fail to account for how habitat suitability changes through time, Stalnaker et al. (Stalnaker et al. 2017) highlight that by incorporating time (via hydrology data), an effective model can assist in identifying these bottlenecks.

Our findings from Study 2 also highlight the importance of selecting discharge metrics with ecological specificity. Targeted metrics reveal nuanced aspects of flow regimes that general statistics often overlook. For instance, low flow metrics like 7Q10 and 30Q2, both with regulatory relevance, capture different dimension of hydrology. 30Q2 reflects more frequent, seasonal low flows that indicate typical stress tolerance, whereas 7Q10 measures infrequent but extreme low flow events which likely exceed the stress tolerance of biota and lead to detrimental effects. Consequently, a conservative approach to eflows, perhaps in a system with a threatened habitat and/or species, may rely on metrics capturing extreme events, while typical stress-range metrics might be sufficient for setting minimum flows. This underscores the need for alignment between modelers and decision-makers regarding which ecological aspects to capture and the importance of metric interpretability.

Despite the site-specific nature of these studies, our findings provide important considerations in determining the most appropriate modeling approach. While greater complexity and the selection of many metrics could provide the most accurate and/or thorough understanding of an ecological system and the subsequent responses to different management scenarios, there are often serious management constraints — limited financial or computational resources or barriers to communicating complex modeling outcomes, for instance — that shape the feasibility, or tractability, of the modeling approach (Addison et al. 2013, Larsen et al. 2016). For example, Study 2 included only a few hydrologic metrics when, by 2003, 171 metrics were

already available (Olden and Poff 2003), and by 2017, that number had grown to at least 612 (Eng et al. 2017). Running hundreds of discharge metrics through even the simplest of hydrologic models could easily surpass the computational capacity available for the study, posing a significant constraint for groups with limited resources. Our findings suggest that targeted metrics, such as 7Q10, which requires only the historical flow record and simple calculations, provide increased ecological insight that is typically associated with increased computational power. Indeed, the capacity for specific ecological insight, has led to the regulatory use of this metric in setting minimum flow requirements, such as monthly minimum flows (mMFLs) associated with 7Q10 for withdrawal strategies. (Novak et al. 2016). However, researchers note the limitations of these metrics, citing a lack of evidence that they adequately protect stream life, such as fish assemblages (e.g., Freeman and Marcinek 2006), and have provided more integrated alternatives such as the sustainability boundary approach – which focuses on defining boundaries to efforts that are based on multiple aspects of the flow regime (Richter 2010). This highlights, however, a fundamental need for a better understanding of flow ecology relationship.

Increases in dimensionality or geo-physical data input cannot reduce uncertainty in ecological phenomena the model is not including. Thus, gains in credibility due to the quality of geo-physical data, model complexity, or post-processing analysis can be undermined by a lack of ecological data in simple hydraulic models. For example, the ecological outcomes in our models are proxies – water-depth and velocity combinations to represent ecologically significant habitat and thus the presence of fish – but provisioning of habitat does not guarantee availability to fish or healthy, productive populations. Decades of prior research in the same study reach has shown that there are myriad fish-flow dynamics that we are ignoring: some fish exhibit resistance to low

flow (Katz and Freeman 2015), and fish species richness can respond to water withdrawals (Freeman and Marcinek 2006), for instance. Further, these simple hydraulic models seldom integrate the energetics of the system, such as inputting data or using metrics describing basal energetics, despite a wealth of prior research showing that basal resources can determine higher-level trophic production, and those same resources are shaped by the hydrology of the system. In the same study reach, prior research has shown that primary producer growth and population size responds to low water velocity and discharges (Pahl 2009b, Wood et al. 2019) and that antecedent conditions – both high and low flows- affect producer identity and biomass (Conn et al. Ch. 2). These primary producers are both energy and habitat for the macroinvertebrates the fish eat, or sometimes even the fish themselves. Thus, in addition to studying the effects of varying geo-physical inputs and increasing complexity, we must also evaluate the direct and potentially interactive effects of differentially incorporating ecological inputs: what trophic level best represents the dynamic being investigated, are ecological proxies appropriate, is post-processing validation with biological data possible?

CONCLUSION

The results of these two studies highlight the importance of creating a model that is appropriate to the system being studied and the questions being asked. There is no one correct level of complexity nor one best set of metrics. Determining the appropriate level of representational and computational detail can be especially challenging with topics like eflows because the information necessary to make decisions requires integrating knowledge and expertise across disciplines with different modeling approaches. Researchers have developed various frameworks to guide the development of models coupling ecological and geophysical systems that include an evaluation of complexity (e.g., Larsen et al. 2016). In practice, balancing

the need for representational and/or computational detail with tractability remains a central challenge in environmental flow modeling. Our results illustrate that decisions about model complexity and hydrologic representation should be explicitly guided by management objectives and tolerance for ecological risk. Further, hydrodynamic complexity alone cannot resolve ecological uncertainty, and continued research into ecological modeling inputs, especially around basal energetics, needs to occur alongside other modeling considerations.

TABLES

Table 4.1. Overview of the study designs evaluating the effects of hydraulic model complexity and hydrologic representation on ecological inference.

Study	Research Question	General Approach	Summary of Results
1	How does ecological inference vary with hydraulic model complexity?	Three fish habitat metrics computed from ten hydraulic-habitat models of varying resolution.	Figure 3
2	How does ecological inference vary with hydrologic representation?	Three fish habitat metrics computed at common hydrologic summary statistics and time-averaged through effectiveness analysis.	Table 3

Table 4.2. Habitat suitability criteria and representative taxa (modified from Bain et al. 1995).Total wetted area comprises the three specific habitat types as well as all remaining habitat categorized as 'other'.

Habitat Type	Water Depth	Water Velocity	Representative Taxa
Deep - fast	> 35 cm	> 45 cm s^{-1}	*Micropterus salmoides* (largemouth bass)
Shallow - fast	≤ 35 cm	≥ 55 cm s^{-1}	*Nocomis leptocephalus* (bluehead chub) *Etheostoma inscriptum* (turquoise shiner)
Shallow - slow	≤ 35 cm	< 35 cm s^{-1}	*Lepomis spp.* (bluegill and sunfish)

Table 4.3: Habitat outcomes derived from alternative indices that differentially incorporate flow variability. Traditional discharge statistics calculate habitat at specific discharge thresholds, while time-weighted statistics calculate habitat while accounting for the frequency of the discharge.

Hydrologic Metric	Associated Discharge (m^3s^{-1})	Total Wetted Area (ha)	Proportion Shallow-Fast Habitat	Habitat Diversity Metric (dimensionless)
Traditional Metrics				
Mean Discharge	14.75	1.29	14.95	0.97
Median Discharge	9.91	1.23	15.58	1.21
10^{th} Percentile of Discharge (low flow)	4.16	1.10	12.63	1.16
90^{th} Percentile of Discharge (high flow)	26.05	1.41	6.87	0.72
Time-weighted Metrics				
Time-weighted Average	—	1.25	12.47	1.22
10^{th} Percentile of Habitat (smallest habitat)	0.23 - 4.16	1.1	8.72	1.07
90^{th} Percentile of Habitat (largest habitat)	26.05 - 356.79	1.41	20.4	0.66
Regulatory Low Flow Metrics				
Annual 7Q10	1.27	0.96	6.29	0.87
Annual 30Q2	4.39	1.11	13.01	1.19

FIGURES

Figure 4.1: Map of study site on the Middle Oconee River at Ben Burton Park in Athens, Georgia. Model cross sections (white lines) indicate the transects where bathymetric data was collected directly from the Middle Oconee River. These cross-sections determined the input data resolution. Elevational data depicted as a heat map are from a previously developed LiDAR-derived digital elevation model of floodplain terrain modified to include a 2D representation of channel bathymetry derived from transect data.

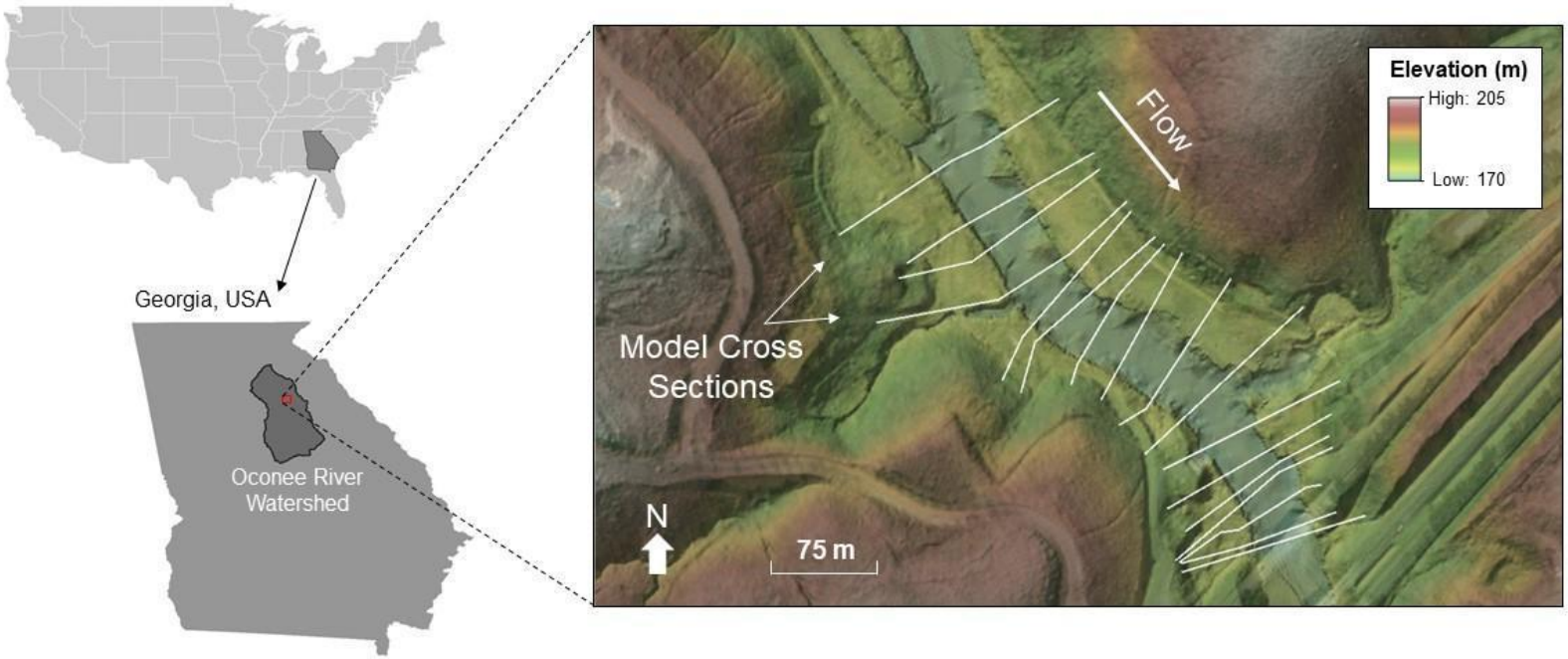
Georgia, USA
Oconee River
Watershed
Model Cross
Sections
Flow
Elevation (m)
High: 205
Low: 170
N
75 m

Figure 4.2: Cumulative habitat rating curve for the two-dimensional, 17 cross-section (2D-17XS) hydraulic-habitat model for the range of recorded discharges. Habitat rating curves were developed for all 10 model scenarios. 2D-17XS is the highest resolution mode.

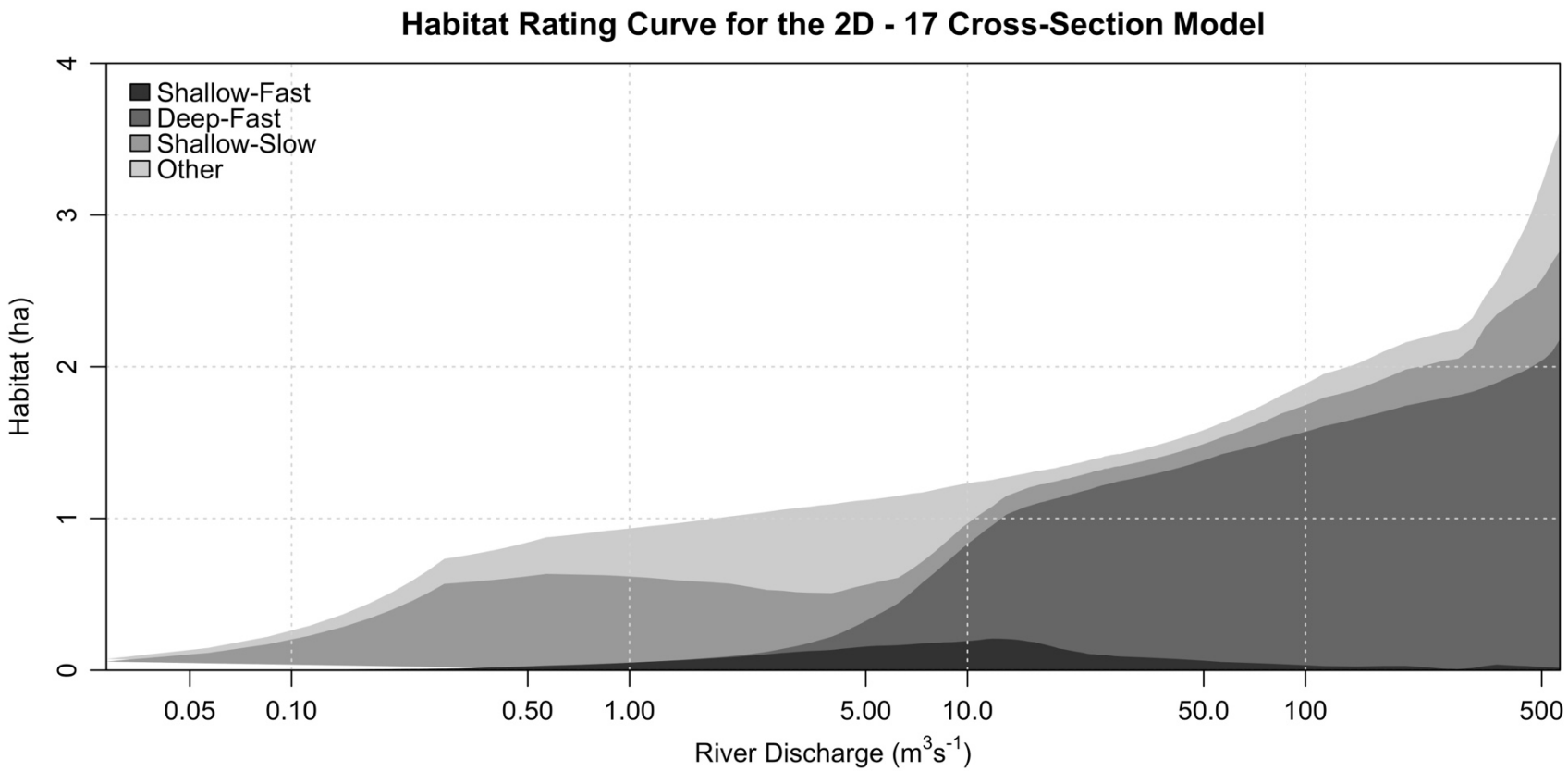
Habitat Rating Curve for the 2D - 17 Cross-Section Model
Shallow-Fast
Deep-Fast
Shallow-Slow
Other
Habitat (ha)
0
1
2
3
4
0.05
0.10
0.50
1.00
5.00
10.0
50.0
100
500
River Discharge (m3s-1)

Figure 4.3: Conceptual depiction of magnitude frequency curve from Bhattacharjee et al. (2019). The habitat rating curve describes the amount of habitat (i.e., magnitude) across different stream discharges while the frequency curve indicates the frequency of the discharges. The effectiveness curve integrates the two, indicating the amount of habitat experienced over time given how often each discharge occurs.

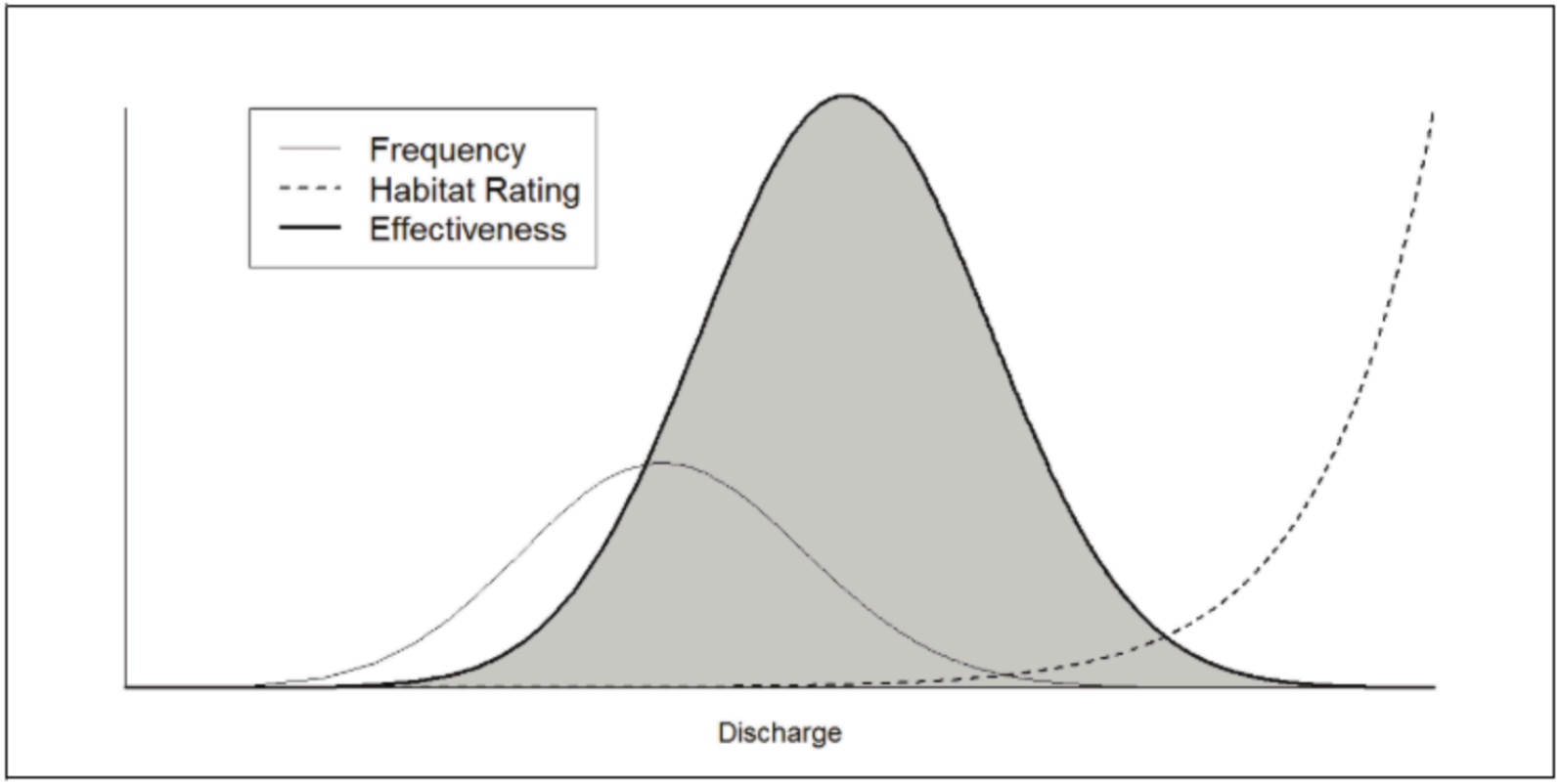
Frequency
Habitat Rating
Effectiveness
Discharge

Figure 4.4: Effects of hydraulic model complexity on habitat modeling outcomes: total wetted area (top), proportion of shallow-fast habitat (middle), and Shannon-Weiner diversity index (bottom). Hydraulic model dimensionality is labeled as one- or two-dimensional (1D and 2D, respectively). Input data resolution is expressed as the number of cross-sections in the hydraulic model (i.e., 5, 9, or 17). Sampling design is shown as stratified by bed slope or evenly spaced. Positive values indicate the model underpredicts relative to the benchmark; negative values indicate overprediction. Each boxplot represents the habitat metrics computed for each discharge executed in the models (i.e., 79 streamflow values).

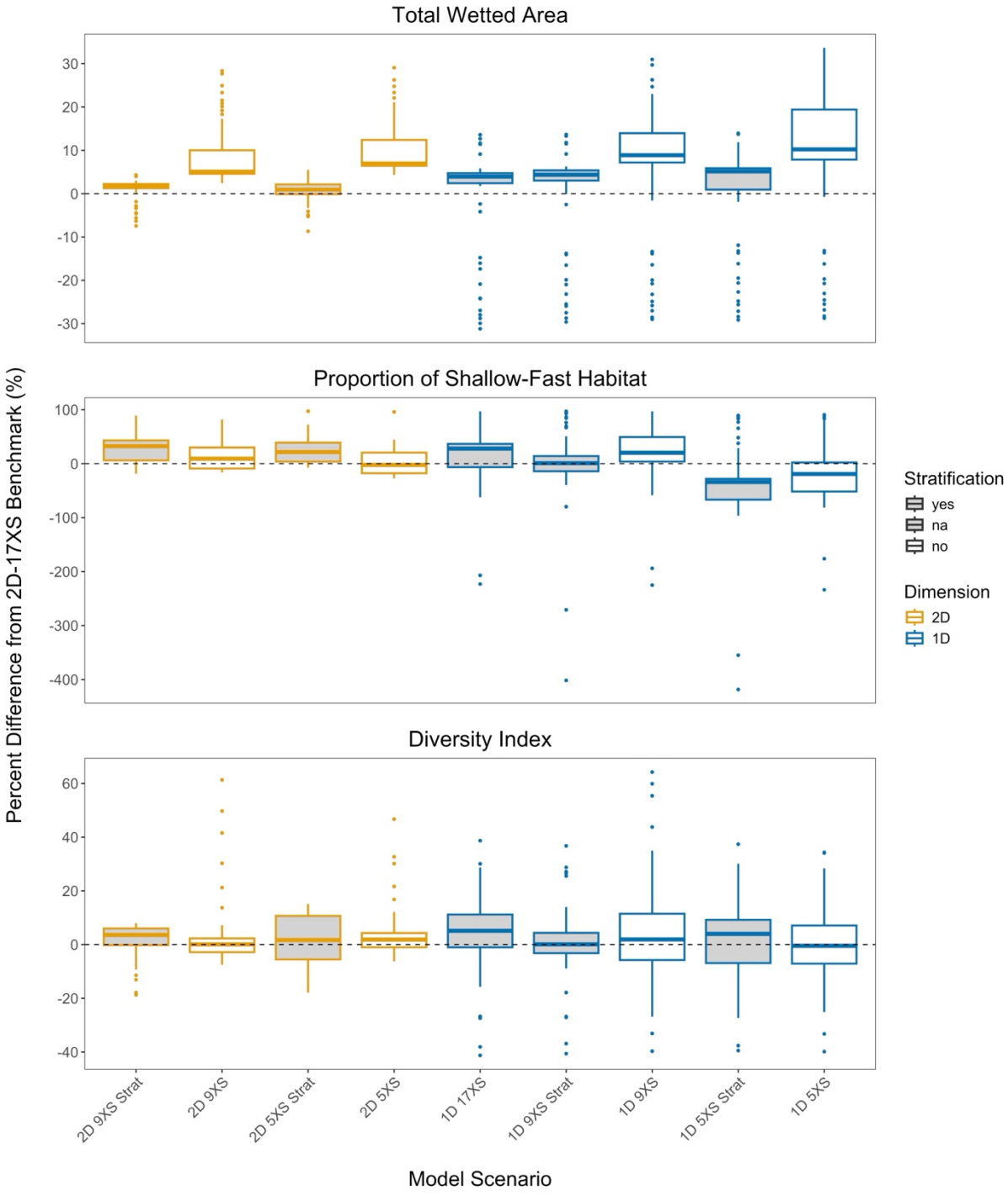
Total Wetted Area
Proportion of Shallow-Fast Habitat
Diversity Index
Percent Difference from 2D-17XS Benchmark (%)
Model Scenario
2D 9XS Strat
2D 9XS
2D 5XS Strat
2D 5XS
1D 17XS
1D 9XS Strat
1D 9XS
1D 5XS Strat
1D 5XS
Stratification
yes
na
no
Dimension
2D
1D

Figure 4.5: Distribution of model outliers (values beyond the 75th percentile) across the full range of discharge (m^3 s^{-1}) in comparison to the 2D-17XS benchmark. Models are separated by dimension (1D vs 2D; top panel) and stratification status (stratified vs non-stratified; bottom panel). The dimension comparison includes all model configurations, while the stratification comparison excludes the 1D-17XS model as there is no stratified counterpart. Positive y-values (above the dashed line) indicate an underprediction; negative y-values (below the dashed line) indicate an over-prediction.

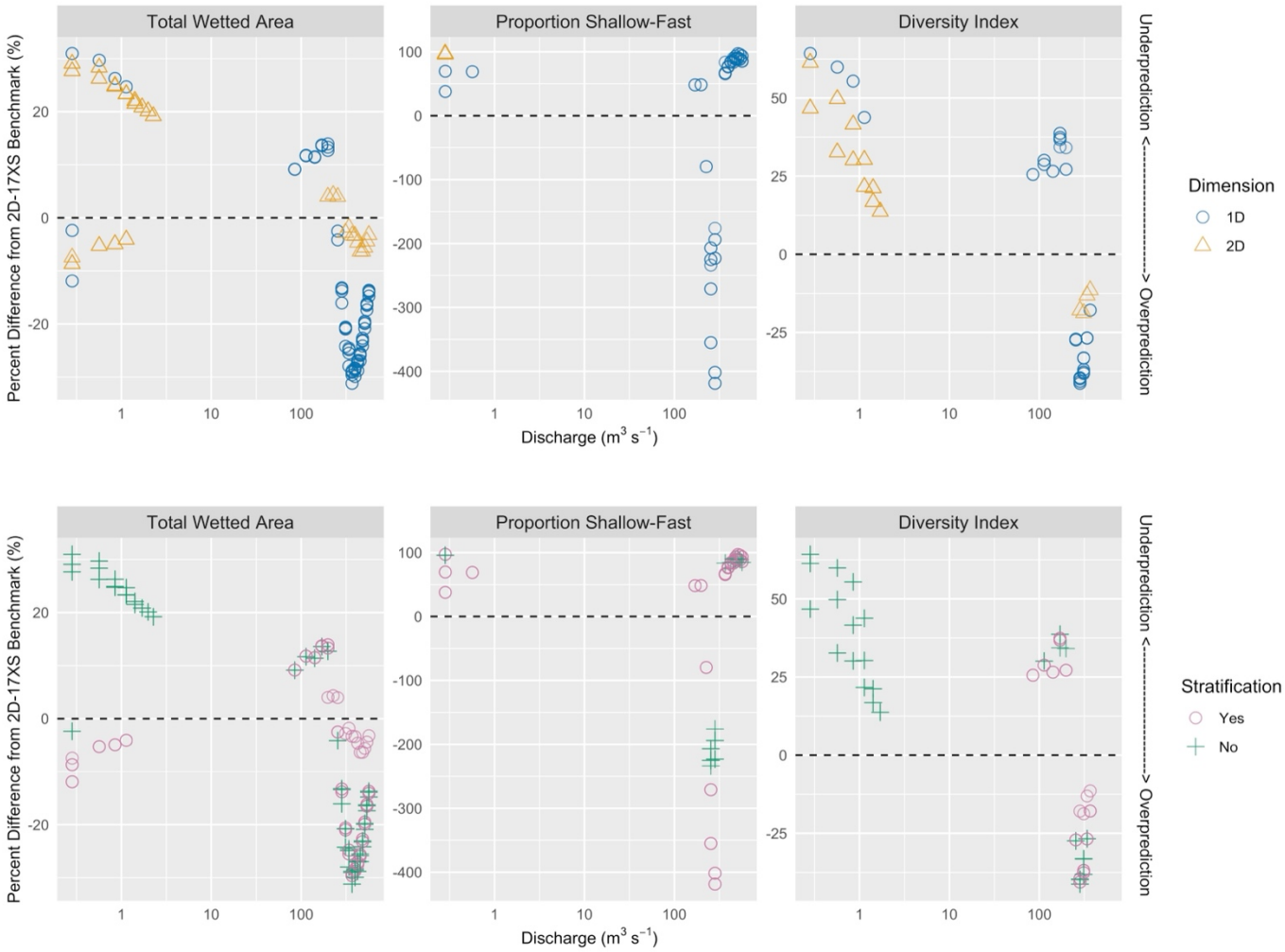
Total Wetted Area
Proportion Shallow-Fast
Diversity Index
Percent Difference from 2D-17XS Benchmark (%)
Discharge (m3 s−1)
Underprediction <----------> Overprediction
Dimension
1D
2D
Stratification
Yes
No

REFERENCES

Addison, P. F. E., L. Rumpff, S. S. Bau, J. M. Carey, Y. E. Chee, F. C. Jarrad, M. F. McBride, and M. A. Burgman. 2013. Practical solutions for making models indispensable in conservation decision-making. Diversity and Distributions 19:490–502.

Annear, T. C. ., Peter. Aarrestad, Allan. Locke, H. Arthur. Beecher, Ian. Chisholm, K. B. . Mayes, John. Marshall, C. E. . Coomer, Joel. Hunt, Rick. Jacobson, Gerrit. Jobsis, John. Kauffman, Gary. Smith, Rod. Wentworth, C. B. . Stalnaker, and C. C. . Estes. 2004. Instream flows for riverine resource stewardship. Instream Flow Council, Cheyenne, WI.

Bain, M. B. 1995. L'habitat a l'echelle locale: distribution multiparametre des poissons d'eau courante. Bulletin Francais de Peche et Pisciculture:165–177.

Bhattacharjee, N. V, J. R. Willis, E. W. Tollner, and S. K. Mckay. 2019. Habitat Provision Associated with Environmental Flows:1–14.

Bovee, K. D., B. L. Lamb, J. M. Bartholow, C. B. Stalnaker, J. Taylor, and J. Henriksen. 1998. Stream Habitat Analysis Using the Instream Flow Incremental Methodology tm m. Washington D.C.

Bowen, Z. H., M. C. Freeman, and K. D. Bovee. 1998. Evaluation of Generalized Habitat Criteria for Assessing Impacts of Altered Flow Regimes on Warmwater Fishes; Evaluation of Generalized Habitat Criteria for Assessing Impacts of Altered Flow Regimes on Warmwater Fishes. Transactions of the American Fisheries Society 127:455–468.

Brauman, K. A., L. L. Bremer, P. Hamel, B. F. Ochoa-Tocachi, F. Roman-Dañobeytia, V. Bonnesoeur, E. Arapa, and G. Gammie. 2021. Producing valuable information from hydrologic models of nature-based solutions for water. Integrated Environmental

Assessment and Management 18:135–147.Davis, J., A. P. O'Grady, A. Dale, A. H. Arthington, P. A. Gell, P. D. Driver, N. Bond, M. Casanova, M. Finlayson, R. J. Watts, S. J. Capon, I. Nagelkerken, R. Tingley, B. Fry, T. J. Page, and A. Specht. 2015. When trends intersect: The challenge of protecting freshwater ecosystems under multiple land use and hydrological intensification scenarios. Science of The Total Environment 534:65–78.

Dietze, M. C., A. Fox, L. M. Beck-Johnson, J. L. Betancourt, M. B. Hooten, C. S. Jarnevich, T. H. Keitt, M. A. Kenney, C. M. Laney, L. G. Larsen, H. W. Loescher, C. K. Lunch, B. C. Pijanowski, J. T. Randerson, E. K. Read, A. T. Tredennick, R. Vargas, K. C. Weathers, and E. P. White. 2018. Iterative near-term ecological forecasting: Needs, opportunities, and challenges. Proceedings of the National Academy of Sciences 115:1424–1432.

Eng, K., T. E. Grantham, D. M. Carlisle, and D. M. Wolock. 2017. Predictability and selection of hydrologic metrics in riverine ecohydrology. https://doi.org/10.1086/694912 36:915–926.

Freeman, M. C., and P. A. Marcinek. 2006. Fish assemblage responses to water withdrawals and water supply reservoirs in piedmont streams. Environmental Management 38:435–450.

Gotvald, A. J. 2017. Methods for estimating selected low-flow frequency statistics and mean annual flow for ungaged locations on streams in North Georgia. Scientific Investigations Report.

Gregory, R. S., and R. L. Keeney. 2002. Making smarter environmental management decisions. Journal of the American Water Resources Association 38:1601–1612.

Harris, A., M. Porter, S. K. McKay, A. Mulchandani, and M. Stone. 2024. Hydraulic analysis for assessing environmental flow selection and ecological model formulation. Ecohydrology 17.

Harris, A., N. Richards, and S. K. Mckay. 2023. Defining levels of effort for ecological models.

Hayes, D., M. Jones, N. Lester, C. Chu, S. Doka, J. Netto, J. Stockwell, B. Thompson, C. K. Minns, B. Shuter, and N. Collins. 2009. Linking fish population dynamics to habitat conditions: Insights from the application of a process-oriented approach to several Great Lakes species. Reviews in Fish Biology and Fisheries 19:295–312.

Larsen, L. G., M. B. Eppinga, P. Passalacqua, W. M. Getz, K. A. Rose, and M. Liang. 2016. Appropriate complexity landscape modeling. Earth-Science Reviews 160:111–130.

McKay, S. K., M. C. Freeman, and A. P. Covich. 2016. Application of Effective Discharge Analysis to Environmental Flow Decision-Making. Environmental Management 57:1153–1165.

Merwade, V., A. Cook, and J. Coonrod. 2008. GIS techniques for creating river terrain models for hydrodynamic modeling and flood inundation mapping. Environmental Modelling & Software 23:1300–1311.

Novak, R., J. G. Kennen, R. W. Abele, C. F. Baschon, D. M. Carlisle, L. Dlugolecki, D. M. Elignor, J. E. Flotemersch, P. Ford, J. Fowler, R. Galer, L. P. Gordon, S. E. Hansen, B. Herbold, T. E. Johnson, J. M. Johnston, C. P. Konrad, B. Leamond, and P. W. Seelbach. 2016. Final EPA-USGS Technical Report: Protecting Aquatic Life from Effects of Hydrologic Alteration.

Olden, J. D., and N. L. Poff. 2003. Redundancy and the choice of hydrologic indices for characterizing streamflow regimes. River Research and Applications 19:101–121.

Pahl, J. P. 2009. Effects of flow alteration on the aquatic macrophyte *Podostemum ceratophyllum* (riverweed); local recovery potential and regional monitoring strategy.

Peterson, J. T., J. M. Wisniewski, C. P. Shea, and C. Rhett Jackson. 2011. Estimation of Mussel Population Response to Hydrologic Alteration in a Southeastern U.S. Stream. Environmental Management 48:109–122.

Poff, N. L., J. D. Allan, M. B. Bain, J. R. Karr, K. L. Prestegaard, B. D. Richter, R. E. Sparks, and J. C. Stromberg. 1997. The Natural Flow Regime. BioScience 47:769–784.

Poff, N. L., C. M. Brown, T. E. Grantham, J. H. Matthews, M. A. Palmer, C. M. Spence, R. L. Wilby, M. Haasnoot, G. F. Mendoza, K. C. Dominique, and A. Baeza. 2016. Sustainable water management under future uncertainty with eco-engineering decision scaling. Nature Climate Change 6:25–34.

Poff, N. L., B. D. Richter, A. H. Arthington, S. E. Bunn, R. J. Naiman, E. Kendy, M. Acreman, C. Apse, B. P. Bledsoe, M. C. Freeman, J. Hendriksen, R. B. Jacobson, J. G. Kennen, D. M. Merritt, J. H. O'keeffe, J. D. Olden, K. Rogers, R. E. Tharme, and A. Warner. 2010. The ecological limits of hydrologic alteration (ELOHA): A new framework for developing regional environmental flow standards. Freshwater Biology 55:147–170.

Poff, N. L. R. 2018. Beyond the natural flow regime? Broadening the hydro-ecological foundation to meet environmental flows challenges in a non-stationary world. Freshwater Biology 63:1011–1021.

Richter, B. D. 2010. Re-thinking environmental flows: From allocations and reserves to sustainability boundaries. River Research and Applications 26:1052–1063.

Richter, B. D., J. V Baumgartner, J. Powell, and D. P. Braun. 1996. A Method for Assessing Hydrologic Alteration within Ecosystems. Conservation Biology 10:1163–1174.

Richter, B. D., A. T. Warner, J. L. Meyer, and K. Lutz. 2006. A collaborative and adaptive process for developing environmental flow recommendations. River Research and Applications 22:297–318.

Risley, J., A. Stonewall, and T. Haluska. 2008. Estimating Flow-Duration and Low-Flow Frequency Statistics for Unregulated Streams in Oregon.

Schultz, M. T., K. N. Mitchell, B. K. Harper, and T. S. Bridges. 2010. ERDC TR-10-12 "Decision Making Under Uncertainty."

Turner, M. G., and S. R. Carpenter. 2017. Ecosystem Modeling for the 21st Century. Ecosystems 20:211–214.

US Army Corps of Engineers. 2019. HEC-RAS River Analysis System. U.S. Army Corps of Engineers, Hydrologic Engineering Center.

Uusitalo, L., A. Lehikoinen, I. Helle, and K. Myrberg. 2015. An overview of methods to evaluate uncertainty of deterministic models in decision support. Environmental Modelling & Software 63:24–31.

Wiens, J. A. 1977. On Competition and Variable Environments: Populations may experience "ecological crunches" in variable climates, nullifying the assumptions of competition theory and limiting the usefulness of short-term studies of population patterns on. American Scientist 65:590–597.

Wolman, M. G., and J. P. Miller. 1960. Magnitude and Frequency of Forces in Geomorphic Processes. https://doi.org/10.1086/626637 68:54–74.

Wood, J. L., J. W. Skaggs, C. Conn, and M. C. Freeman. 2019. Water velocity regulates macro-consumer herbivory on the benthic macrophyte Podostemum ceratophyllum Michx. Freshwater Biology 64:2037–2045.

AUTHOR CONTRIBUTIONS

Author C. C. Conn developed the code, conducted all analyses, interpreted results with the assistance from S. K. McKay, and wrote the manuscript with input from M. C. Freeman and written contributions from S. K. McKay and T. A. Keys. Co-author S. K. McKay conceived of the presented idea and secured funding. Co-author T. A. Keys developed and implemented the HEC-RAS model. The author and all co-authors contributed to the study design.

All co-authors agree that the work may be included in this thesis or dissertation.

CHAPTER 5

CONCLUSION

As pressure on riverine ecosystems continues to increase, water managers are tasked with balancing ecological integrity with societal demands for freshwater. The ultimate goal of my research is to improve predictions of ecological responses to better inform those water management decisions. To do so requires building a mechanistic understanding of the biotic links between streamflow and stream function while also identifying reliable methods for using that knowledge to inform decision-making. The contributions of this dissertation are twofold: (1) filling an ecological knowledge gap by quantifying individual steps in the producer-mediated pathway of streamflow affecting function and (2) filling a modeling knowledge gap by evaluating how modeling decisions influence the uncertainty associated with predicting ecological responses to streamflow.

Identifying existing flow ecology relationships is a key step in determining how ecosystems will respond to future climate and management scenarios (Poff and Zimmerman 2010b). Palmer and Ruhi (2019) identify a critical point in this research as the 'flow-biota-ecosystem-process-nexus'. This term highlights the dual roles of ecological structure and function as well as the dynamic, multi-directional nature of the three-way relationship. Primary producer biomass represents a foundational metric of ecosystem structure – food and habitat to other stream biota, while gross primary productivity is the critical function that structure provides, and one inextricably linked to other ecosystem processes. In Chapter 2, I focused on the first two elements of the nexus – antecedent flow conditions and primary producers. In

Chapter 3, I connected the same primary producers to the third element of the nexus – the process of primary production.

Our findings in Chapter 2 show that antecedent flow conditions, both high and low flows, are strong drivers of the biomass and distribution of *Podostemum ceratophyllum*, biofilms containing algae, and filamentous algae. The predictor variables we used to model primary producer biomass represent unique combinations of the defining characteristics of a flow regime: magnitude, frequency, duration, timing, and rate of change of discharge. By examining temporal patterns in peak biomass, we found that sustained drought and floods had strong producer-specific effects. *Podostemum* and filamentous algae benefited from longer periods of high flows, while being negatively affected by low flows. In contrast, biofilm was the only group to be positively affected by low flows. These results are consistent with other empirical studies elucidating different bottom-up and top-down controls of producer biomass, such as water velocity and herbivory (Peterson and Stevenson 1992, Rosemond et al. 1993, Wood et al. 2019). Further, they provide empirical support for current theory which implicates differences in organismal traits, largely growth form, as the determinants of producer-specific resistance and resilience to disturbance (Biggs et al. 1998, Dodds and Biggs 2002, Schneck and Melo 2012, Lange et al. 2016). Thus, our research identifies producer-specific responses to antecedent flow conditions – shaped by distinctions in organismal traits – as an important mechanism occurring in the nexus.

In Chapter 3, we found that the same primary producers, separated by broad distinctions in morphology and associated substrate, varied in their mass-specific gross primary productivity. Further separating the producer groups into types, based on stream light environment and/or substrate or taxon, revealed distinct responses to irradiance: saturating, non-saturating, or

photoinhibition. While the productivity rates of *Podostemum*, rock biofilm, and soft substrate biofilm differed by sometimes orders of magnitude, samples of each producer group taken from the sun, along with the green alga *Rhizoclonium*, exhibited a similar functional response: a non-saturating relationship to light. In contrast, samples from the shade and the cyanobacteria *Lyngbya* appeared to similarly exhibit saturation, if not photoinhibition. Soft substrate biofilm, and some samples of seston, exhibited an overall negative relationship with light, though seston was highly variable. In the context of the biodiversity ecosystem functioning framework, distinct GPP-light relationships indicate the presence of functional diversity (Shahid and Justin 2003). Further, similarities in GPP-light relationships of types across producer groups demonstrate that it does not perfectly align with morphological or taxonomic diversity. Our research identifies functional diversity as another important mechanism occurring in the nexus.

When Chapter 3 mass-specific productivity rates were combined with Chapter 2 biomass data, the patterns in productivity rates did not match the patterns in biomass. Rock biofilm and filamentous algae had a higher capacity for productivity than *Podostemum* and soft substrate biofilm. However, *Podostemum* and soft substrate biofilm consistently dominated segments of the stream reach (lower shoal and run, respectively). This decoupling of biomass and productivity produces multiple mechanisms by which producers can affect stream productivity. *Podostemum*, disproportionately contributed to areal stream productivity throughout the study period due to high biomass, which we previously connected to a positive relationship to long term high flows. In contrast, filamentous algae exhibited a high relative GPP contribution, providing more to areal stream productivity than biomass alone would indicate, though only periodically affecting total areal stream productivity due to periods of low or no biomass. Thus, filamentous algae's contribution was both a combination of producer-specific high GPP, which

laboratory trials have indicated would only increase with increasing light availability, and positive and negative relationships with high and low flow conditions, respectively, which we previously connected to the patterns in biomass. These data illustrate the potential for fluctuating stream productivity due to the combination of functional diversity and producer-specific relationships to antecedent flow condition. While the addition of productivity data elucidated a greater portion of the flow-biota-ecosystem-process nexus, it is pivotal that these illustrative projections be empirically validated by connecting organismal GPP to community scale productivity (Suding et al. 2008) as well as fully linking them to whole stream productivity (Bernhardt et al. 2018).

Our findings from Chapters 2 and 3 provide a strong foundation for continued ecological research into the flow ecology relationships that are needed to inform water management decisions. This decision-making process increasingly relies upon integrated modeling, which provides a formal structure for linking complex ecological and geophysical processes (Gregory and Keeney 2002, Addison et al. 2013, Harris et al. 2023). This allows managers to forecast the outcomes of potential scenarios, such as species abundance under different eflow strategies (Gregory and Keeney 2002, Davis et al. 2015, Dietze et al. 2018, Poff 2018). In Chapter 4, I focused on a current challenge in the modeling process: identifying how common aspects of model complexity interact and potentially affect ecological inference about habitat provisioning. While this chapter shifts from primary producers to fish habitat, we modeled the specific streamflow-habitat scenarios in the same Middle Oconee system. Further, our findings provide important insights for modeling the flow-biota-ecosystem-process-nexus.

We found that higher resolution models consistently outperformed simpler models, especially for the less common shallow-fast habitat. We also found that a complementary

approach using both time-weighted and targeted discharge statistics provided the most accurate and comprehensive understanding of how streamflow variability affects habitat provisioning, which was necessary to capture to the non-monotic relationship between flow and the shallow-fast habitat. Model development often presents a challenging between simplicity/complexity and resolution/accuracy (Larsen et al. 2016, Turner and Carpenter 2017), and these results highlight that for sensitive, more rare ecological attributes (structure or function) the investment may be worth it due to the increased risk associated with uncertainty (Schultz et al. 2010).

Podostemum ceratophyllum, whose habitat type generally corresponds to the rarer shallow-fast habitat, presents a high-risk scenario due to its functional importance to both primary (Conn et. al, Ch.2) and secondary production and current population declines (Wood and Freeman 2017). Thus, inaccuracies in model predictions could disproportionately affect the stream ecosystem. Current research indicates how important it is for the representational and computational detail of a model to be informed by management objectives (Larsen et al. 2016), yet simple hydraulic models fail to adequately capture the flow-biota-ecosystem-process nexus Palmer and Ruhi (2019) describe as key to river management. These models often use proxies for ecological outcomes (e.g., habitat provisioning for fish populations) and seldom consider energetic processes, proxies or otherwise. As a foundation species with demonstrated flow-ecology relationships, *Podostemum ceratophyllum* presents an opportunity to improve model predictions of ecosystem processes.

Next Steps

Developing more effective approaches to protecting freshwater integrity is imperative. My dissertation moves research forward in identifying mechanisms underlying the streamflow – stream function relationship and considerations and potential leverage points in current modeling

practices. However, this work has occurred in one, well-studied system: an aspect integral to understanding the underlying mechanisms, but also a major limitation of their use. There remains important links to identify and validate across both community and ecosystem scales. Integrated modeling must also move forward in adequately capturing these mechanisms. This continued movement will allow us to better understand, predict, and protect ecosystem processes under increasing global change and management.

REFERENCES

Addison, P. F. E., L. Rumpff, S. S. Bau, J. M. Carey, Y. E. Chee, F. C. Jarrad, M. F. McBride, and M. A. Burgman. 2013. Practical solutions for making models indispensable in conservation decision-making. Diversity and Distributions 19:490–502.

Bernhardt, E. S., J. B. Heffernan, N. B. Grimm, E. H. Stanley, J. W. Harvey, M. Arroita, A. P. Appling, M. J. Cohen, W. H. McDowell, R. O. Hall, J. S. Read, B. J. Roberts, E. G. Stets, and C. B. Yackulic. 2018. The metabolic regimes of flowing waters. Limnology and Oceanography 63:S99–S118.

Biggs, B. J., D. G. Goring, and V. I. Nikora. 1998. Subsidy and stress responses of stream periphyton to gradients in water velocity as a function of community growth form. Journal of Phycology. 34:598–607.

Davis, J., A. P. O'Grady, A. Dale, A. H. Arthington, P. A. Gell, P. D. Driver, N. Bond, M. Casanova, M. Finlayson, R. J. Watts, S. J. Capon, I. Nagelkerken, R. Tingley, B. Fry, T. J. Page, and A. Specht. 2015. When trends intersect: The challenge of protecting freshwater ecosystems under multiple land use and hydrological intensification scenarios. Science of The Total Environment 534:65–78.

Dietze, M. C., A. Fox, L. M. Beck-Johnson, J. L. Betancourt, M. B. Hooten, C. S. Jarnevich, T. H. Keitt, M. A. Kenney, C. M. Laney, L. G. Larsen, H. W. Loescher, C. K. Lunch, B. C. Pijanowski, J. T. Randerson, E. K. Read, A. T. Tredennick, R. Vargas, K. C. Weathers, and E. P. White. 2018. Iterative near-term ecological forecasting: Needs, opportunities, and challenges. Proceedings of the National Academy of Sciences 115:1424–1432.

Dodds, W. K., and B. J. F. Biggs. 2002. Water velocity attenuation by stream periphyton and macrophytes in relation to growth form and architecture. Journal of the North American Benthological Society 21:2–15.

Gregory, R. S., and R. L. Keeney. 2002. Making smarter environmental management decisions. Journal of the American Water Resources Association 38:1601–1612.

Harris, A., N. Richards, and S. K. McKay. 2023. Defining levels of effort for ecological models. Vicksburg.

Lange, K., C. R. Townsend, and C. D. Matthaei. 2016. A trait-based framework for stream algal communities. Ecology and Evolution 6:23–36.

Larsen, L. G., M. B. Eppinga, P. Passalacqua, W. M. Getz, K. A. Rose, and M. Liang. 2016. Appropriate complexity landscape modeling. Earth-Science Reviews 160:111–130.

Palmer, M., and A. Ruhi. 2019. Linkages between flow regime, biota, and ecosystem processes: Implications for river restoration. Science 365:147–170.

Peterson, C. G., and R. J. Stevenson. 1992. Resistance and resilience of lotic algal communities: importance of disturbance timing and current. Ecology 73:1445–1461.

Poff, N. L. R. 2018. Beyond the natural flow regime? Broadening the hydro-ecological foundation to meet environmental flows challenges in a non-stationary world. Freshwater Biology 63:1011–1021.

Poff, N. L., and J. K. H. Zimmerman. 2010. Ecological responses to altered flow regimes: a literature review to inform the science and management of environmental flows. Freshwater Biology 55:194–205.

Rosemond, A. D., P. J. Mulholland, and J. W. Elwood. 1993. Top-down and bottom-up control of stream periphyton: effects of nutrients and herbivores. Ecology 74:1264–1280.

Schneck, F., and A. S. Melo. 2012. Hydrological disturbance overrides the effect of substratum roughness on the resistance and resilience of stream benthic algae. Freshwater Biology 57:1678–1688.

Schultz, M. T., K. N. Mitchell, B. K. Harper, and T. S. Bridges. 2010. ERDC TR-10-12 "Decision Making Under Uncertainty."

Shahid, N., and P. W. Justin. 2003. Disentangling biodiversity effects on ecosystem functioning: deriving solutions to a seemingly insurmountable problem. Ecology Letters 6:567–579.

Suding, K. N., S. Lavorel, F. S. Chapin, J. H. C. Cornelissen, S. Díaz, E. Garnier, D. Goldberg, D. U. Hooper, S. T. Jackson, and M. Navas. 2008. Scaling environmental change through the community-level: a trait-based response-and-effect framework for plants. Global Change Biology 14:1125–1140.

Turner, M. G., and S. R. Carpenter. 2017. Ecosystem Modeling for the 21st Century. Ecosystems 20:211–214.

Wood, J. L., J. W. Skaggs, C. Conn, and M. C. Freeman. 2019. Water velocity regulates macro-consumer herbivory on the benthic macrophyte *Podostemum ceratophyllum* Michx. Freshwater Biology 64:2037–2045.

APPENDIX A

CHAPTER 2 SUPPLEMENTARY MATERIALS

DATA AVAILABILITY

DOI for all versions of published primary producer biomass data: 10.5281/zenodo.16422069

Repository access: https://doi.org/10.5281/zenodo.16422069

Zenodo Version 1 Record Number 16422070

SUPPLEMENTARY TABLES

Table A1: Comparison of river discharge from the USGS gage 02217500 during the historic record (1929-2015) and the study period (Jan 2016 – Aug 2018). Units for flow are cubic meters per second (m3 s–1). Daily flows are averaged for that calendar day over the years of the timeframe summarized.

Description	Historic record daily flows	Study period daily flows
Lowest daily minimum flow	0.11	1.19
Lowest 5th percentile of daily flows	≤ 0.91	≤ 1.25
State-declared low flow*	≤ 1.28	
Lowest 10th percentile of daily flows	≤ 1.42	≤ 1.30
Lowest 25th percentile of daily flows	≤ 2.78	≤ 1.47
Mean 50th percentile of daily flows	9.94	8.81
Mean daily flow	14.19	10.19
Highest 75th percentile of daily flows	≥ 29.68	≥ 66.69
Highest 95th percentile of daily flows	≥ 104.04	≥ 128.98
Highest daily maximum	376.61	138.19

**This is set at the 7Q10 of a given river system, which is the lowest 7-day mean flow that occurs, on mean, once every 10 years* (United States Environmental Protection Agency 2009).

Table A2: Occurrence and co-occurrence rates of larger producers and/or quantities out of 644 samples. PC = *Podostemum ceratophyllum*. FA = filamentous algae, including *Rhizoclonium* sp. LM = *Lemanea* sp. PF = *Potamogeton foliosus*. BR = bryophytes. DI = diatom mass large enough to be caught in sieve. These producers are categorized as macrophytes (*Podostemum ceratophyllum*, *Potamogeton foliosus* and a third unidentified taxon), bryophytes (2 unidentified morphotypes), filamentous algae (*Rhizoclonium* sp. and *Lyngbya* sp.), red algae (*Lemanea sp.*), and biofilms containing green algae, cyanobacteria, and diatoms.

	PC *n = 378*	**FA** *n = 96*	**LM** *n = 11*	**PF** *n = 11*	**BR** *n = 5*	**DI** *n = 4*
PC		0.85	0.18	1.0	0.4	0.75
FA	0.22		0.27	0.27	0.8	0
LM	0.003	0.03		0	0	0
PF	0.03	0.03	0		0	0
BR	0.005	0.04	0	0		0
DI	0.008	0	0	0	0	
Total Occurrence	0.57	0.15	0.02*	0.02	0.008	0.006*

**LM is a cold-weather species & sampling only occurred during one consecutive winter and spring compared to 3 summers and 2 falls. ** DI total is only of diatom quantities large enough to be caught in a sieve.*

Table A3: Top models (ΔAIC < 2 and for hard substrate also $R^2 > 0.25$) predicting mean and maximum biomass of biofilm (Chl-*a*) across the entire reach, on soft substrate (soft sediment or sand), and on hard substrate (small and large removable rock). Biomass is measured as Chl-*a* per mg m^{-2}. Timeframes: short-term (7d, 14d, 30d), mid-term (90d), long-term (180d). Predictor variables are scaled, and dominant variables are in bold text.

Top Models	R^2	High Flow Coefficient Estimate	High Flow Standard Error	Low Flow Coefficient Estimate	Low Flow Standard Error	ΔAIC	AIC wt.
Biofilm (Chl-*a*)							
mean ~ standard.spate.90 + **x.low.90**	0.88	- 4.97	1.19	10.86	1.14	—	0.53
max ~ standard.spate.30 + **x.low.90**	0.86	- 47.95	21.83	167.18	20.51	—	0.17
max ~ standard.spate.90 + **x.low.90**	0.86	- 44.42	20.34	179.04	19.53	0.05	0.17
Biofilm (Chl-*a*) soft substrate							
mean ~ standard.spate.90 + **x.low.90**	0.88	- 8.63	2.27	20.47	2.18	—	0.49
max ~ standard.spate.90 + **x.low.90**	0.86	- 45.46	20.27	179.40	19.46	—	0.18
max ~ standard.spate.30 + **x.low.90**	0.86	- 47.70	21.96	167.67	20.63	0.28	0.16
Biofilm (Chl-*a*) on hard substrate							
mean ~ standard.spate.180 + min.90	0.29	-2.40	1.01	-1.96	1.00	—	0.01
mean ~ standard.spate.90 + min.90	0.28	-2.18	0.94	-1.73	0.95	0.19	0.01
mean ~ x.high.180 + min.14	0.28	1.46	0.83	-1.85	0.88	0.32	0.01
max ~ x.high.180 + min.14	0.36	20.78	8.31	-18.88	8.79	—	0.03
max ~ x.high.180 + min.30	0.35	21.30	8.47	-18.82	9.04	0.26	0.03

Figure A1: Monthly mean AFDM of seston and biofilm over time. Biofilm AFDM is a mean across the entire reach and is measured in g m^{-2} while seston AFDM is a mean of 2-3 grab samples and is measured in g L^{-1}. Regression of biofilm AFDM predicting seston AFDM: $y = 0.001x + 1.9$ ($R^2 = 0.005$, p-value = 0.79).

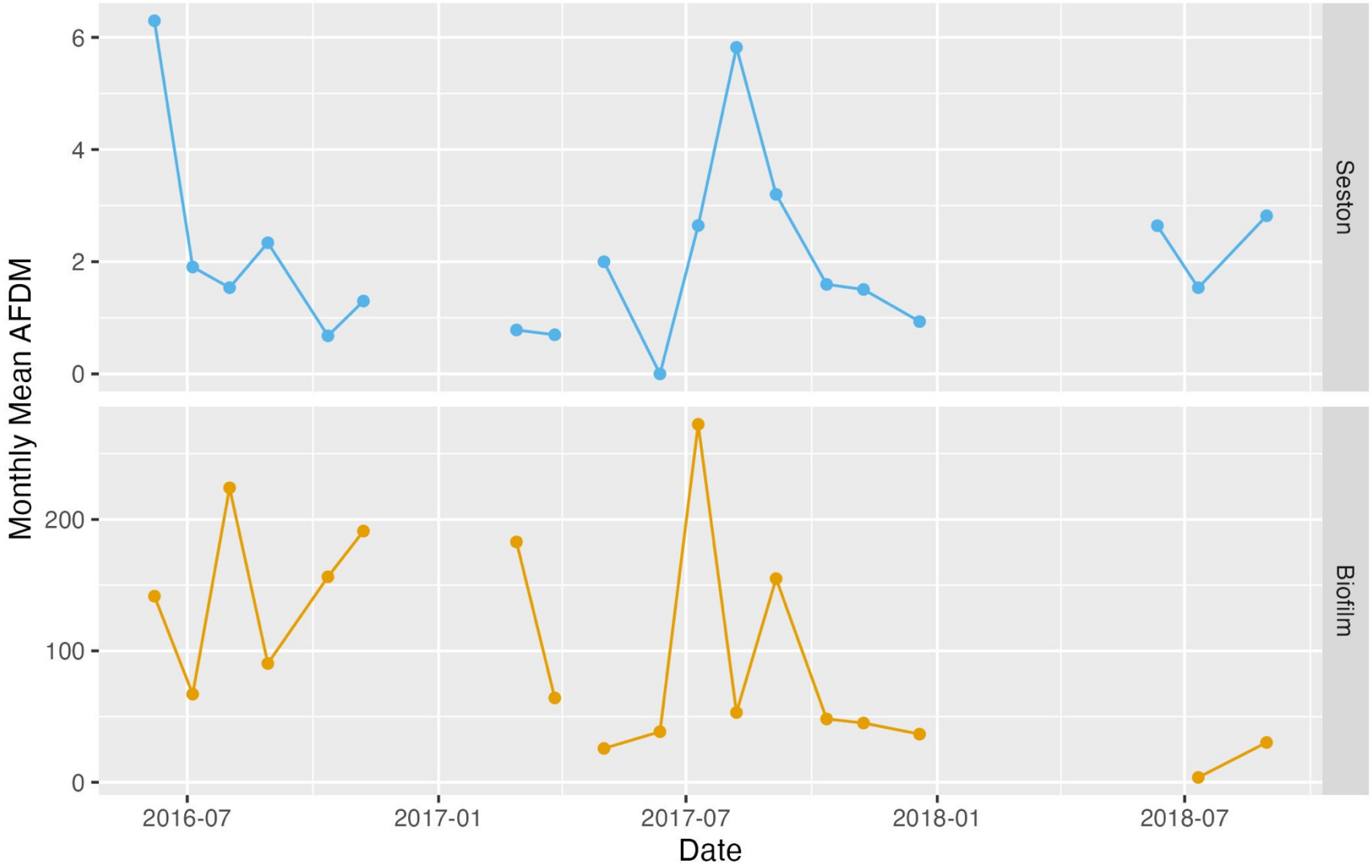
Monthly Mean AFDM
6
4
2
0
200
100
0
Seston
Biofilm
2016-07
2017-01
2017-07
2018-01
2018-07
Date

Figure A2: Proportion of producer mean monthly biomass on each substrate type across the entire reach. Biofilm Chl-*a* was not quantified for bedrock and fixed rock (*). Units for AFDM are g m^{-2} whereas units for Chl-*a* are mg m^{-2}. Error bars indicate standard error of the mean of monthly biomass (n = 18). BR.FR = bedrock or fixed rock, LR = large removable rock, SR = small removable rock, SS = soft

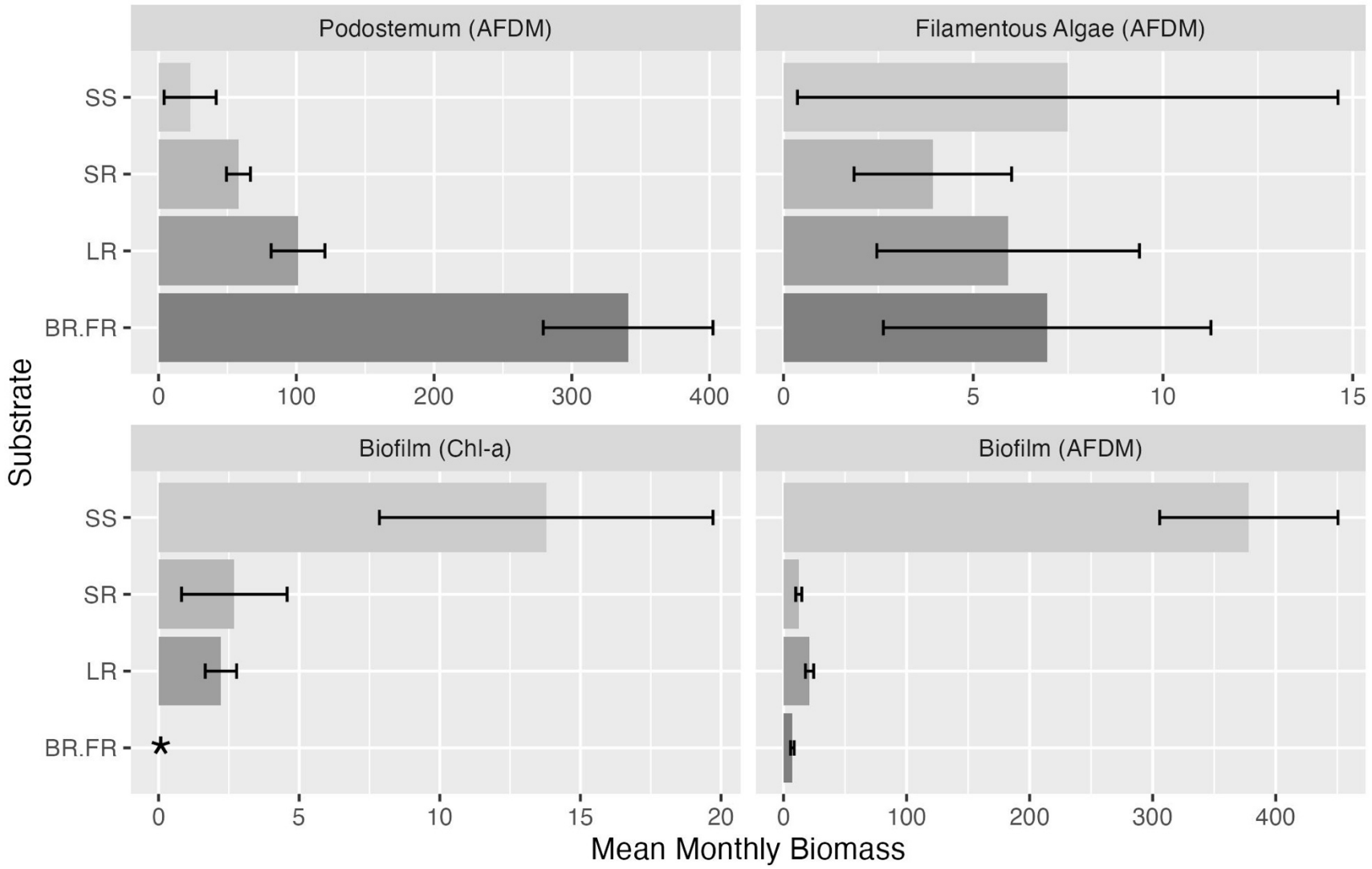
Podostemum (AFDM)
Filamentous Algae (AFDM)
Biofilm (Chl-a)
Biofilm (AFDM)
SS
SR
LR
BR.FR
Substrate
0
100
200
300
400
5
10
15
20
Mean Monthly Biomass

APPENDIX B

CHAPTER 3 SUPPLEMENTARY MATERIALS

DATA AVAILABILITY

DOI for all versions of published primary producer functional data: 10.5281/zenodo.17545386

Repository access: https://doi.org/10.5281/zenodo.17545386

Zenodo Version 1 Record Number 17545387

See Appendix A for published primary producer biomass data.

DOI for all versions of published whole stream functional and environmental monitoring data of the study reach: 10.5281/zenodo.17612952

Repository access: https://doi.org/10.5281/zenodo.17612952

Zenodo Version 1 Record Number 17612953

SUPPLEMENTARY FIGURES

Figure B1: Mass-specific gross primary productivity across producer groups by light treatment separated into high and low GPP rates. Boxplots display GPP (mg O_2 g^{-1} h^{-1}) by experimental light treatment (µmol photons m^{-2} s^{-1}). Boxes represent the interquartile range (25th-75th percentiles) with median line; whiskers extend to 1.5×IQR. Sample sizes ~ 30 ± 2 for all groups except seston. Seston sample size = 43

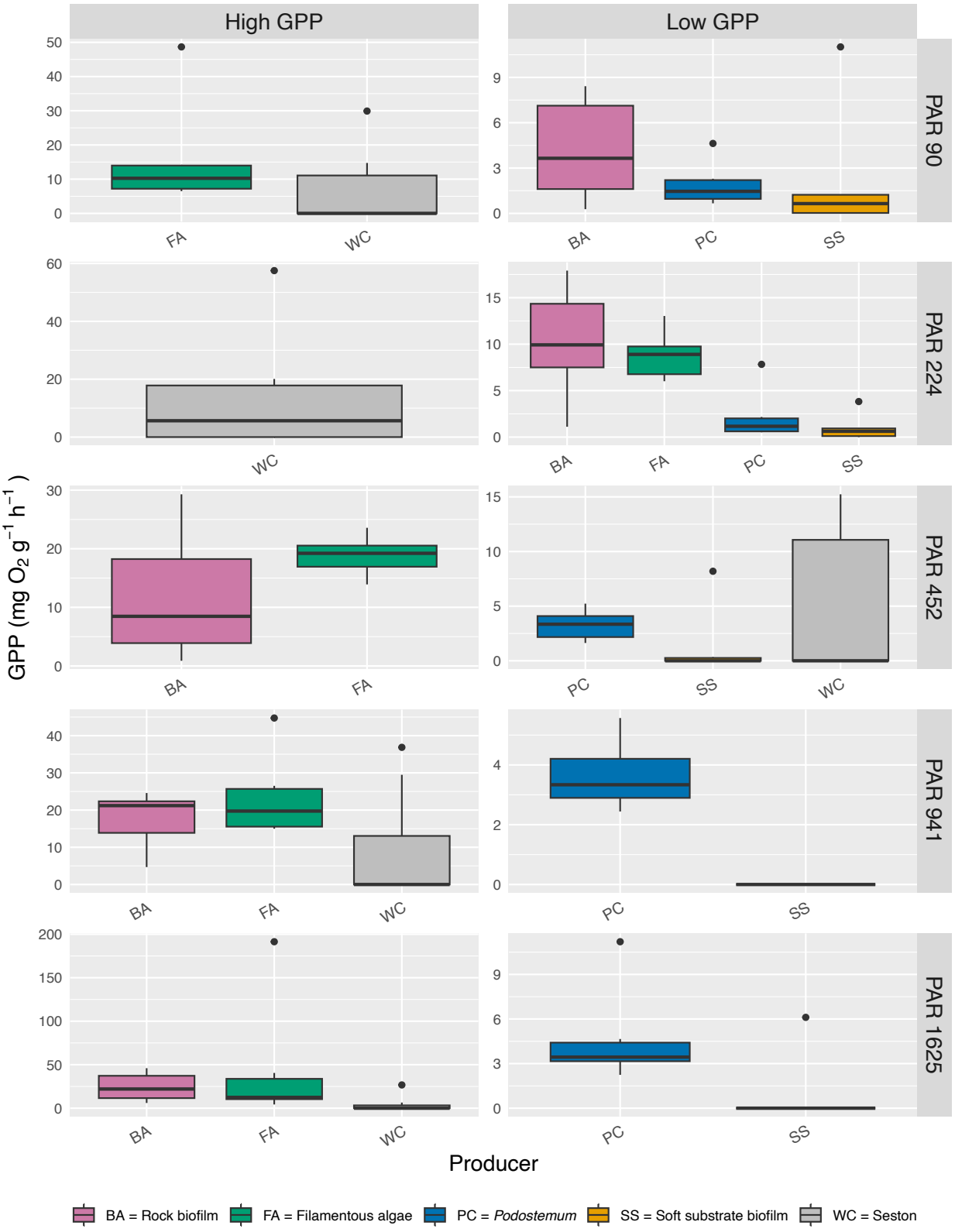
High GPP
Low GPP
PAR 90
PAR 224
PAR 452
PAR 941
PAR 1625
GPP (mg O2 g-1 h-1)
Producer
BA = Rock biofilm
FA = Filamentous algae
PC = Podostemum
SS = Soft substrate biofilm
WC = Seston

Figure B2: Mass-specific gross primary productivity across producer types by light treatment separated into high and low GPP rates. Boxplots display GPP (mg O_2 g^{-1} h^{-1}) by experimental light treatment (μmol photons m^{-2} s^{-1}). Boxes represent the interquartile range (25th-75th percentiles) with median line; whiskers extend to 1.5×IQR. Sample sizes $\sim 15 \pm 2$ for all producer types.

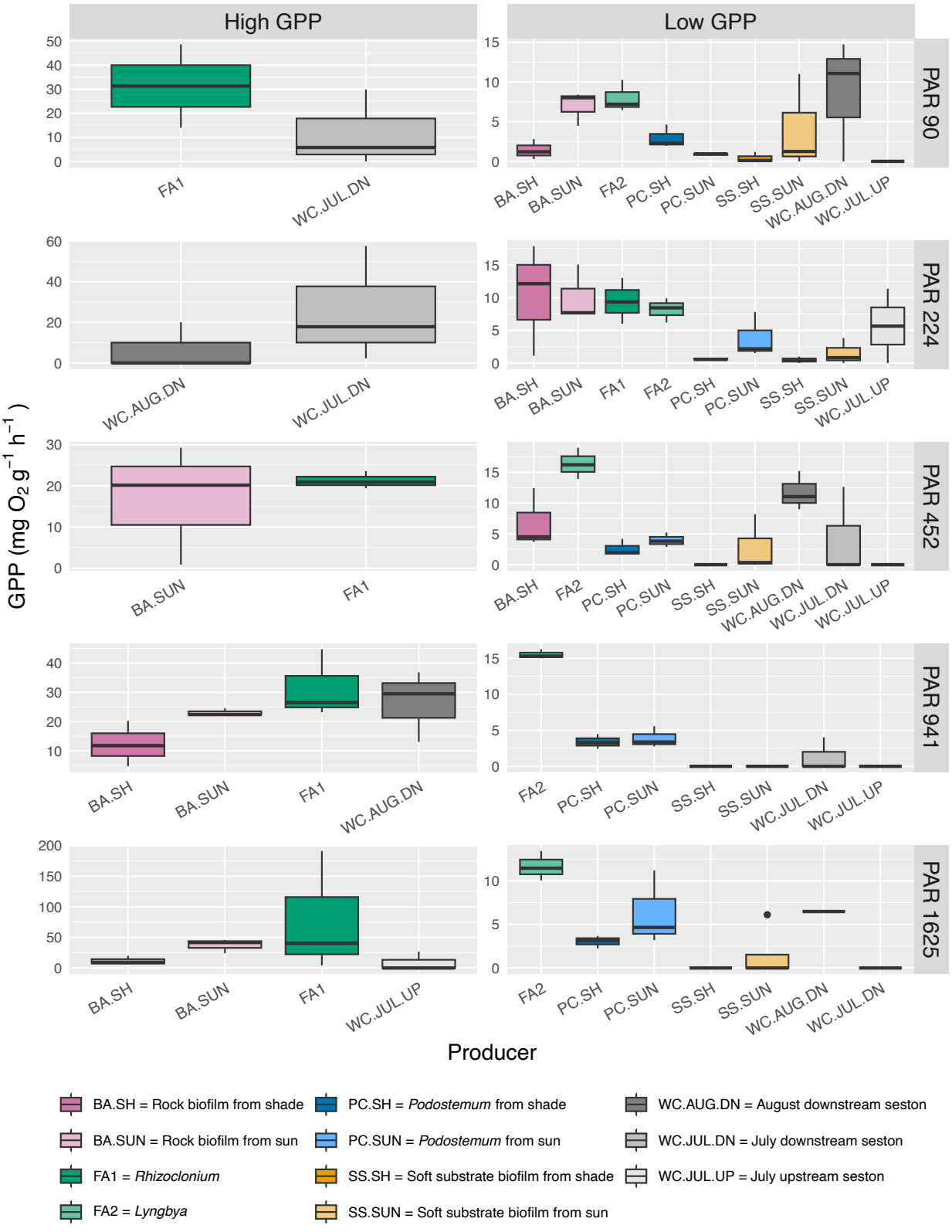
High GPP
Low GPP
PAR 90
PAR 224
PAR 452
PAR 941
PAR 1625
GPP (mg O2 g−1 h−1)
Producer
BA.SH = Rock biofilm from shade
BA.SUN = Rock biofilm from sun
FA1 = Rhizoclonium
FA2 = Lyngbya
PC.SH = Podostemum from shade
PC.SUN = Podostemum from sun
SS.SH = Soft substrate biofilm from shade
SS.SUN = Soft substrate biofilm from sun
WC.AUG.DN = August downstream seston
WC.JUL.DN = July downstream seston
WC.JUL.UP = July upstream seston

SUPPLEMENTARY IMAGES

Image B1: Example water bath setups with shade cloths (left) for one of the four shaded light treatments – PAR of 90, 224, 452, or 941 – and without shade cloths (right) for a full light treatment – PAR of 1625.

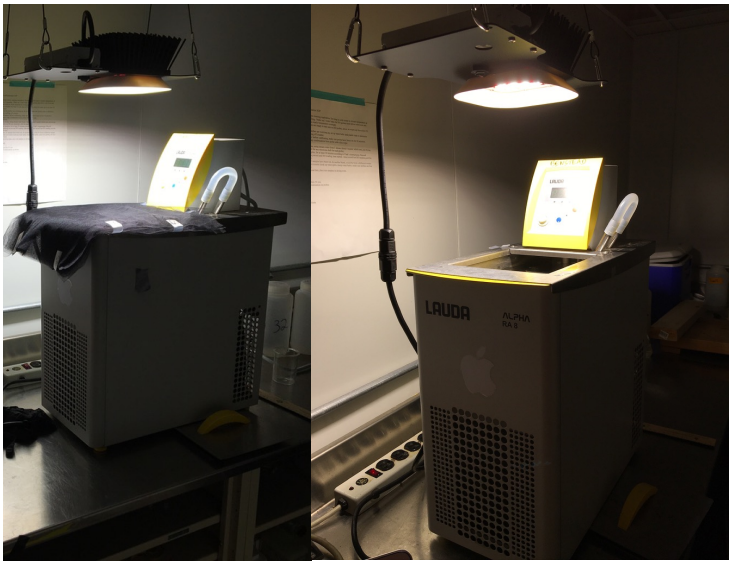

APPENDIX C

CHAPTER 4 SUPPLEMENTARY MATERIALS

DATA AVAILABILITY

DOI for continued versions of published data: 10.5281/zenodo.17613023

Repository access: https://doi.org/10.5281/zenodo.17613023

Zenodo Version 1 Record Number 17613024